Αλληλεπίδραση Η/Μ ακτινοβολίας με την ύλη

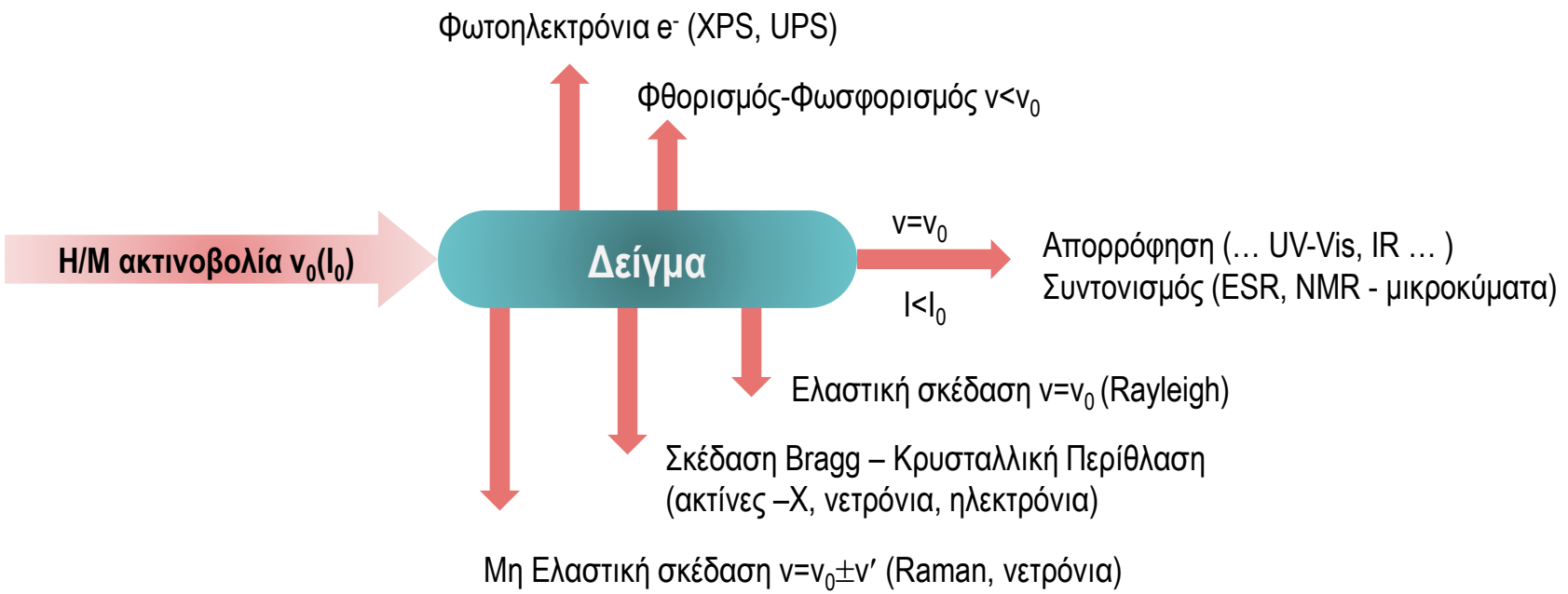

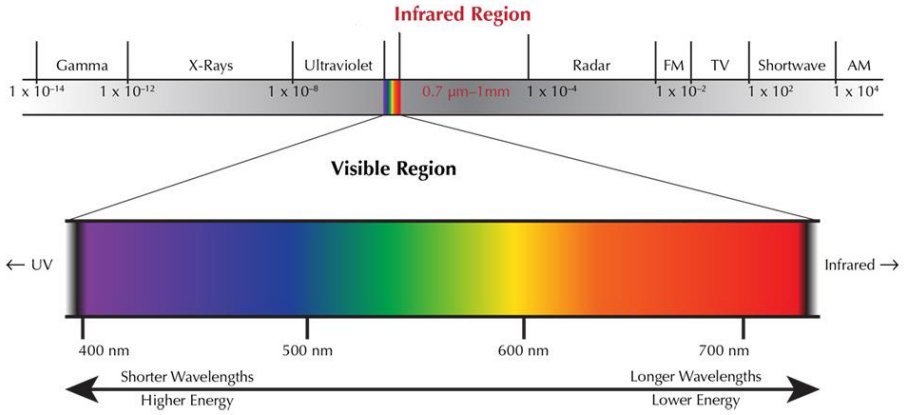

	Abbreviation	Wavelength
Near-Infrared	NIR	0.75–1.5 μm
Mid-Infrared	MIR	1.5–15 μm
Far-Infrared	FIR	15–1000 μm

Spectral intensity and width

Transition probability: Fermi's golden rule

$$\lambda_{if} = \frac{2\pi}{\hbar}\left|M_{if}\right|^2 \rho_f$$

Fermi's Golden Rule

Transition probability — *Matrix element for the interaction* — *Density of final states*

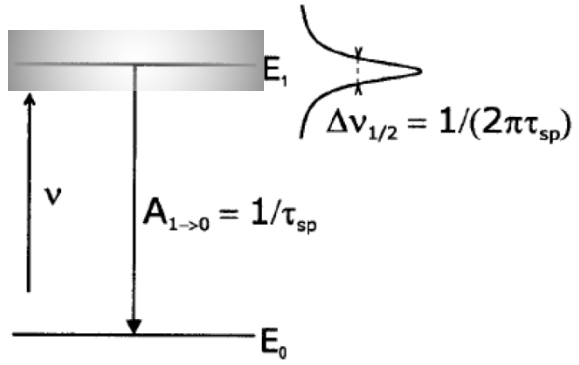

$$\Delta E \Delta t \geq \hbar \Leftrightarrow \Delta \nu \Delta t \geq \frac{1}{2\pi}$$

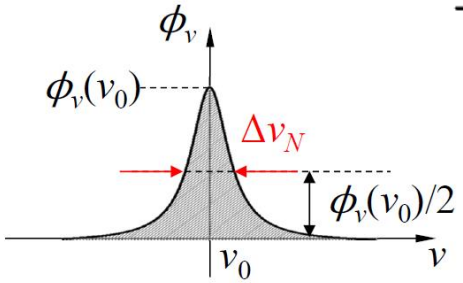

- Frequency
- Width
- Intensity

Light-matter interaction

Wavefunction for final state — *Wavefunction for initial state*

$$M_{if} = \int \Psi_f^* V \Psi_i \, dv$$

Operator for the physical interaction which couples the initial and final states of the system.

Electric dipole

$$V = -\mu \cdot E$$

Magnetic dipole

$$V = -\mu_S \cdot B = g_S \mu_B S \cdot B$$

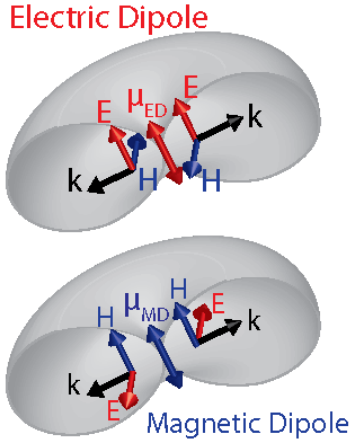

Spectral intensity and width

Absorption

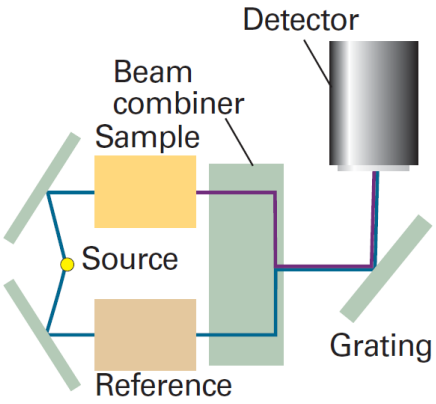

Emission

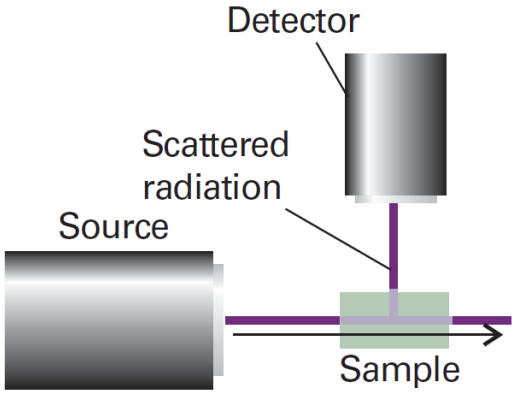

Scattering

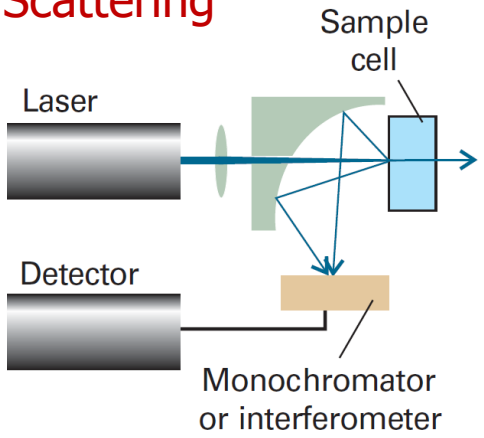

Material "quantity" (light path length, scattering volume)

Beer-Lambert Law

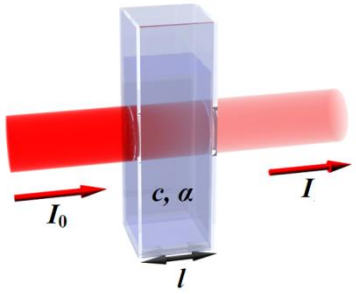

$$A = -\log\frac{I}{I_0} = \varepsilon l c$$

ε: extinction coefficient
l: length
c: concentration

Scattering volume)

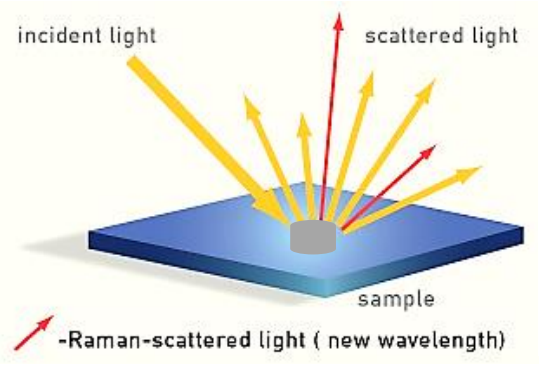

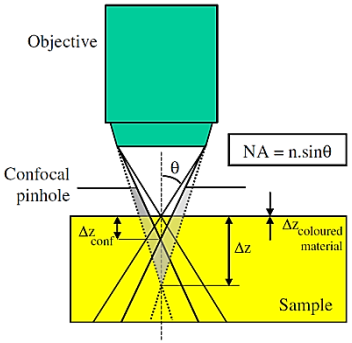

Spectral intensity and width

Full width at half maximum-FWHM

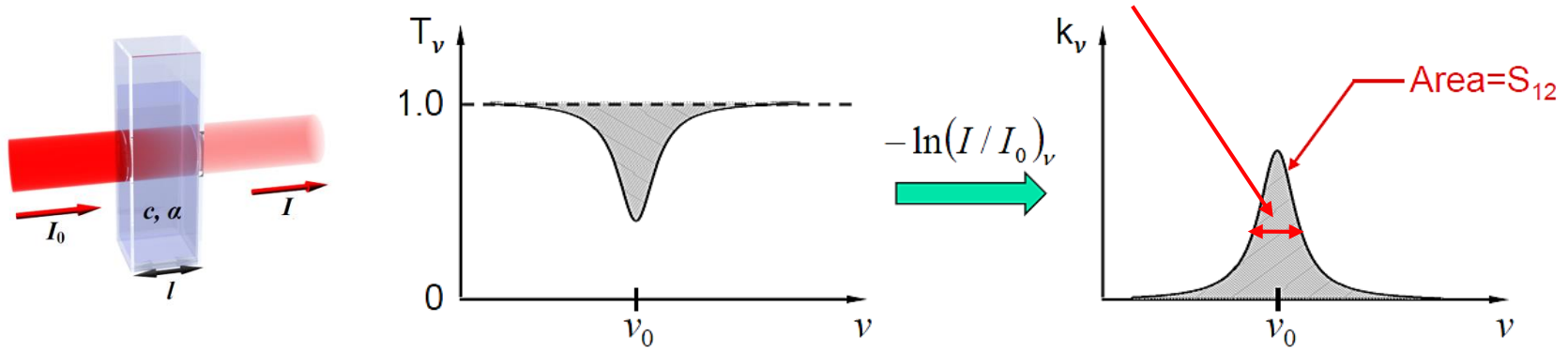

Lineshape functions

Lorentz

A,w>0
offset:y0=0
center:xc=5
width:w=2
area:A=1

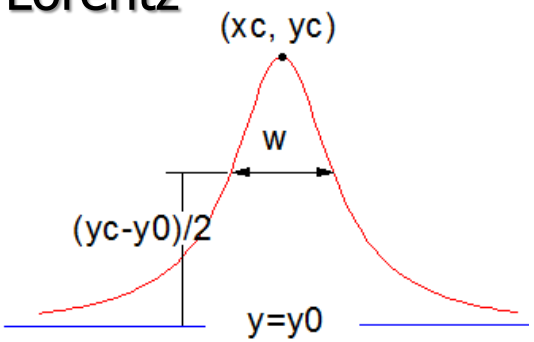

yc=y0+2A/(w*pi)

$$y = y_0 + \frac{2A}{\pi}\frac{w}{4(x-x_c)^2 + w^2}$$

Gauss

A>0
offset:y0=1
center:xc=2
width:w=1.5
area:A=5

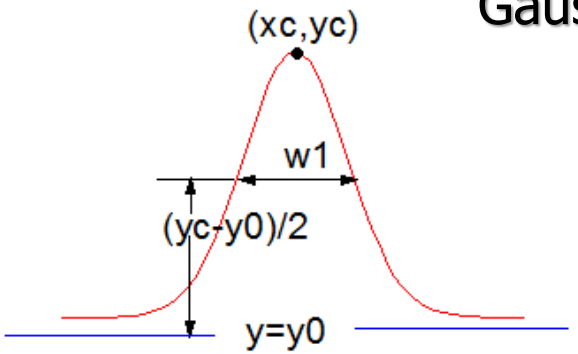

yc=y0+A/(w*sqrt(pi/2))
w=w1/sqrt(ln(4))

$$y = y_0 + \frac{A}{w\sqrt{\pi/2}} e^{-2\frac{(x-x_c)^2}{w^2}}$$

Spectral resolution

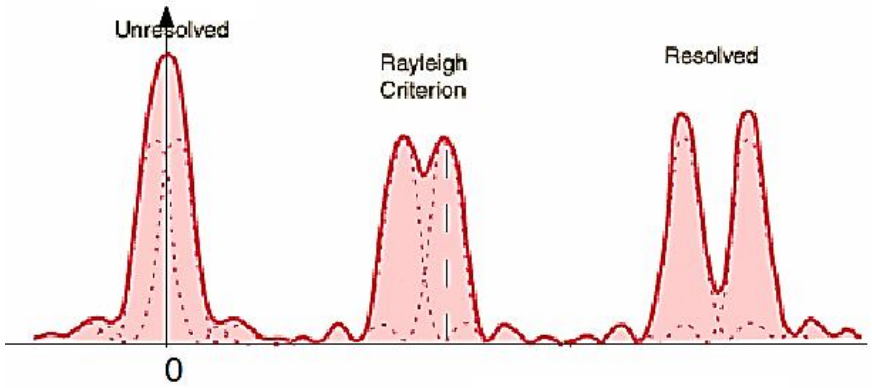

Homogeneous vs inhomogeneous broadening

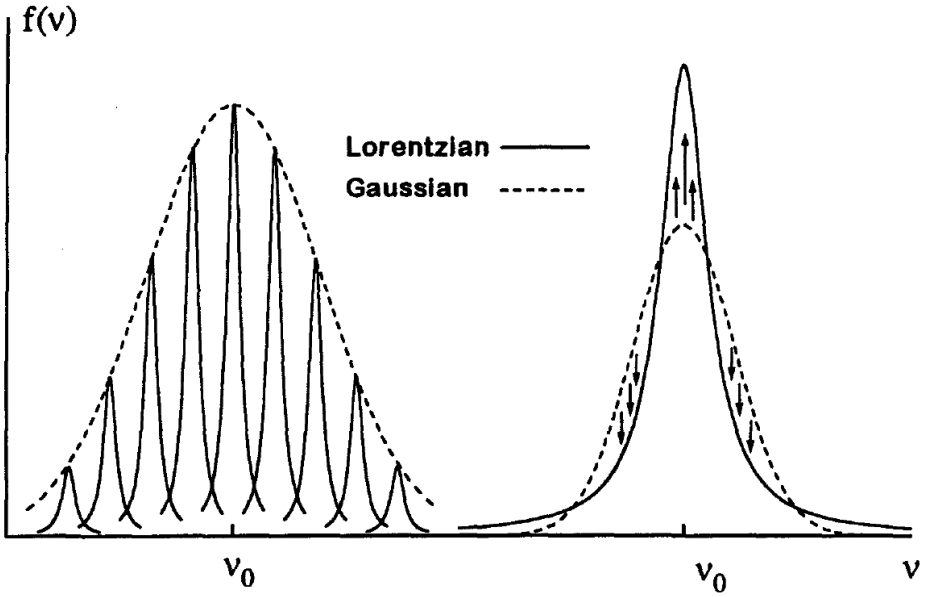

Multi-peak fitting

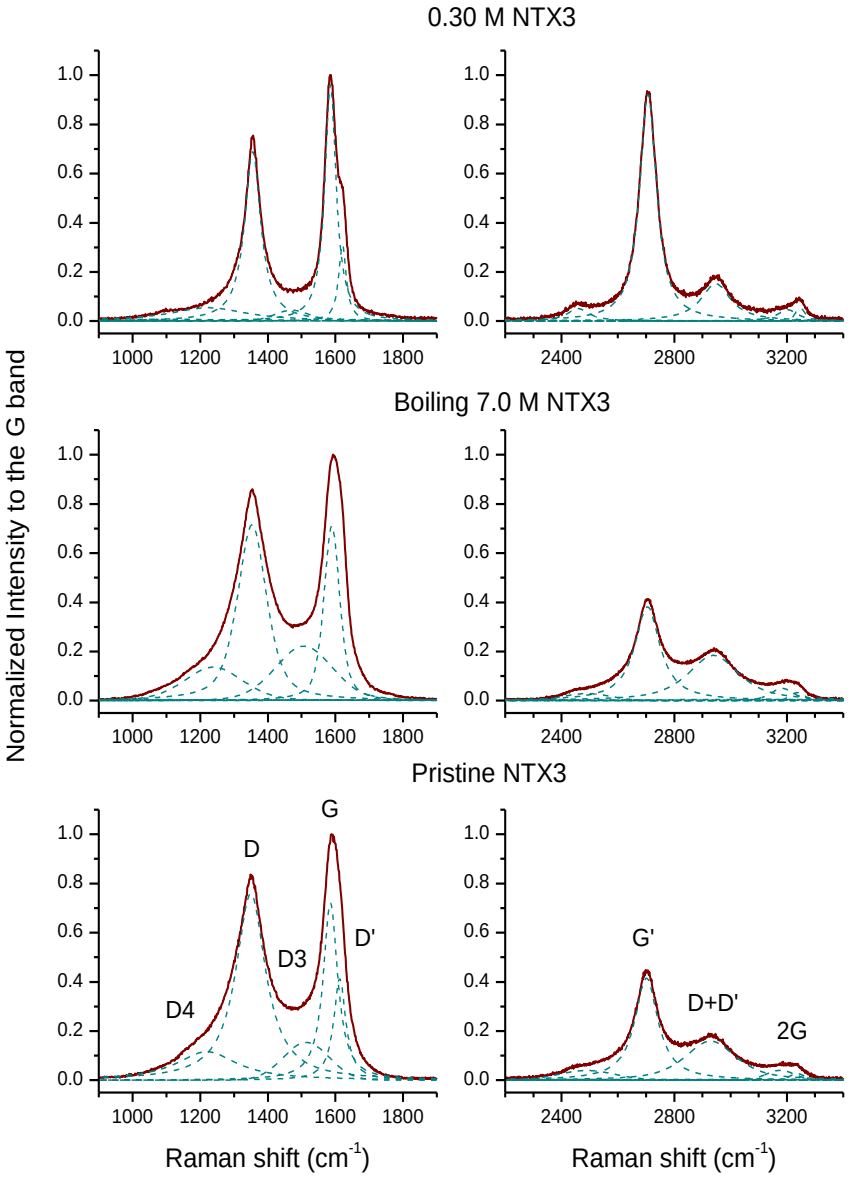

Electron Paramagnetic (Spin) Resonance

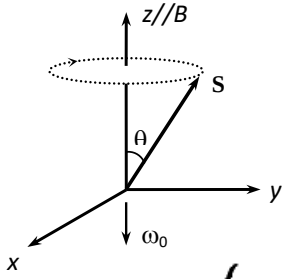

Zeeman effect

$$\hat{H} = -\vec{\mu}_S \cdot \vec{H} = \mu_B \vec{S} \cdot \vec{g} \cdot \vec{H}$$

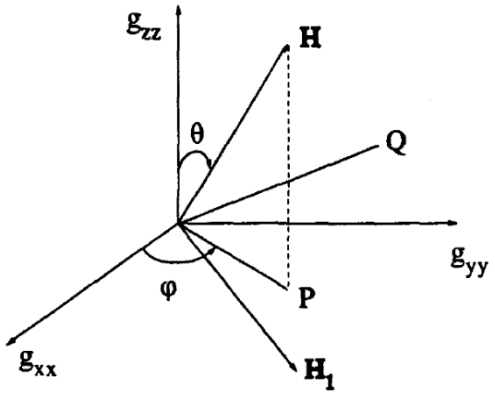

$$H_S = \mu_B H\left(\cos\theta\, g_{zz} S_z + \sin\theta\cos\phi\, g_{xx} S_x + \sin\theta\sin\phi\, g_{yy} S_y\right)$$

	$\lvert\psi_1\rangle$	$\lvert\psi_2\rangle$
$\langle\psi_1\rvert$	$-\frac{1}{2}\mu_B g_{zz} H\cos\theta$	$\frac{1}{2}\mu_B\left(g_{xx} H\sin\theta\cos\phi + i g_{yy}\sin\theta\sin\phi\right)$
$\langle\psi_2\rvert$	$\frac{1}{2}\mu_B\left(g_{xx} H\sin\theta\cos\phi - i g_{yy}\sin\theta\sin\phi\right)$	$\frac{1}{2}\mu_B g_{zz} H\cos\theta$

$$E_{2,1} = \pm\tfrac{1}{2}\mu_B H\left(g_{xx}^{\,2}\sin^2\theta\cos^2\phi + g_{yy}^{\,2}\sin^2\theta\sin^2\phi + g_{zz}^{\,2}\cos^2\theta\right)^{1/2} = \pm\tfrac{1}{2} g_{\text{eff}}\mu_B H$$

$$\Delta E = h\nu = g\mu_B H_r$$

$$g = \frac{0.77448\times\nu(\text{GHz})}{H_r(kG)}$$

$$\hat{H}_1 = \mu_B \mathbf{S}\cdot g_S \cdot H_1\cos\omega t \qquad P_{12} = \frac{\mu_B^{\,2}}{\hbar^2}\left|\langle\psi_1\left|H_1\cdot \mathrm{g_S}\cdot\mathbf{S}\right|\psi_2\rangle\right|^2 f(\nu) \Rightarrow H_1 \perp H_0$$

Electron Paramagnetic (Spin) Resonance

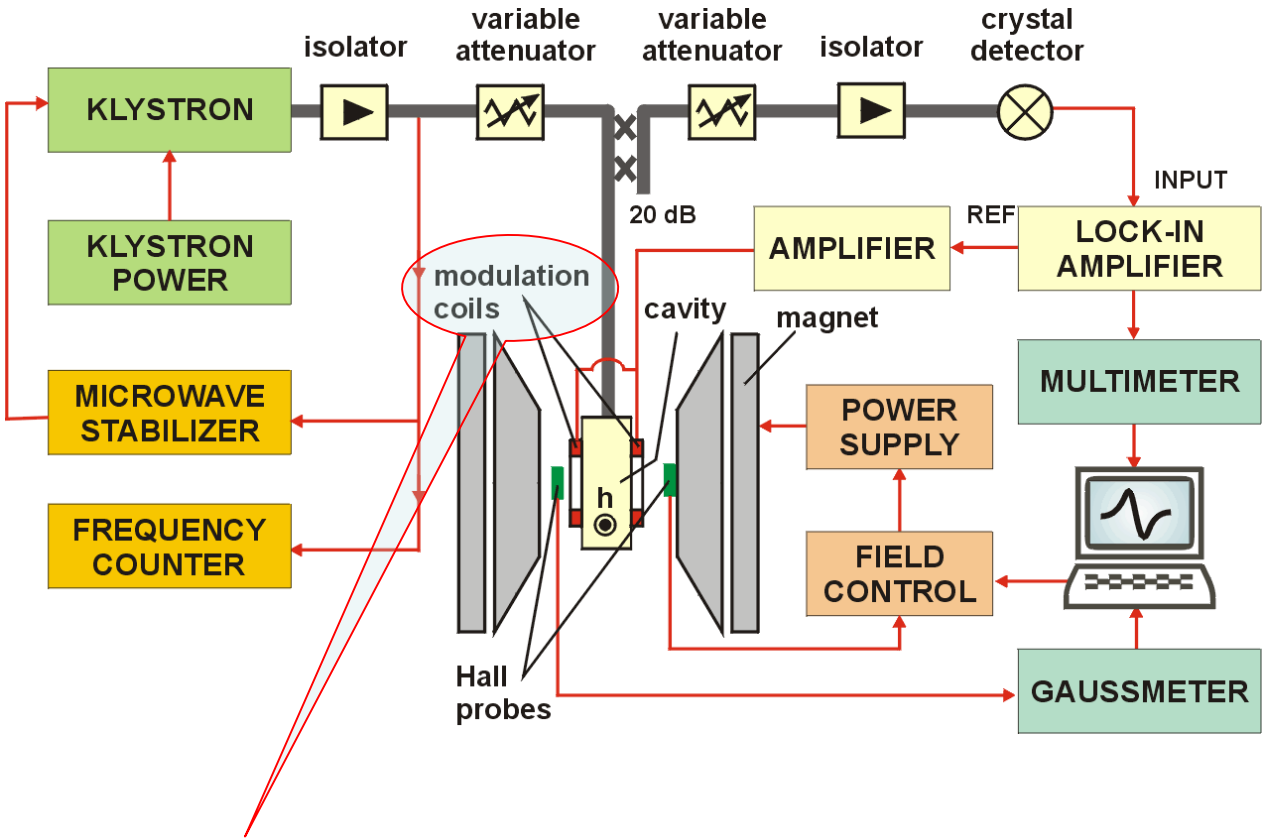

Field modulation (100 kHz): absorption derivative dP/dH - Increase of S/N

Electron Paramagnetic (Spin) Resonance

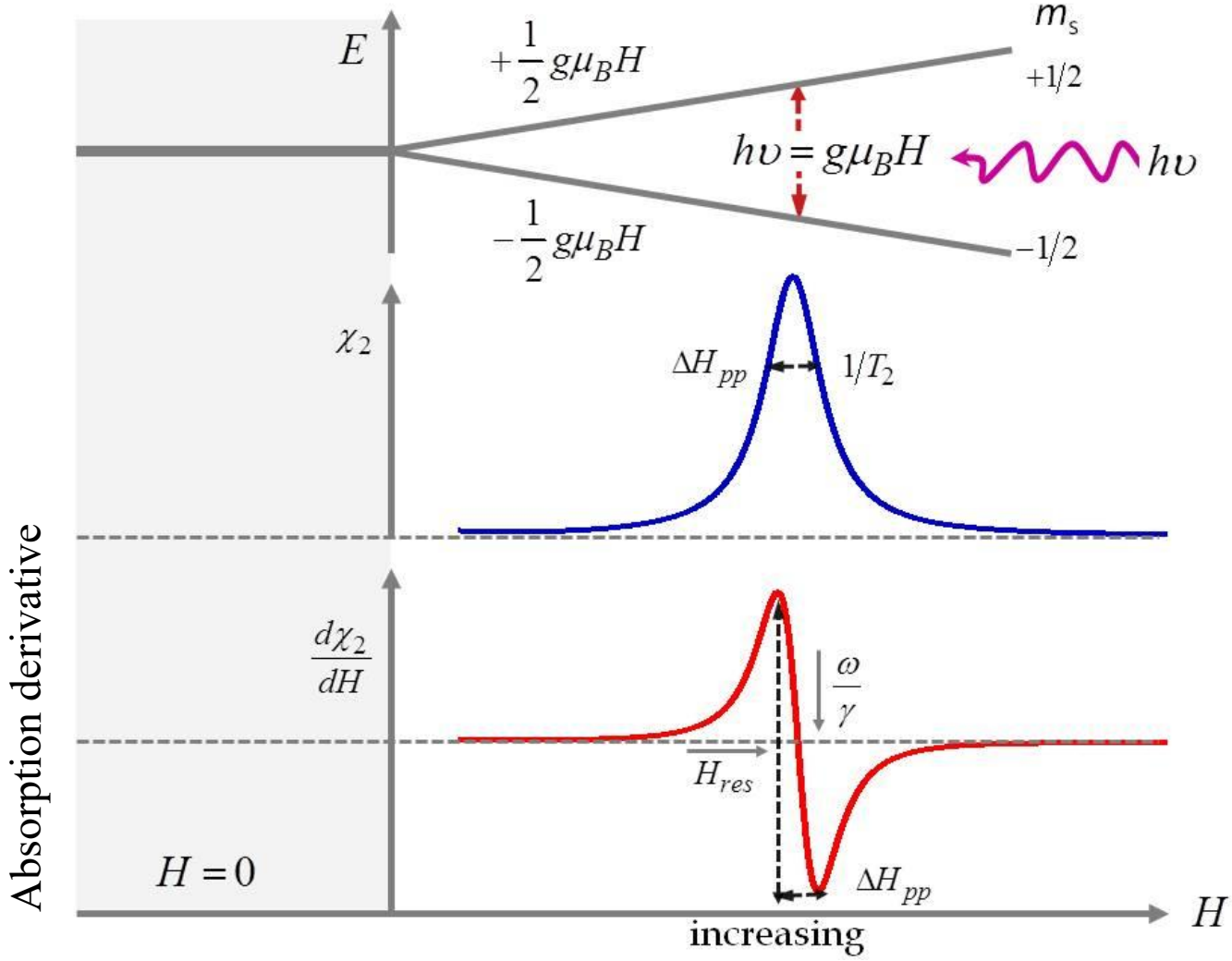

Polycrystalline (powder) EPR spectra

$$I(H) = \int_0^{\pi}\int_0^{\pi} \langle g_1^2 \rangle \left|\frac{dH_0}{d\nu}\right| f(H - H_0, \Delta H)\sin\theta\, d\theta\, d\phi$$

Axial symmetry
$g_{||} \neq g_{\perp}$

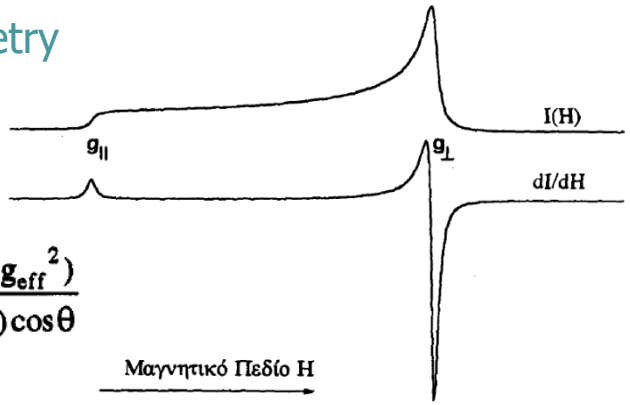

$$I(H) \approx \frac{g_{\perp}^2(g_{//}^2 + g_{eff}^2)}{(g_{//}^2 - g_{\perp}^2)\cos\theta}$$

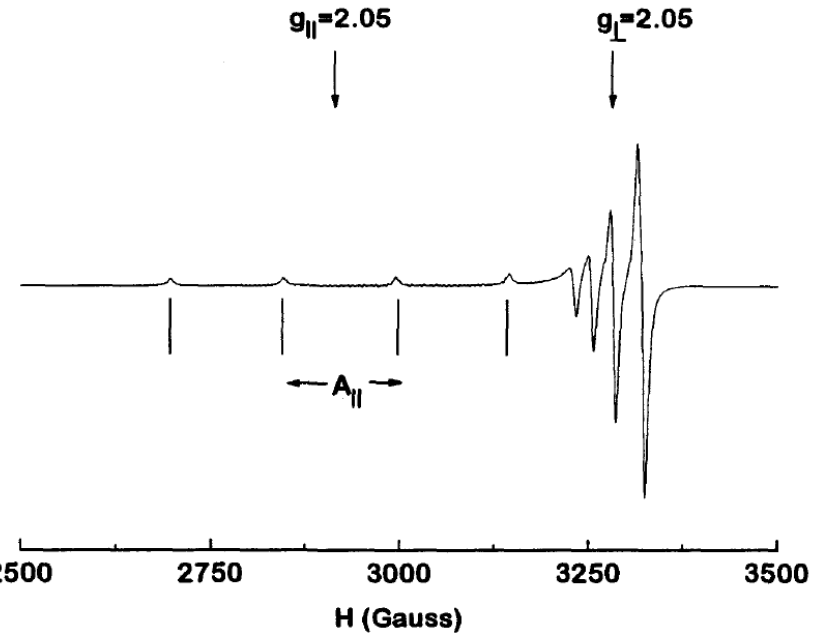

Rhombic symmetry
$g_x \neq g_y \neq g_z$

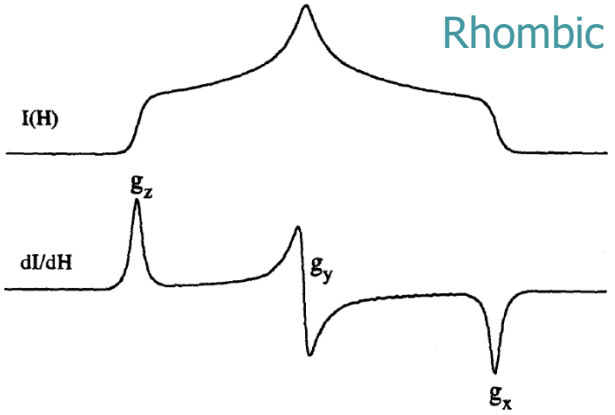

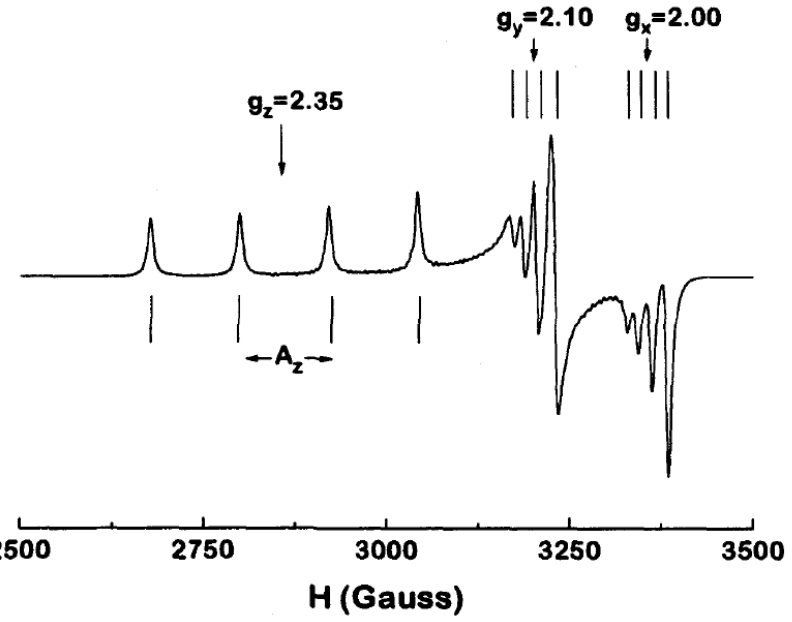

Inelastic Raman Scattering

Rayleigh scattering
Laser line

$I_{Raman} \sim 10^{-3} I_{Rayleigh}$

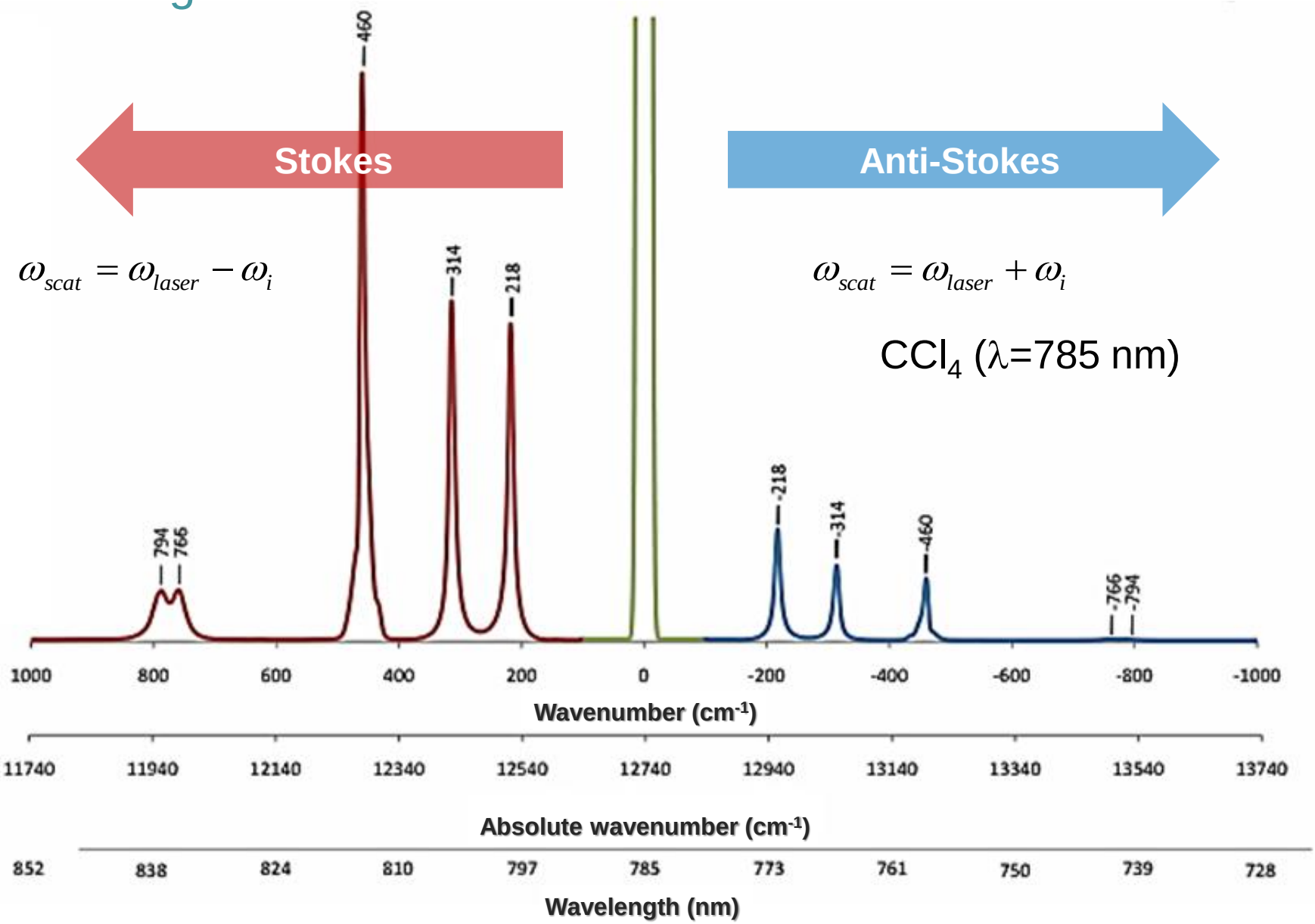

Σκέδαση Raman: Κλασική ερμηνεία

$$\vec{E} = \vec{E}_0 \cos\omega_0 t$$

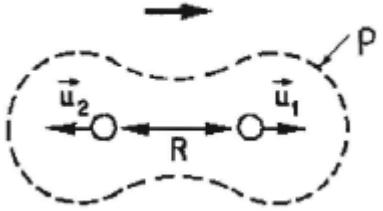

$$\vec{M}(t) = \sum e_i \vec{r}_i(t)$$

$$\vec{M} = a\vec{E} + \beta\vec{E}^2/2 + \ldots$$

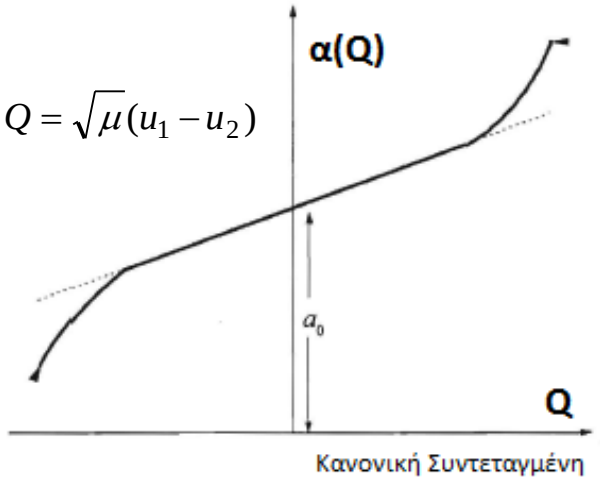

Ηλεκτρονική Πολωσιμότητα

$$a = a_0 + \left(\frac{\partial\alpha}{\partial Q}\right)_0 Q + \frac{1}{2}\left(\frac{\partial^2\alpha}{\partial Q^2}\right)_0 Q^2 + \ldots$$

Raman

$1^{ης}$ τάξης $2^{ης}$ τάξης

$$Q = Q_0 \cos\omega_j t$$

$$a(t) = a_0 + \left(\frac{\partial\alpha}{\partial Q}\right)_0 Q_0 \cos\omega_j t$$

$$M(t) = a_0 E_0 \cos\omega_0 t + \frac{1}{2}\left(\frac{\partial\alpha}{\partial Q}\right)_0 Q_0 E_0 \left[\cos(\omega_0 - \omega_j)t + \cos(\omega_0 + \omega_j)t\right]$$

Elastic Stokes Anti-Stokes

Φέρον κύμα

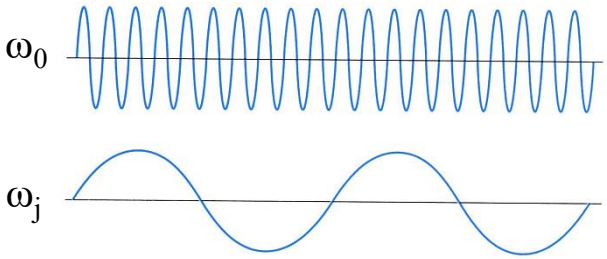

Διαμόρφωση κατά πλάτος

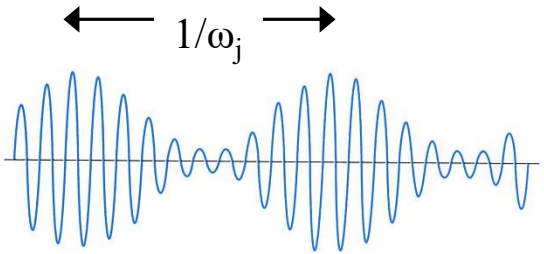

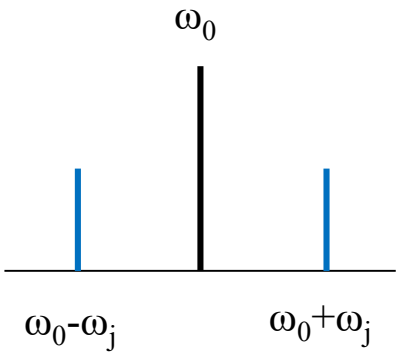

Εκπομπή Η/Μ ταλαντούμενου διπόλου

Ένταση ακτινοβολίας ανα μονάδα στερεάς γωνίας

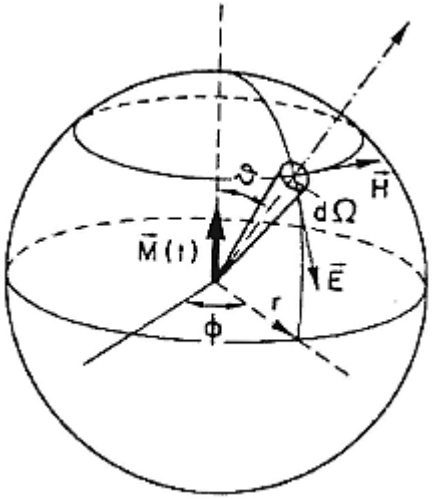

$$I(t) = \frac{1}{4\pi c^3}\sin^2\theta\,|\ddot{M}(t)|^2 = A\,|\ddot{M}(t)|^2$$

$$I(t) = AE_0^2[k_0^2\cos^2\omega_0 t + k_1^2\cos^2(\omega_0-\omega_j)t + k_2^2\cos^2(\omega_0+\omega_j)t + \ldots$$

$$k_0^2 = \alpha_0^2\omega_0^4 \qquad k_1^2 = \frac{1}{4}\left(\frac{\partial\alpha}{\partial Q}\right)_0^2 Q_0^2(\omega_0-\omega_j)^4 \qquad k_2^2 = \frac{1}{4}\left(\frac{\partial\alpha}{\partial Q}\right)_0^2 Q_0^2(\omega_0+\omega_j)^4$$

Φάσμα Ισχύος $$P(\omega) = A\lim_{\tau\to\infty}\frac{2}{\tau}\left|\int_{-\tau/2}^{\tau/2}\ddot{M}(t)e^{-it\omega}dt\right|^2$$

$$P(\omega) = \pi AE_0^2\{k_0^2\delta(\omega-\omega_0) + k_1^2\delta[\omega-(\omega_0-\omega_j)] + k_2^2\delta[\omega-(\omega_0+\omega_j)]\}$$

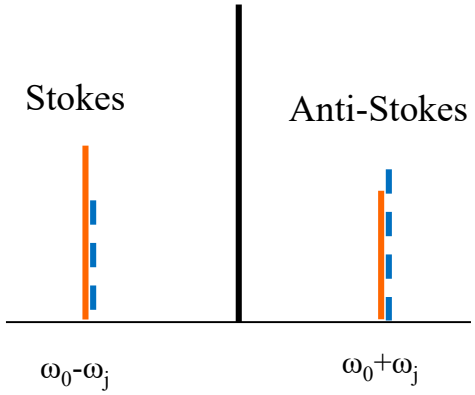

$$\frac{I_{Stokes}}{I_{Anti-Stokes}} = \frac{(\omega_0-\omega_j)^4}{(\omega_0+\omega_j)^4} < 1$$

Σκέδαση Raman vs Απορρόφηση Υπερύθρου (IR)

Πόλωση διπόλου $\vec{P} = \vec{\mu} + \vec{a} \cdot \vec{E}$

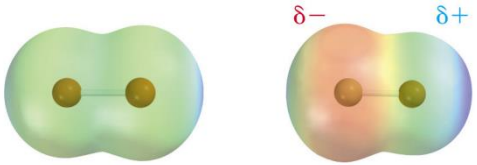

$$\vec{r} = \vec{r}_{eq} + \Delta\vec{r}\cos(\omega_j t) \qquad \vec{\mu} = \vec{\mu}_{eq} + \Delta\vec{\mu}\cos(\omega_j t) \qquad \vec{a} = \vec{a}_{eq} + \Delta\vec{a}\cos(\omega_j t)$$

$$\vec{P} = \vec{\mu}_{eq} + \Delta\vec{\mu}\cos(\omega_j t) + \vec{a}_{eq}\vec{E}_0\cos(\omega_0 t) + \frac{1}{2}\Delta\vec{a}\cdot\vec{E}_0\left[\cos(\omega_0+\omega_j)t + \cos(\omega_0-\omega_j)t\right]$$

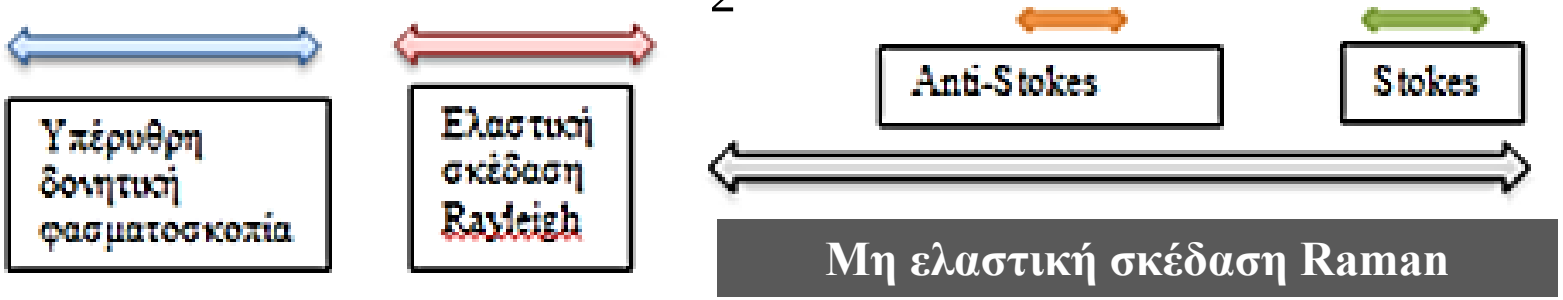

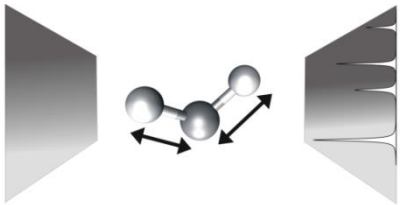

$$\left(\frac{\partial\mu}{\partial r}\right)_{r=r_0} \neq 0$$ Ταλάντωση ενεργή κατά IR

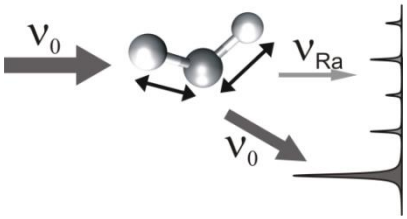

$$\left(\frac{\partial a}{\partial r}\right)_{r=r_0} \neq 0$$ Ταλάντωση ενεργή κατά Raman

Απορρόφηση Υπερύθρου (IR)

Πιθανότητα μετάβασης

$$R_\nu = \int \psi_\nu^{'*} \mu \psi_\nu^{''} dx$$

Μόνιμη διπολική ροπή

$$\mu = \mu_e + \left(\frac{\partial \mu}{\partial x}\right)_e x + \frac{1}{2!}\left(\frac{\partial^2 \mu}{\partial x^2}\right)_e x^2 + \ldots$$

$x \equiv r - r_0$ η μετατόπιση της διατομικής απόστασης από την ισορροπία

$$R_\nu = \mu_e \int \psi_\nu^{'*} \psi_\nu^{''} dx + \left(\frac{\partial \mu}{\partial x}\right)_e \int \psi_\nu^{'*} x \psi_\nu^{''} dx + \ldots$$

($\int \psi_\nu^{'*} \psi_\nu^{''} dx = 0$)

$$R_\nu = \left(\frac{\partial \mu}{\partial x}\right)_e \int \psi_\nu^{'*} x \psi_\nu^{''} dx + \ldots$$

Ενεργό φορτίο

$$\eta = \frac{\partial \mu}{\partial x} \neq 0$$

Ταλάντωση ενεργή κατά IR

Σκέδαση Raman: Κβαντική ερμηνεία

$$\text{H/M ακτινοβολία} \equiv \phi\omega\tau\acute{o}\nu\iota\alpha\ \varepsilon\nu\acute{\varepsilon}\rho\gamma\varepsilon\iota\alpha\varsigma\ E_i = \hbar\omega_i,\ o\rho\mu\acute{\eta}\varsigma\ \vec{p}_i = \hbar\vec{k}_i,\ \acute{o}\pi o\upsilon\ \omega_i = ck_i\ \kappa\alpha\iota\ k_i = 2\pi/\lambda_i$$

$$\Phi\omega\nu\acute{o}\nu\iota\alpha\ \varepsilon\nu\acute{\varepsilon}\rho\gamma\varepsilon\iota\alpha\varsigma\ E_0 = \hbar\omega_0,\ o\rho\mu\acute{\eta}\varsigma\ \vec{p}_0 = \hbar\vec{q}_0,\ \acute{o}\pi o\upsilon\ \omega_0 = \omega(q)$$

$\chi \equiv$ ηλεκτρική επιδεκτικότητα

$$\vec{P} = \varepsilon_0\left(\tilde{\chi}_0 + \frac{\partial\tilde{\chi}}{\partial Q}Q\right)\vec{E}$$

$$H = -\int_V \vec{P}\cdot\vec{E}\,d^3r$$

Κανόνας Fermi

$$\frac{1}{\tau} = \frac{2\pi}{\hbar}\sum_f \left|\langle f|H_{Raman}|i\rangle\right|^2 \delta\left(E_f - E_i\right)$$

Διατήρηση Ενέργειας

$$\hbar\omega_i = \hbar\omega_S \pm \hbar\omega_0$$

Διατήρηση ορμής

$$\hbar\vec{k}_i = \hbar\vec{k}_S \pm \hbar\vec{q}_0$$

$\vec{k}_i \equiv$ *incident wavevector* $\quad \vec{k}_S \equiv$ *scattered wavevector* $\quad \vec{q}_0 \equiv$ *phonon wavevector*

$$\left(\frac{1}{\tau}\right)_{Stokes} = \frac{2\pi}{\hbar}\left|\frac{\partial\tilde{\chi}}{\partial Q}\right|^2 \frac{\hbar}{2\rho\omega_q}\frac{\omega_{k'}^4}{(c/\eta)^3}(1+n_q)$$

$$\left(\frac{1}{\tau}\right)_{Anti-Stokes} = \frac{2\pi}{\hbar}\left|\frac{\partial\tilde{\chi}}{\partial Q}\right|^2 \frac{\hbar}{2\rho\omega_q}\frac{\omega_{k'}^4}{(c/\eta)^3}n_q$$

Bose-Einstein

$$n_q(T) = \frac{1}{e^{\frac{\hbar\omega_q}{k_BT}} - 1}$$

$$\frac{I_{Stokes}}{I_{Anti-Stokes}} = \left(\frac{\omega_S{}^{Stokes}}{\omega_S{}^{Anti-Stokes}}\right)^4 e^{\frac{\hbar\omega_0}{k_BT}} = \left(\frac{\omega_i-\omega_0}{\omega_i+\omega_0}\right)^4 e^{\frac{\hbar\omega_0}{k_BT}} > 1$$

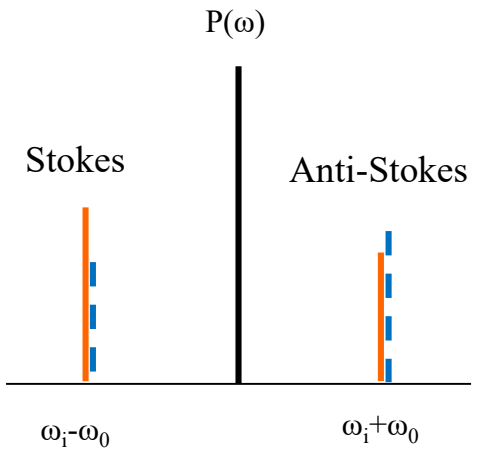

Σκέδαση Raman: Κβαντική ερμηνεία

Διατήρηση Ενέργειας

Rayleigh	Stokes	Anti-Stokes
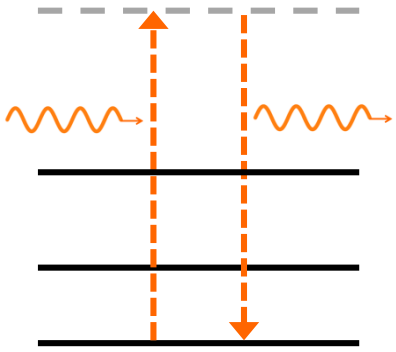	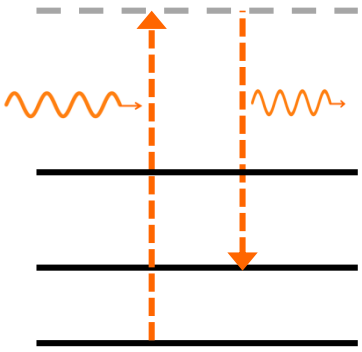	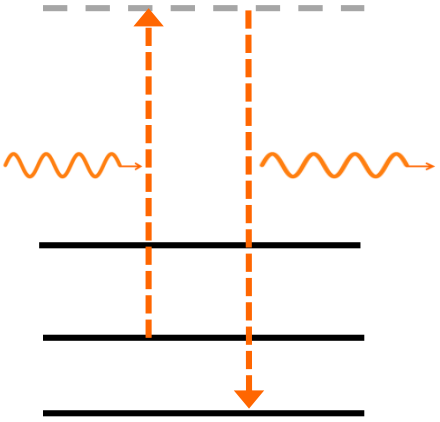
$\hbar\omega_i = \hbar\omega_S$	$\hbar\omega_i = \hbar\omega_S + \hbar\omega_0$	$\hbar\omega_i = \hbar\omega_S - \hbar\omega_0$
Ελαστική σκέδαση	"Εκπομπή" δημιουργία φωνονίου ορμής q	"Απορρόφηση" καταστροφή φωνονίου ορμής q

Εικονική κατάσταση
(virtual state)

Σκέδαση Raman: Κβαντική ερμηνεία

Διατήρηση ορμής

Stokes

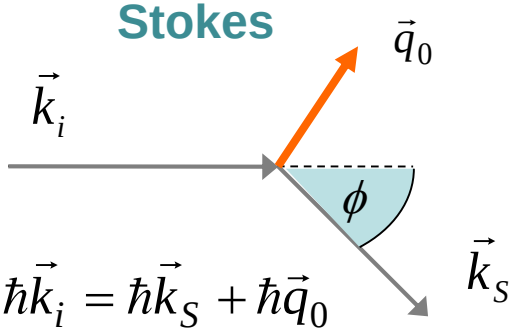

$$\hbar\vec{k}_i = \hbar\vec{k}_S + \hbar\vec{q}_0$$

Anti-Stokes

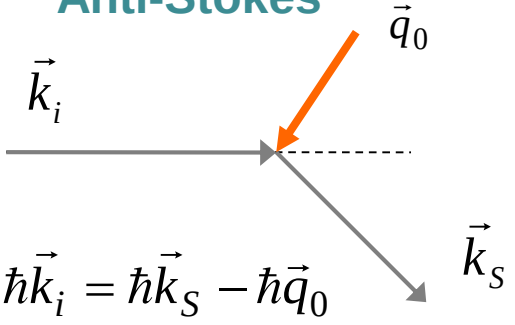

$$\hbar\vec{k}_i = \hbar\vec{k}_S - \hbar\vec{q}_0$$

$\vec{k}_i \equiv$ *incident wavevector* $\quad \vec{k}_S \equiv$ *scattered wavevector* $\quad \vec{q}_0 \equiv$ *phonon wavevector*

Incident Laser in the visible range λ_i=514 nm

$$\bar{\nu}_i \equiv \frac{\nu}{c} = \frac{1}{\lambda_i} = 1/500 \text{ nm} = 20000 \text{ cm}^{-1} = \frac{\omega_i}{2\pi c}$$

$$\bar{\nu}_0 = \frac{\omega_0(q)}{2\pi c} \approx 50 - 3000 \text{ cm}^{-1}$$

$$\omega_i \approx \omega_S$$

$$k_i = \frac{2\pi}{\lambda_i} = \frac{\omega_i}{c} \approx \frac{\omega_S}{c} = k_S$$

$$k_i \approx k_S$$

$$q = 2k_i \sin(\phi/2) \Rightarrow 0 \le q \le 2k_i$$

$$q_{\max} = 2k_i = \frac{4\pi}{\lambda} \approx 2.5\times10^5 \text{ cm}^{-1} << q_{\max} = \frac{2\pi}{a} \text{(1st Brillouin Zone)} \approx 10^8 \text{ cm}^{-1}$$

Backscattering (ϕ=180°) k_S=-k_i

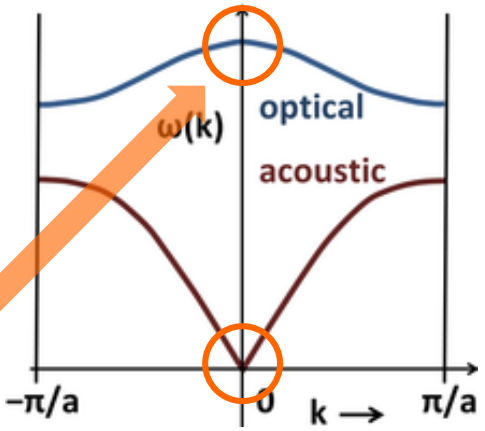

$q \approx 0$

Neutrons λ~1 Å ?

Absorption, Raman Scattering, and Resonant Raman Scattering

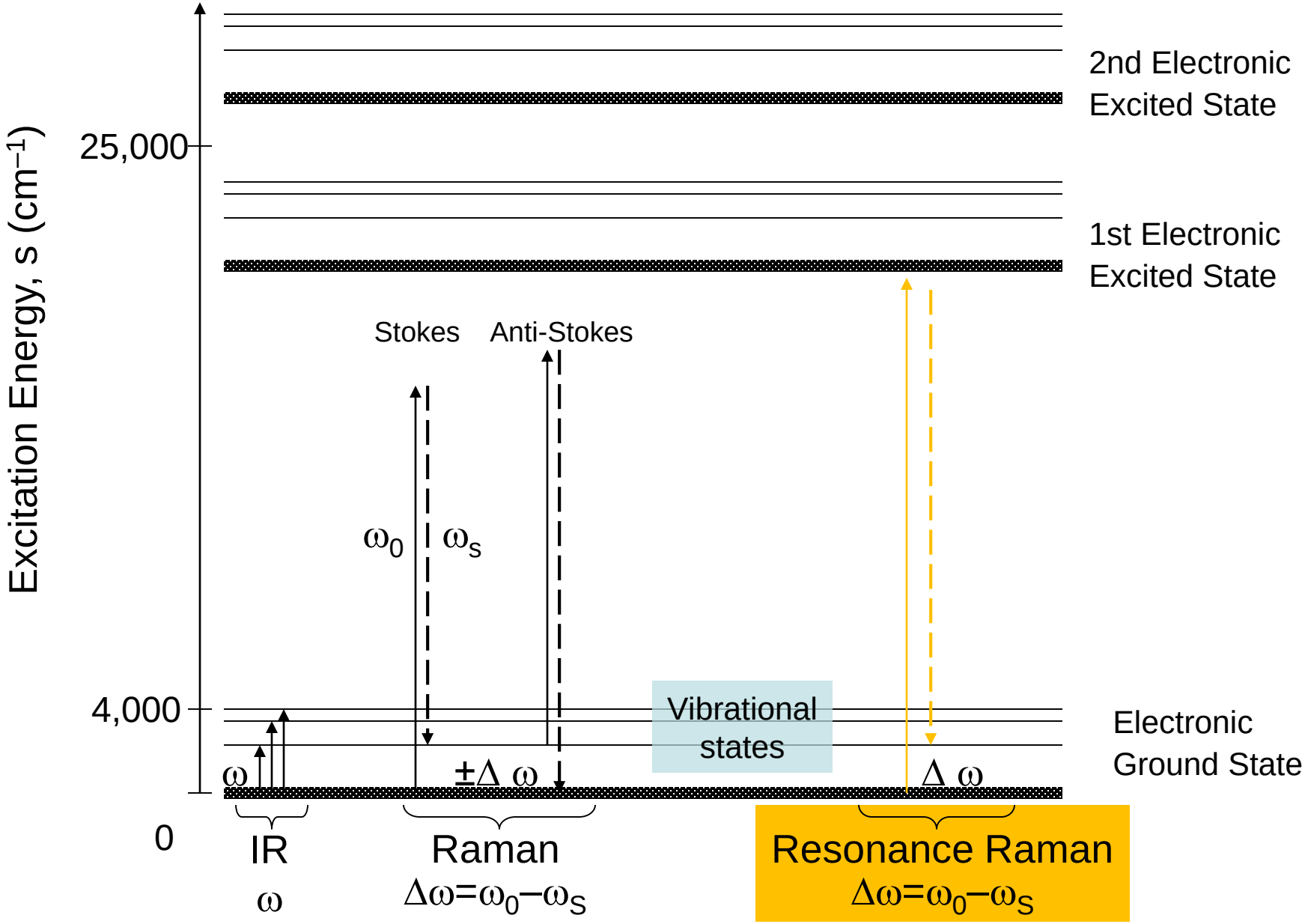

Absorption, Raman Scattering, and Fluorescence

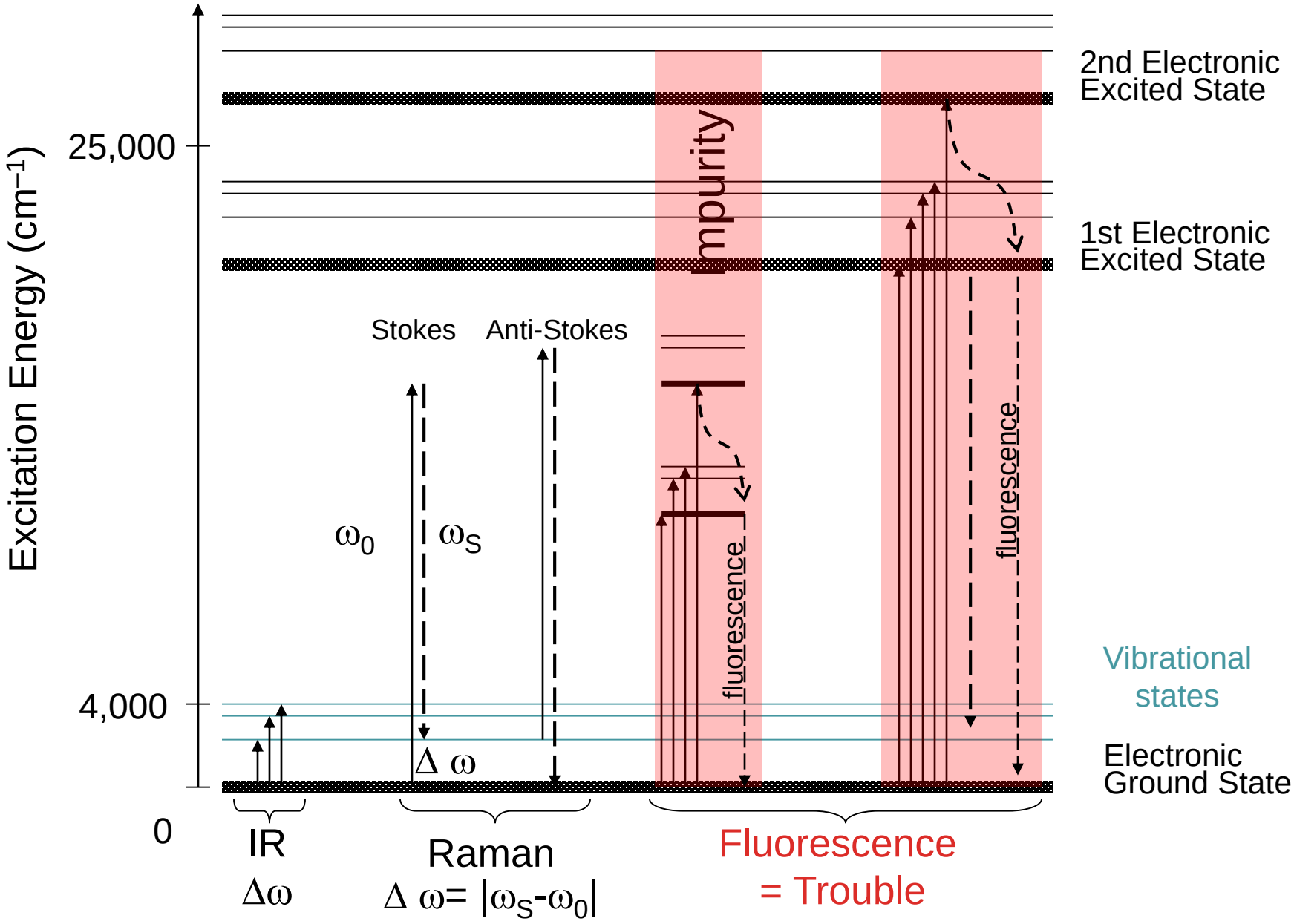

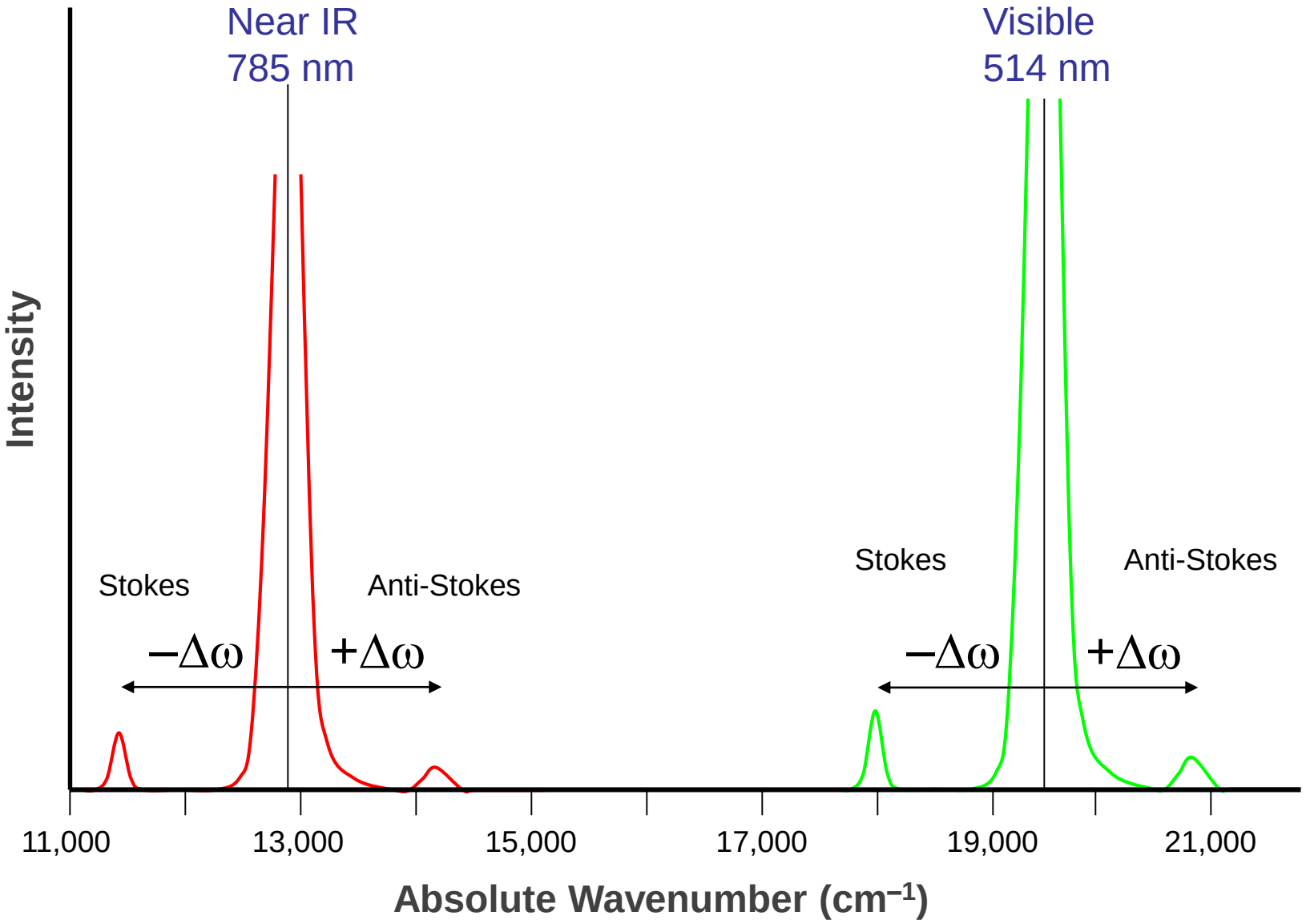
Near IR
785 nm
Visible
514 nm
Intensity
Stokes
Anti-Stokes
−Δω
+Δω
Stokes
Anti-Stokes
−Δω
+Δω
11,000
13,000
15,000
17,000
19,000
21,000
Absolute Wavenumber (cm⁻¹)

Raman Scattering vs Fluorescence

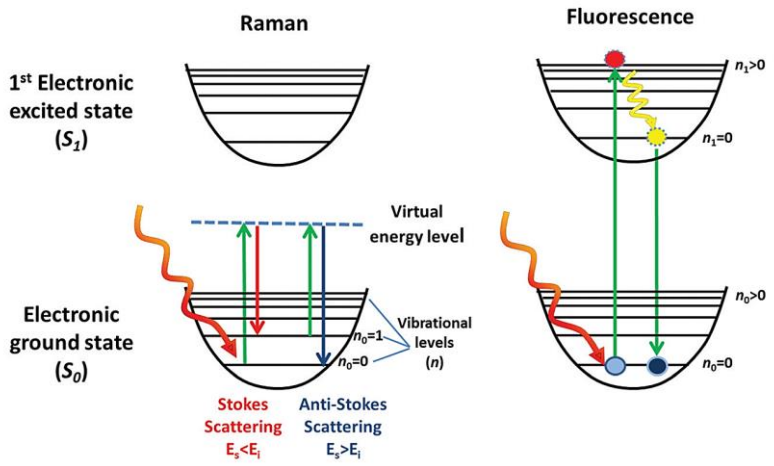

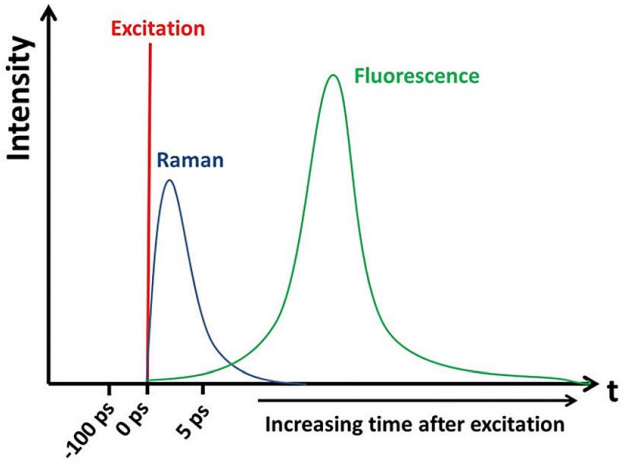

$LiPF_6$

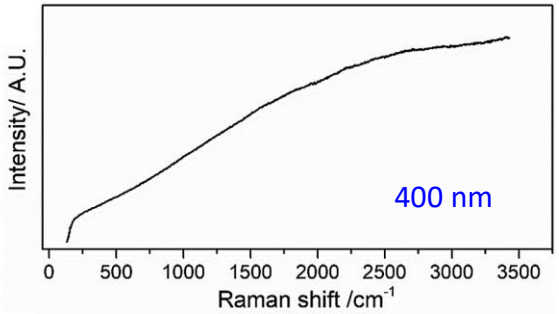

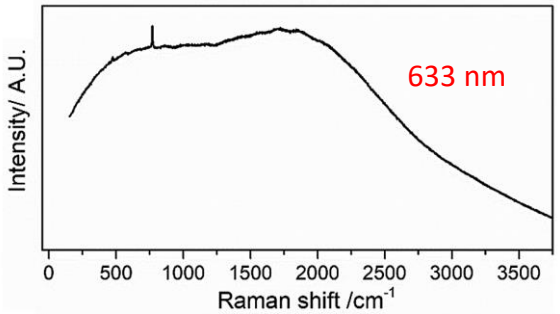

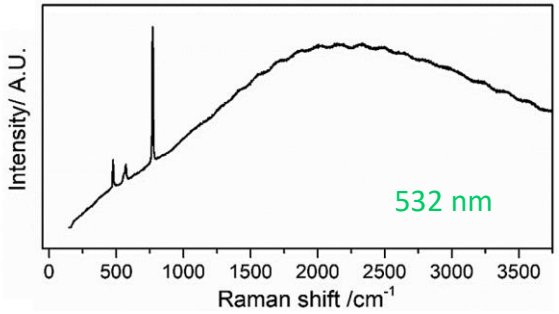

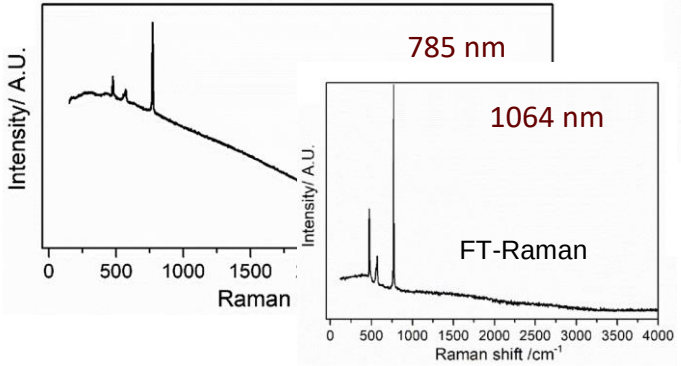

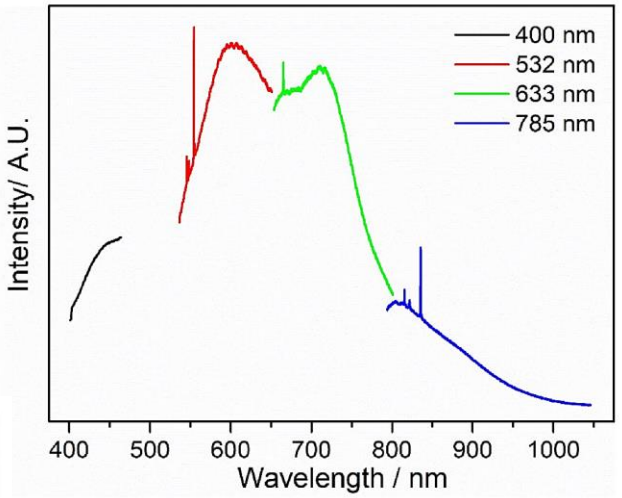

Laurence J. Hardwicket al., Phys.Chem.Chem.Phys., 2019,21, 23833

Σκέδαση Raman: Κανόνες επιλογής - Συμμετρία

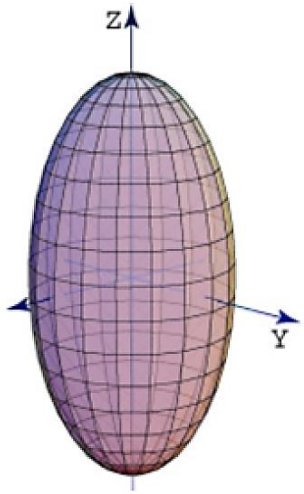

$$\vec{M} = a\vec{E} \Rightarrow M_\rho = \sum_\rho a_{\rho\sigma} E_\sigma \Rightarrow \begin{pmatrix} M_x \\ M_y \\ M_z \end{pmatrix} = \begin{pmatrix} a_{xx} & a_{xy} & a_{xz} \\ a_{yx} & a_{yy} & a_{yz} \\ a_{zx} & a_{zx} & a_{zz} \end{pmatrix} \begin{pmatrix} E_x \\ E_y \\ E_z \end{pmatrix}$$

$$\alpha_{\rho\sigma} = \alpha_{\rho\sigma}^{(0)} + \sum_j \alpha_{\rho\sigma,j} Q_j + \frac{1}{2} \sum_{j'j''} \alpha_{\rho\sigma,j'j''} Q_{j'} Q_{j''} + \ldots$$

Ελλειψοειδές πολωσιμότητας
$r_i \sim 1/\sqrt{a_i}$

$$\Delta\alpha_{\rho\sigma} = \alpha_{\rho\sigma,j} Q_j = \left(\frac{\partial \alpha_{\rho\sigma}}{\partial Q_j} \right)_0 Q_j$$

Ταυστής Raman

$$\alpha_{\rho\sigma,j} = \left(\frac{\partial \alpha_{\rho\sigma}}{\partial Q_j} \right)_0$$

$$\delta\alpha^{(j)} = \begin{pmatrix} \alpha_{xx,j} & \alpha_{xy,j} & \alpha_{xz,j} \\ \alpha_{yx,j} & \alpha_{yy,j} & \alpha_{xz,j} \\ \alpha_{zx,j} & \alpha_{zy,j} & \alpha_{zz,j} \end{pmatrix}$$

$$\left(P_{scatt}\right)_i \sim \sum_{j=x,y,z} \left(\frac{\partial \chi_{ij}}{\partial Q} \right)_{Q=0} E_j \qquad i = x, y, z$$

$$R_{ij,Q} \equiv \left(\frac{\partial \chi_{ij}}{\partial Q} \right)_{Q=0}$$

Σκέδαση Raman: Κανόνες επιλογής - Συμμετρία

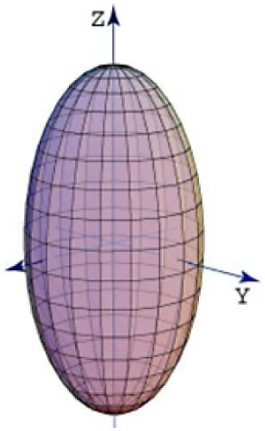

$$r \sim \frac{1}{\sqrt{a}}$$

Διατομικό μόριο π.χ. H_2

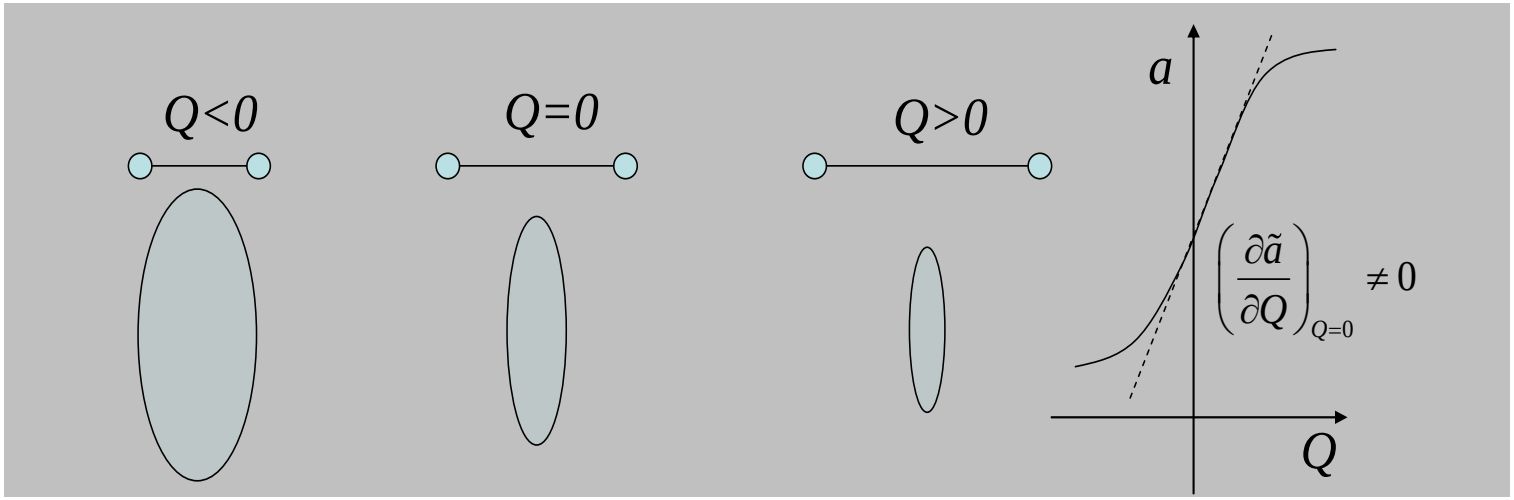

$\alpha<\alpha_0$ α_0 $\alpha>\alpha_0$

$\partial\alpha/\partial Q \neq 0$ ενεργή Raman $\partial\mu/\partial Q = 0$ ανενεργή IR

$$\omega = \frac{c}{2\pi}\sqrt{\frac{k(m_1+m_2)}{m_1 m_2}} = \frac{c}{2\pi}\sqrt{\frac{k}{\mu}}$$

Ετεροπυρηνικά διατομικά μόρια (π.χ. HF, HCl): $\partial\alpha/\partial Q \neq 0$ (Raman) και $\partial\mu/\partial Q \neq 0$ (IR)

Σκέδαση Raman: Κανόνες επιλογής - Συμμετρία

Γραμμικό τριατομικό μόριο π.χ. CO_2

Συμμετρική ταλάντωση έκτασης

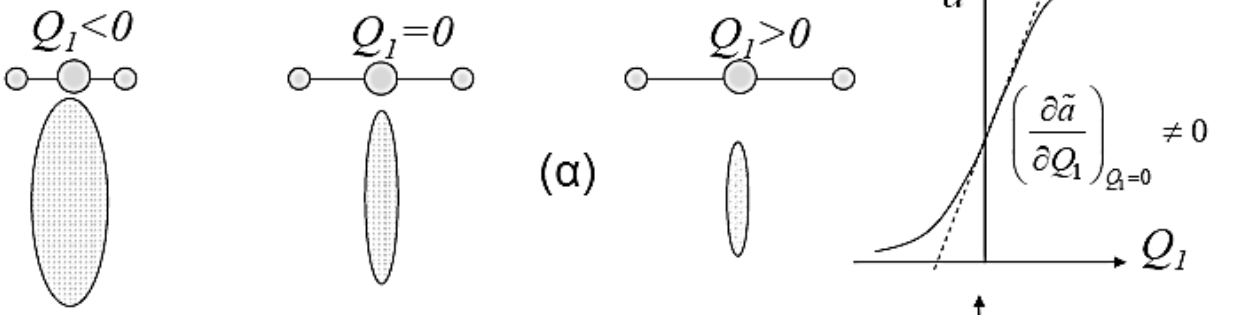

Raman

Αντισυμμετρική ταλάντωση έκτασης

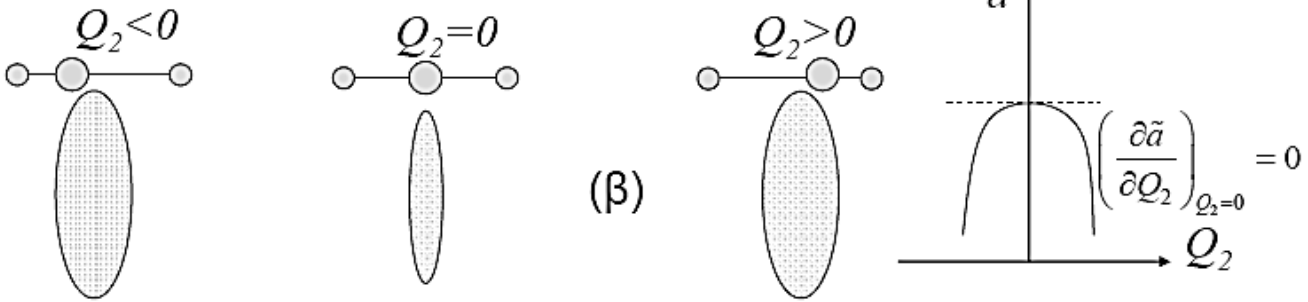

IR

Ταλάντωση κάμψης

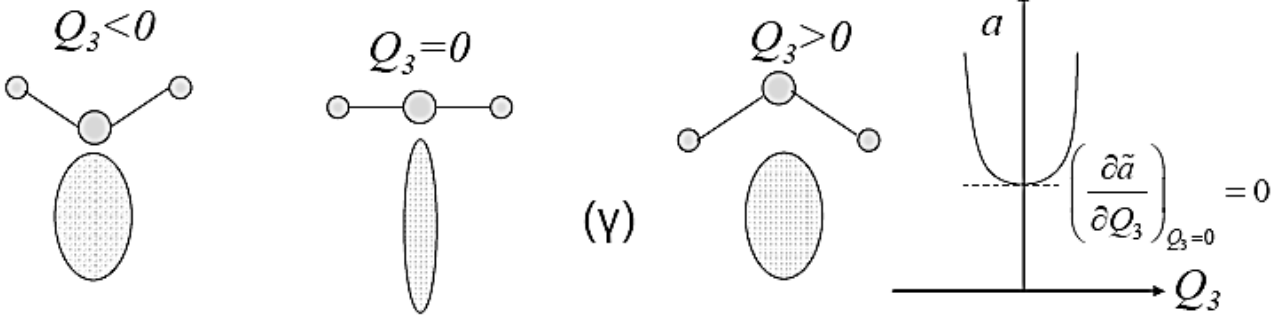

IR

Σκέδαση Raman: Κανόνες επιλογής - Συμμετρία

Μη Γραμμικό τριατομικό μόριο π.χ. H_2O

Κάμψη

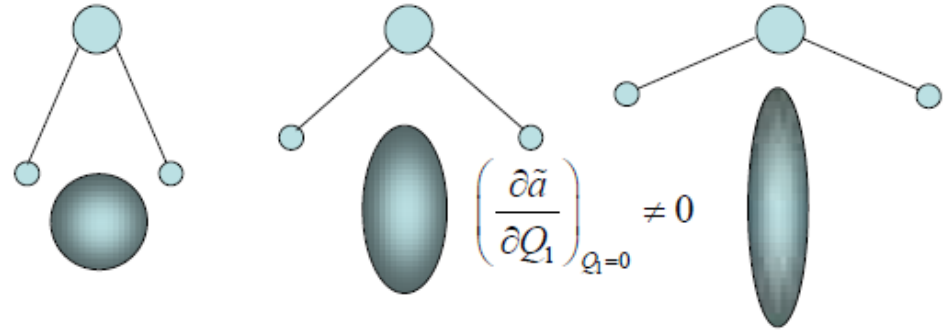

Raman+IR

Συμμετρική έκταση

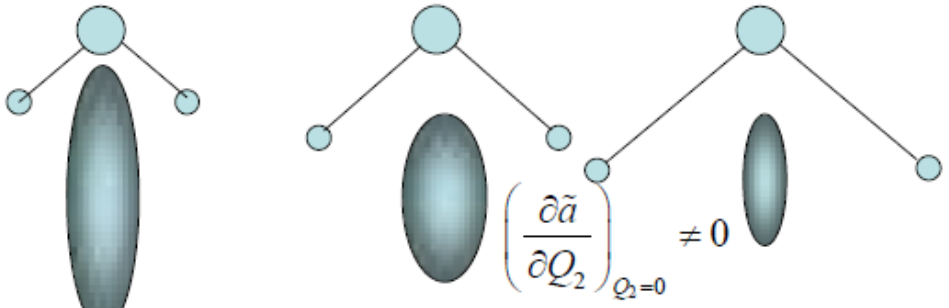

Raman+IR

Αντισυμμετρική έκταση

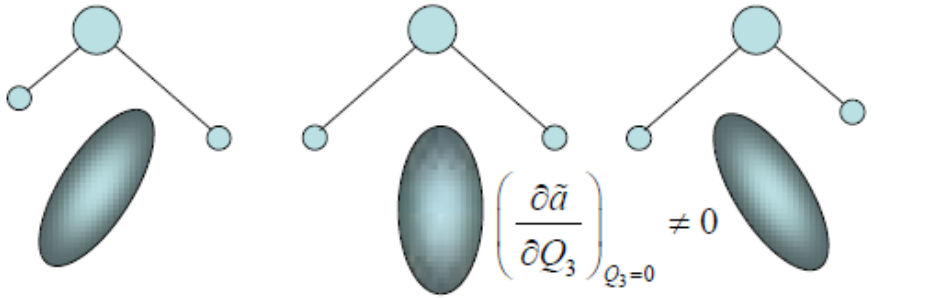

Raman+IR

Σκέδαση Raman: Κανόνες επιλογής - Συμμετρία

Μόρια AB_3

		Επίπεδο e.g. NO_3^-	**Πυραμίδα** e.g. ClO_3^-	
Symmetric Stretching	Raman	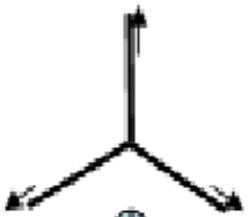		Raman+IR
Symmetric Bending	IR	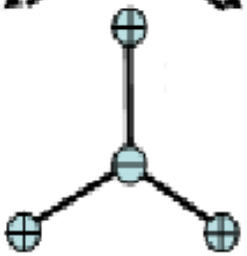	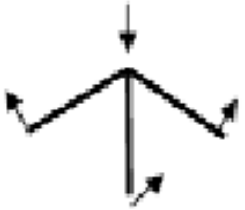	Raman+IR
Asymmetric Stretching	Raman+IR	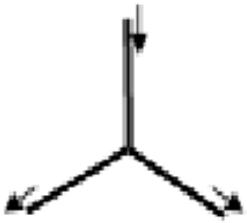		Raman+IR
Asymmetric Bending	Raman+IR	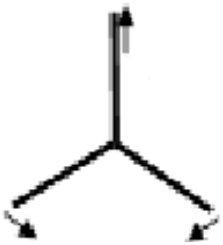		Raman+IR

Σκέδαση Raman: Κανόνες επιλογής - Συμμετρία

- Αριθμός κανονικών τρόπων ταλάντωσης

  3N – 6 (γενικά) ή 3N - 5 (γραμμικά μόρια)

- Συχνότητα αρμονικού ταλαντωτή

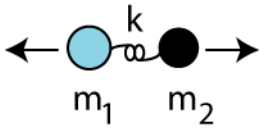

$$\omega = \frac{c}{2\pi}\sqrt{\frac{k(m_1+m_2)}{m_1 m_2}}$$

- Κανόνες επιλογής

Αρχή αμοιβαίου αποκλεισμού (∃ κέντρο συμμετρίας)

Συμμετρική = ενεργός Raman - Αντισυμμετρική = ενεργός IR

CO_2	H_2O
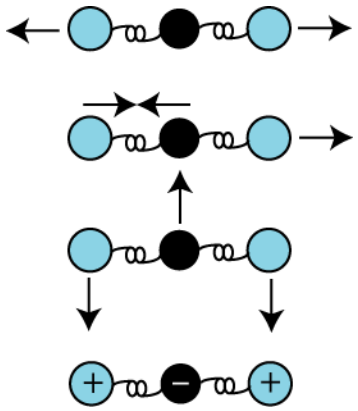 Raman: 1335 cm^{-1} IR: 2349 cm^{-1} IR: 667 cm^{-1}	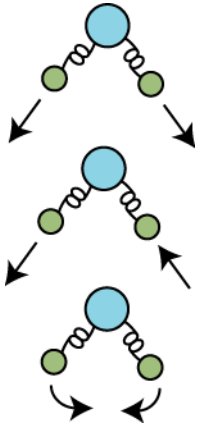 Raman + IR: 3657 cm^{-1} Raman + IR: 3756 cm^{-1} Raman + IR: 1594 cm^{-1}

IR vs Raman

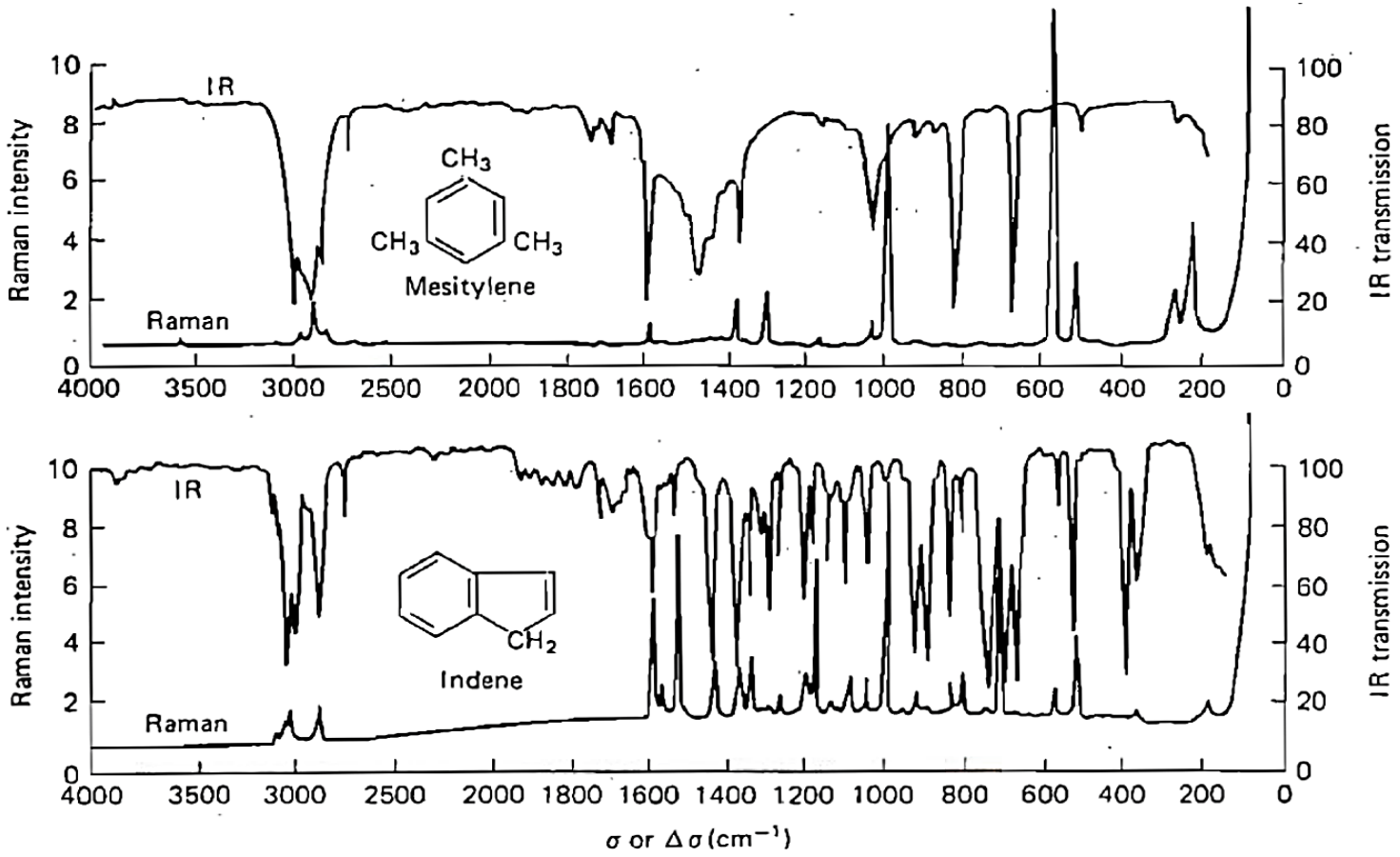

C-H C=C C-C Bending

- Συχνότητες δόνησης → Ταυτοποίηση χημικών δεσμών
- Η συμμετρία καθορίζει αν ένας τρόπος ταλάντωσης είναι ενεργός/ανενεργός κατά Raman ή IR (*Συμπληρωματικότητα μεθόδων*)

diatomic chain

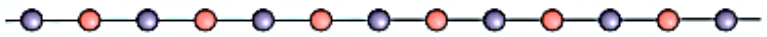

Acoustic phonon: $\mathbf{u}_1$, $\mathbf{u}_2$, in-phase

Optical phonon: $\mathbf{u}_1$, $\mathbf{u}_2$, out-of-phase

phonon dispersion: $\omega_{ac}(\mathbf{q}) \neq \omega_{op}(\mathbf{q})$, for $q \approx 0$, $\omega_{op} > \omega_{ac}$

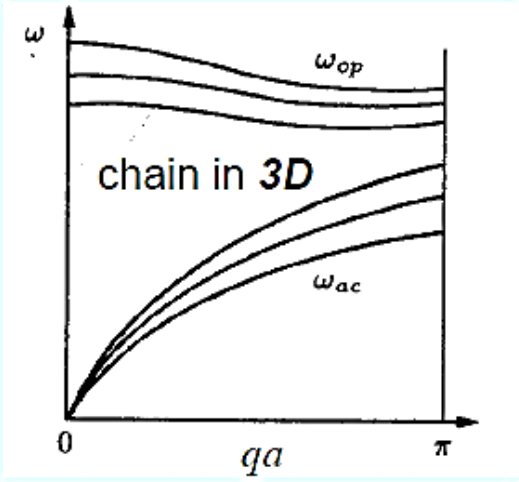

3*D* crystal with ***N*** atoms per cell :

3 acoustic and **3*N* – 3** optical phonons

induced dipole moment
⇨ *interact with light*

1 Longitudinal: wave polarization (**u**) || wave propagation (**q**)

2 Transverse: wave polarization (**u**) ⊥ wave propagation (**q**)

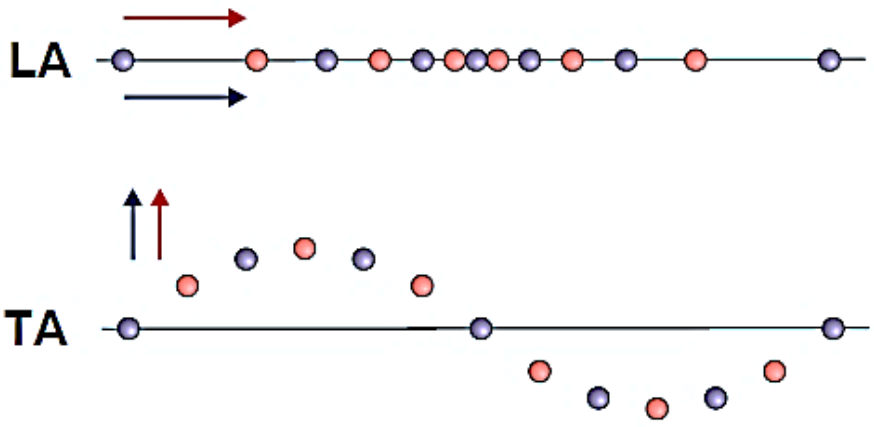

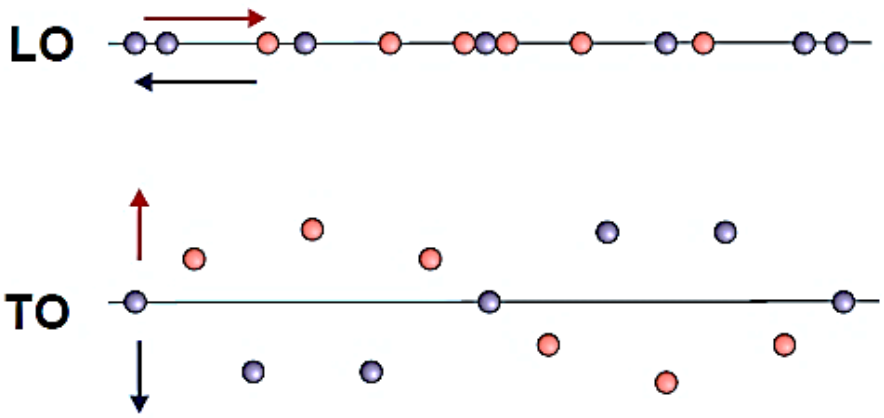

Isolated TO_4 group ⟶ Crystal: $Pb_3(PO_4)_2$, $R\bar{3}m$

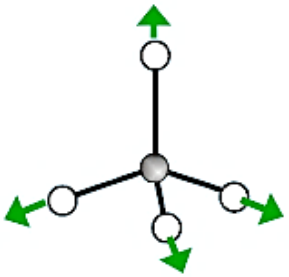

Raman-active

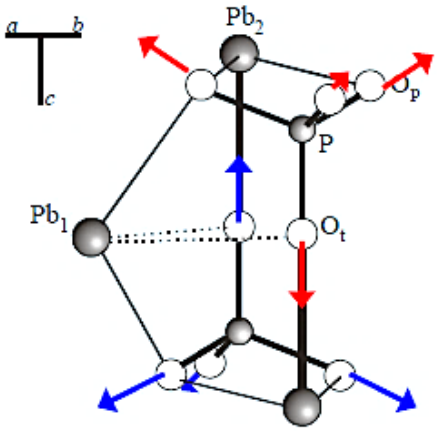

Raman-active

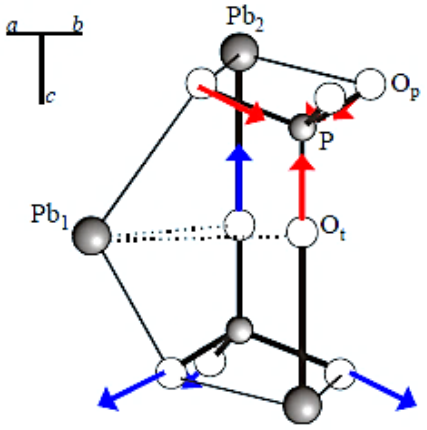

IR-active

IR-active

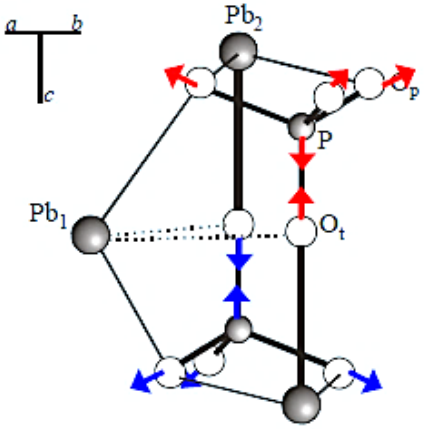

Raman-active

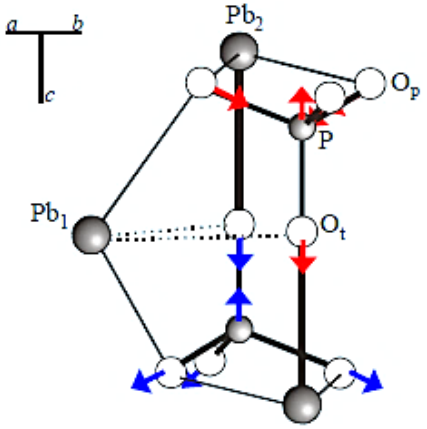

IR-active

Σκέδαση Raman: Πόλωση

Raman intensity

$$I \propto (\alpha_{\alpha\beta})^2$$

Directions of the propagation of incident (i) and scattered (s) light

$$k_i (E_i E_s) k_s$$

Directions of the polarisation of incident (i) and scattered (s) light

Geometry Sample Laser Polarisation

Backscattering (180°)

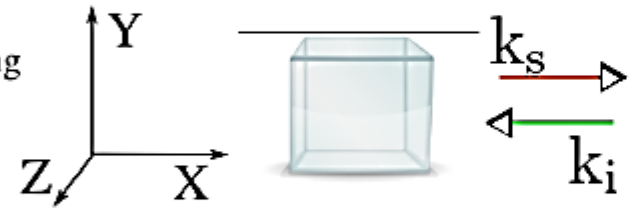

$\overline{X}(YY)X$ $\overline{X}(YZ)X$ $\overline{X}(ZZ)X$

$E_i \,||\, E_s$ $E_i \,|/\, E_s$ $E_i \,//\, E_s$

α_{YY} α_{YZ} α_{ZZ}

$\alpha^n_{\alpha\beta}$ n: X= LO and Y,Z = TO

Right angle

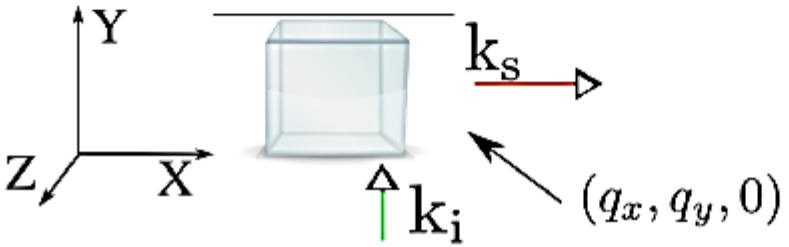

$Y(XZ)X$ $Y(XY)X$ $Y(ZZ)X$

$E_i \,—/\, E_s$ $E_i \,—|\, E_s$ $E_i \,//\, E_s$

α_{XZ} α_{XY} α_{ZZ}

$\alpha^n_{\alpha\beta}$ n: X,Y= LO+TO and Z = TO

$k_i = k_s + q$, E is always $\perp$ to k

Σκέδαση Raman: Πόλωση

180° backscattering geometry

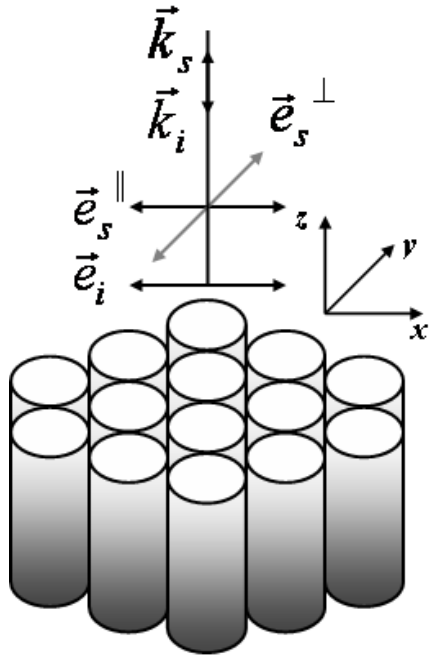

$$I_{\text{Raman}} \propto \alpha_{\alpha\beta}{}^2$$

$$I \sim \left| \hat{e}_i^{\mu} \cdot \vec{\vec{R}}_{ij} \cdot \hat{e}_S^{\nu} \right|^2 \quad \mu,\nu = x,y,z$$

$\mathbf{k}_i \equiv$ propagating vector of the incident laser beam
$\mathbf{k}_S \equiv$ propagating vector of the scattered laser beam
$\mathbf{e}_i \equiv$ incident unit polarization vector
$\mathbf{e}_i \equiv$ scattered unit polarization vector

Porto's notation: A(BC)D
A, D - directions of the propagation of incident ($\mathbf{k}_i$) and scattered ($\mathbf{k}_s$) light,
B, C – directions of the polarization incident ($\mathbf{E}_i$) and scattered ($\mathbf{E}_s$) light

back-scattering geometry

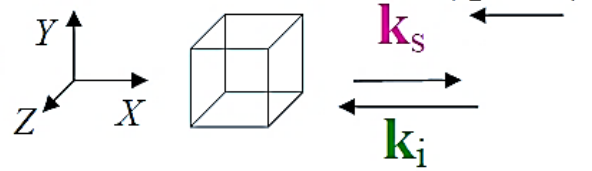

$\bar{X}(YY)X$	$\bar{X}(ZZ)X$	$\bar{X}(YZ)X$
$\mathbf{E}_i$ $\mathbf{E}_s$	$\mathbf{E}_i$ $\mathbf{E}_s$	$\mathbf{E}_i$ $\mathbf{E}_s$
α_{yy}	α_{zz}	α_{yz}
$\alpha_{yy}{}^n$	$\alpha_{zz}{}^n$	$\alpha_{yz}{}^n$

$n = x$ ⇨ LO
$n = y, z$ ⇨ TO

($\mathbf{k}_i = \mathbf{k}_s + \mathbf{q}$, $\mathbf{E}$ is always $\perp$ to $\mathbf{k}$)

Polarized micro-Raman scattering
Crystallite's orientation

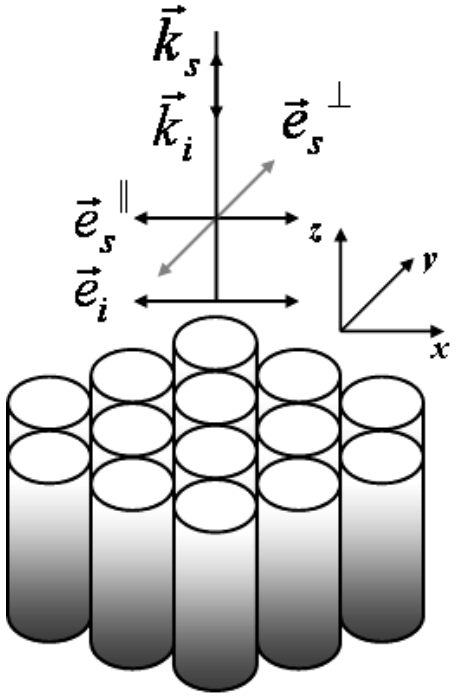

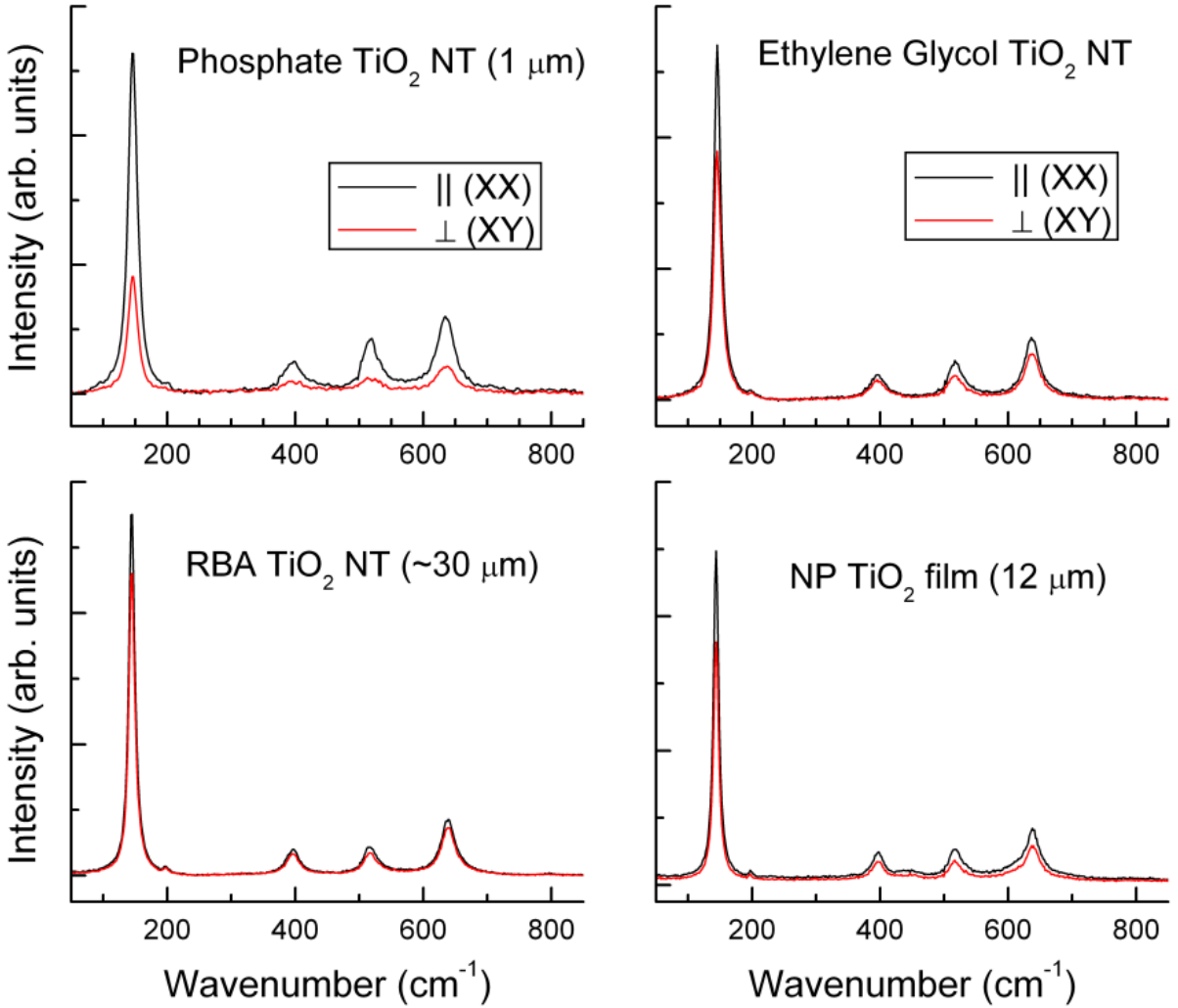

Demokritos
National Centre for Scientific Research
Institute of Physical Chemistry

Crystallographic orientation of anatase crystallites in TiO_2 nanotubes

Depolarization ratio

$$\rho = \frac{I_{\perp}}{I_{\parallel}}$$

Random orientation

E_g	$\rho=3/4$
B_{1g}	$\rho=3/4$
A_{1g}	$1/8 \leq \rho \leq 1/3$

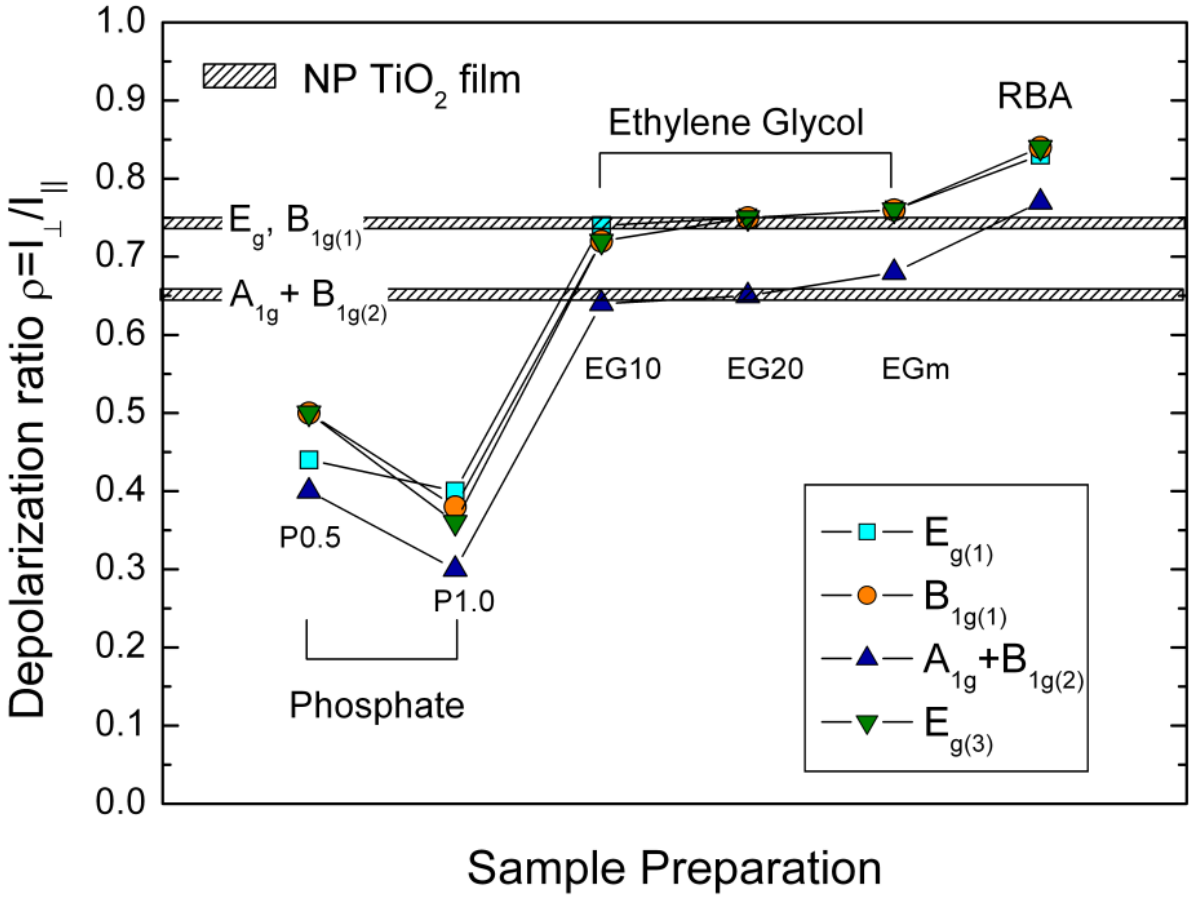

- **Phosphate short (0.5 μm, 1.0 μm) tubes ⇒ Partial crystallographic orientation (occasional highly polarized spectra)**
- **Ethylene glycol + RBA tubes ⇒ Random orientation similar to nanoparticulate films**

LO-TO splitting

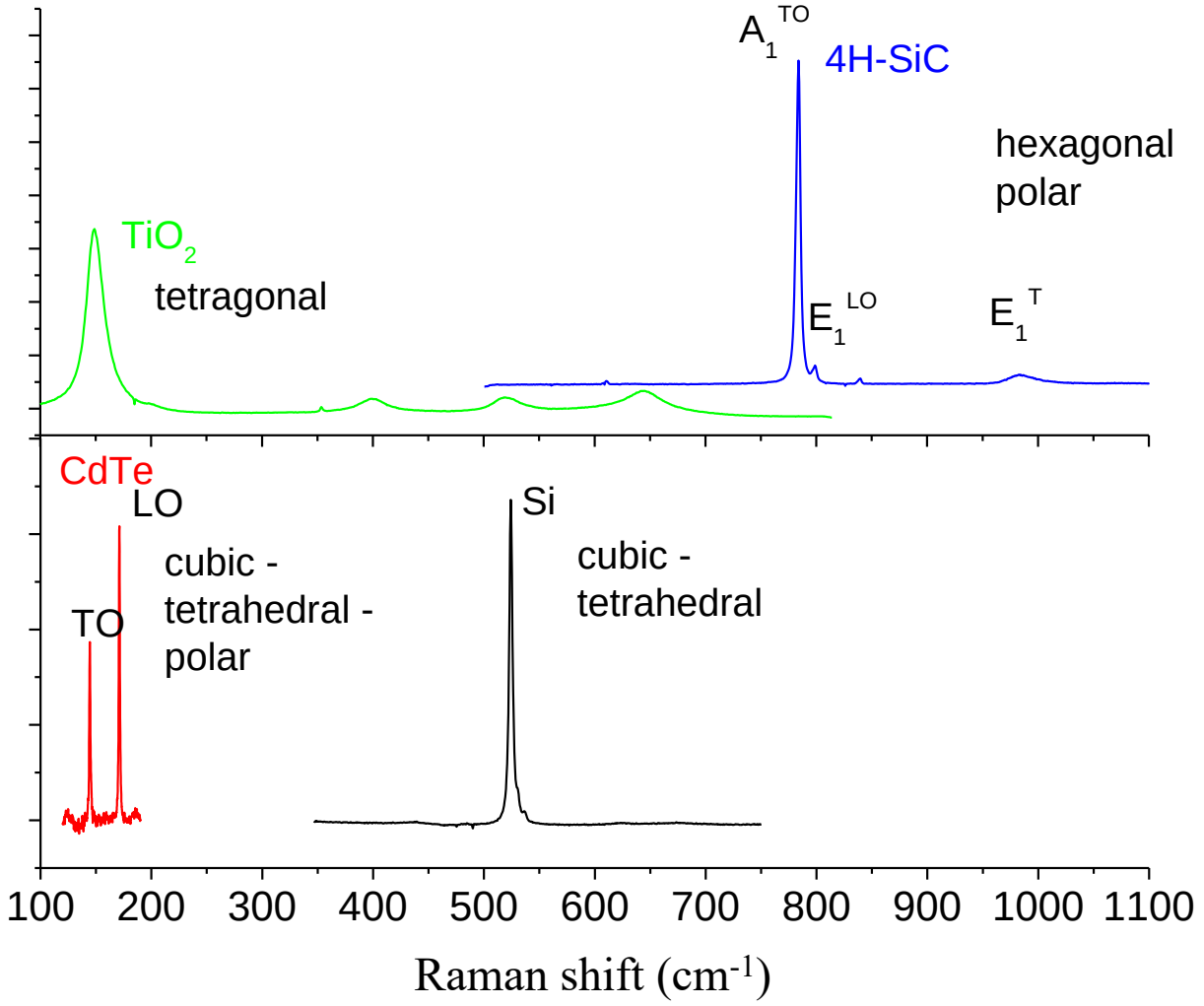

Επιπρόσθετο ηλεκτρικό πεδίο λόγω πολικού /ιοντικού δεσμού στη διαμήκη ταλάντωση (LO: U+E), αντίθετα με την εγκάρσια (TO: U) → ενίσχυση δύναμης επαναφοράς → ω(*LO*) >ω(*TO*)

ΠΕΙΡΑΜΑΤΙΚΕΣ ΤΕΧΝΙΚΕΣ

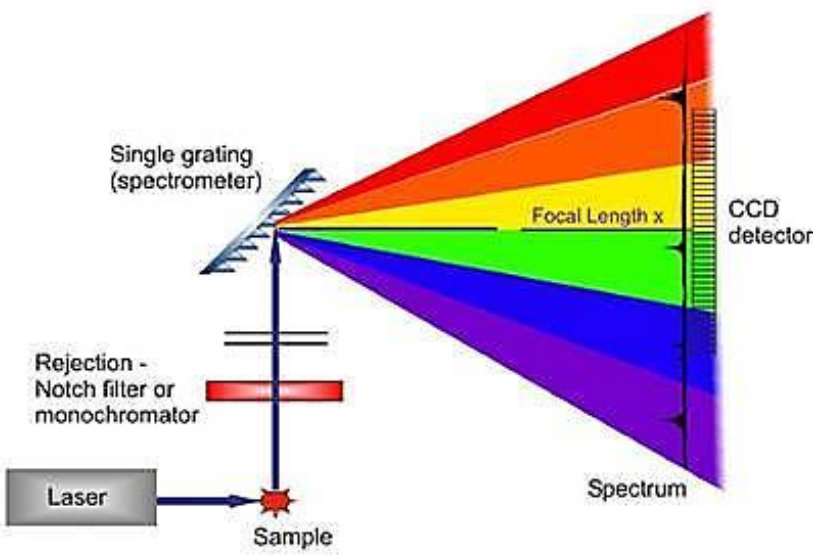

Dispersive Raman spectrometer

- Laser
- Rayleigh Rejection filter
- **Diffraction grating**
- Detector (CCD)

Diffraction grating- spectral resolution proportional to ***grating density*** and **focal length**

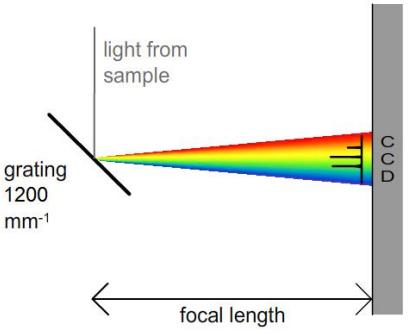

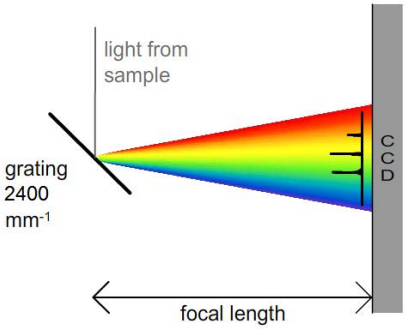

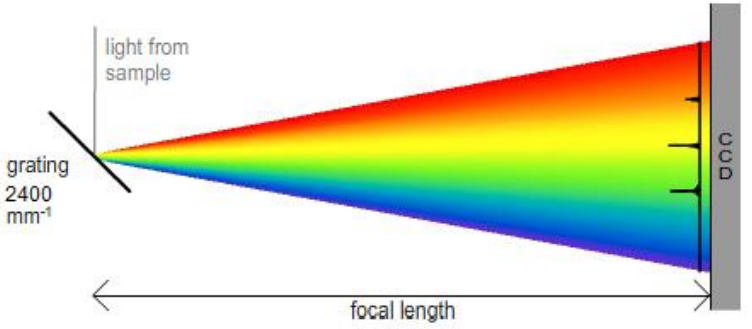

ΠΕΙΡΑΜΑΤΙΚΕΣ ΤΕΧΝΙΚΕΣ

Dispersive Raman spectrometer

Μονοχρωμάτορας Czerny–Turner

Spectral analysis

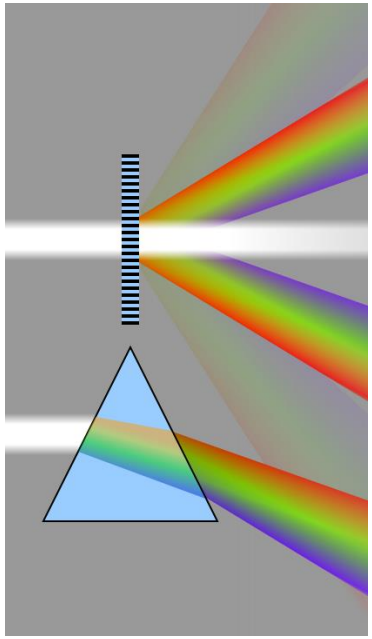

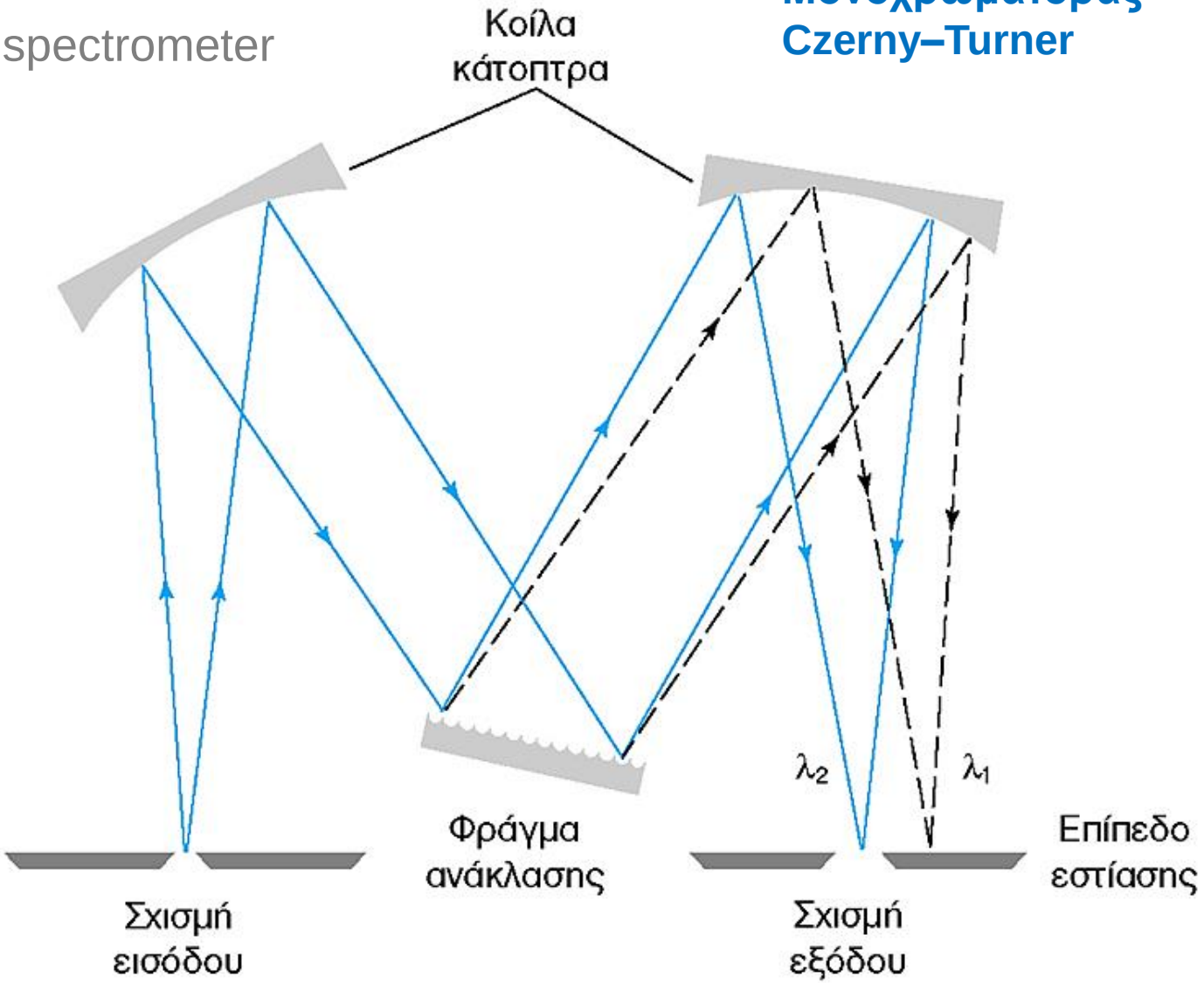

ΠΕΙΡΑΜΑΤΙΚΕΣ ΤΕΧΝΙΚΕΣ

Dispersive Raman spectrometer

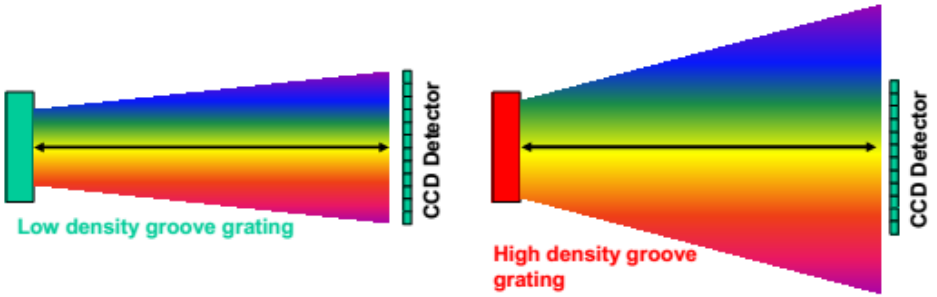

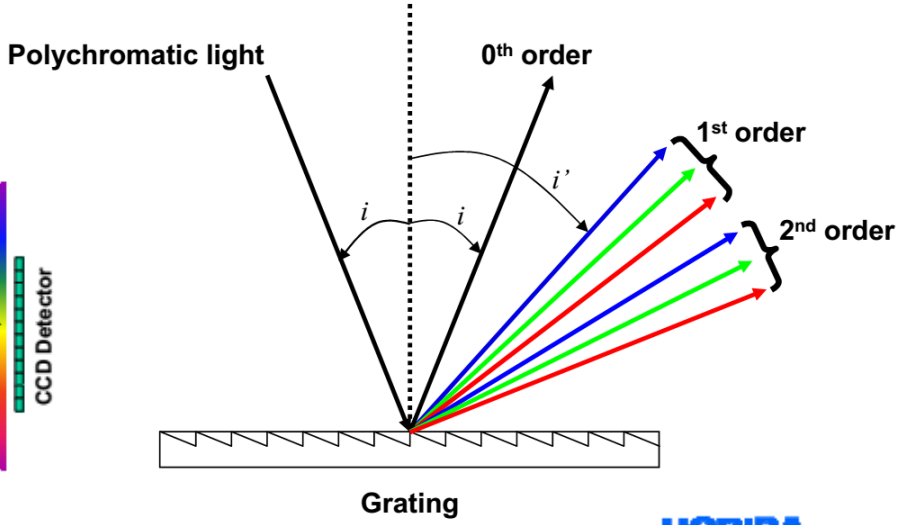

HORIBA Scientific

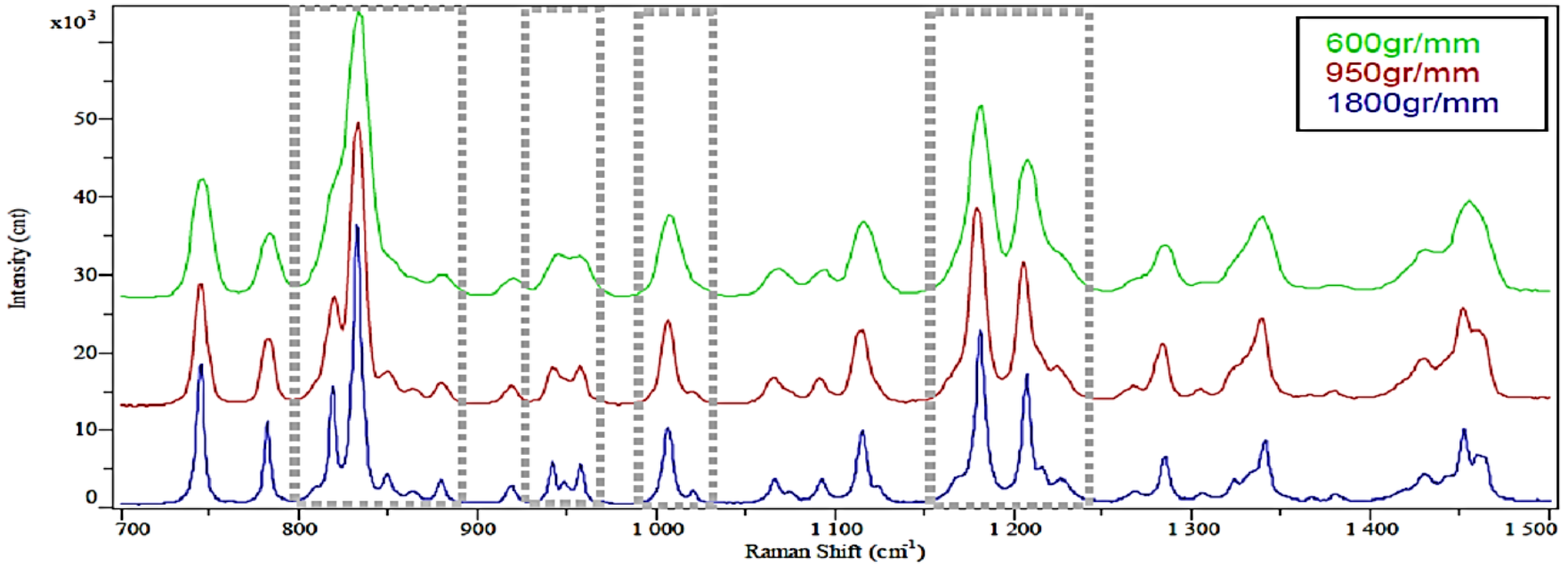

ΠΕΙΡΑΜΑΤΙΚΕΣ ΤΕΧΝΙΚΕΣ

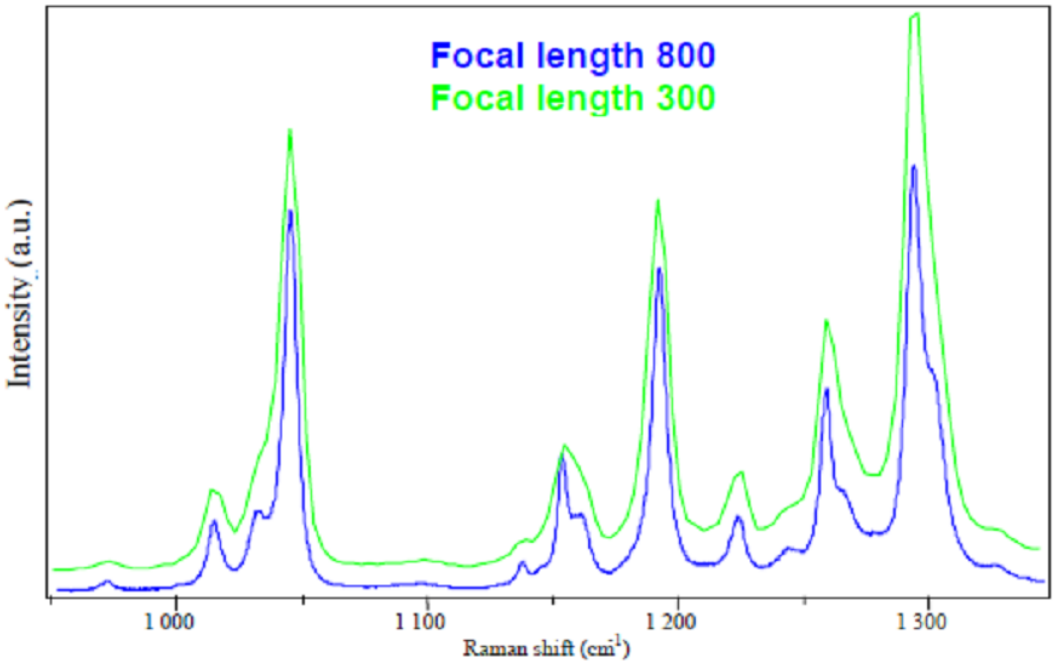

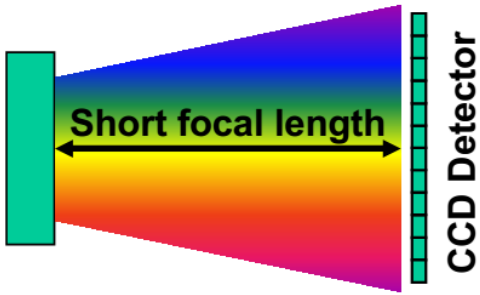

Same grating
Same excitation wavelength

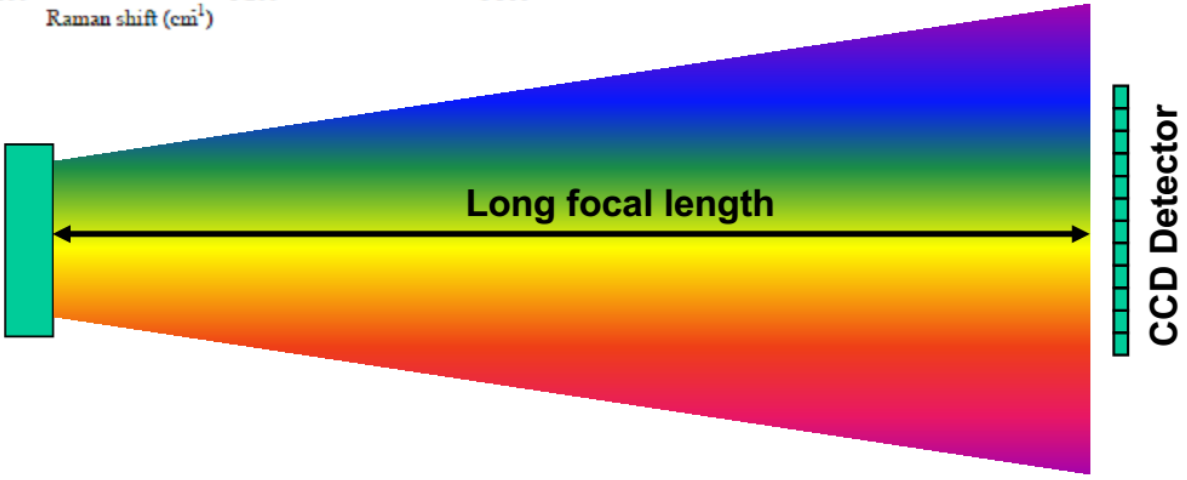

HORIBA Scientific

ΠΕΙΡΑΜΑΤΙΚΕΣ ΤΕΧΝΙΚΕΣ

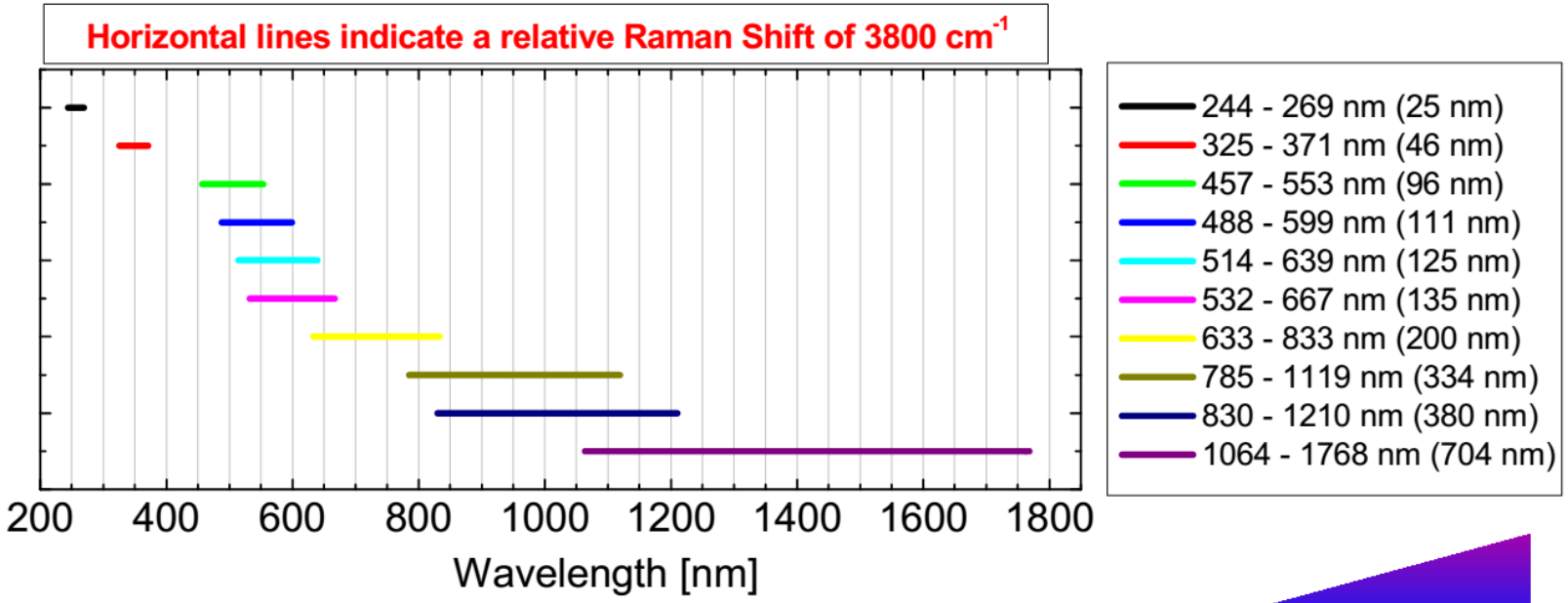

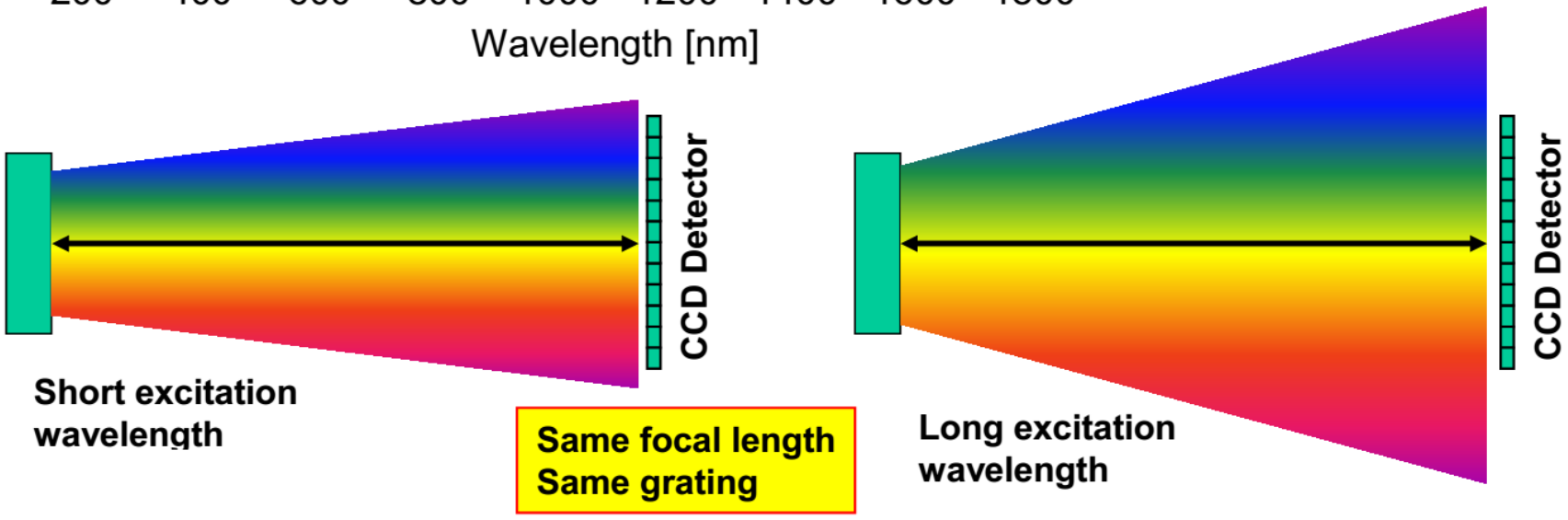

ΠΕΙΡΑΜΑΤΙΚΕΣ ΤΕΧΝΙΚΕΣ

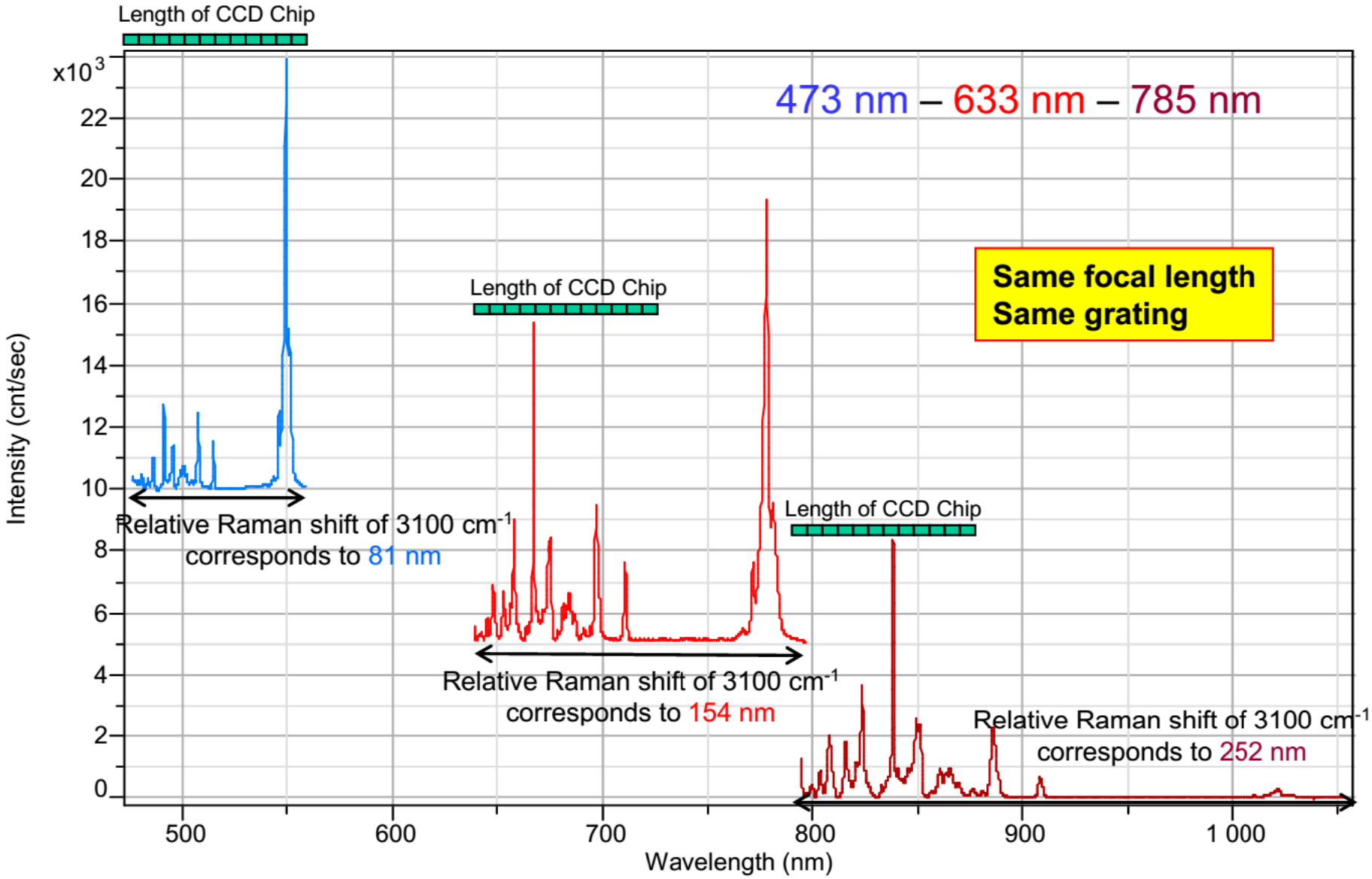

ΠΕΙΡΑΜΑΤΙΚΕΣ ΤΕΧΝΙΚΕΣ

Dispersive Raman spectrometer

Triple spectrometer

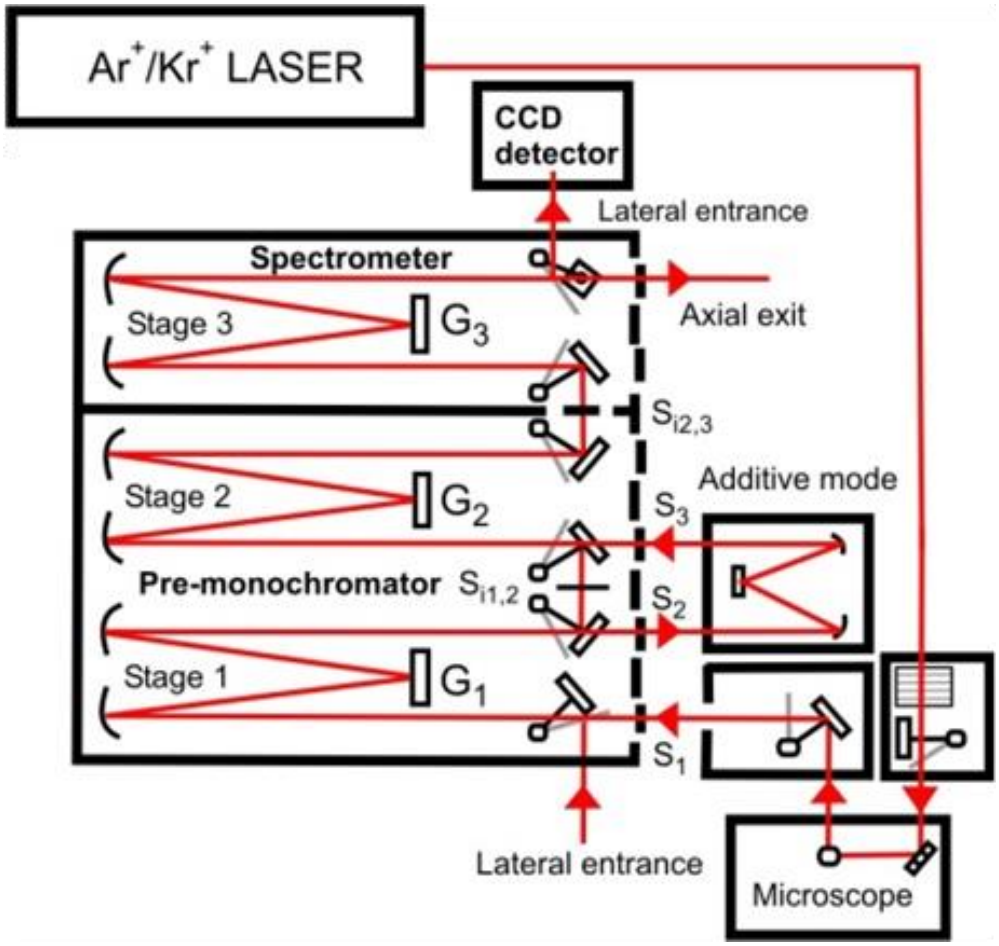

- Laser
- Rayleigh Rejection filter
- **Diffraction grating**
- Detector (CCD)

ΠΕΙΡΑΜΑΤΙΚΕΣ ΤΕΧΝΙΚΕΣ

- **Laser**
- Rayleigh Rejection filter
- Diffraction grating
- Detector (CCD)

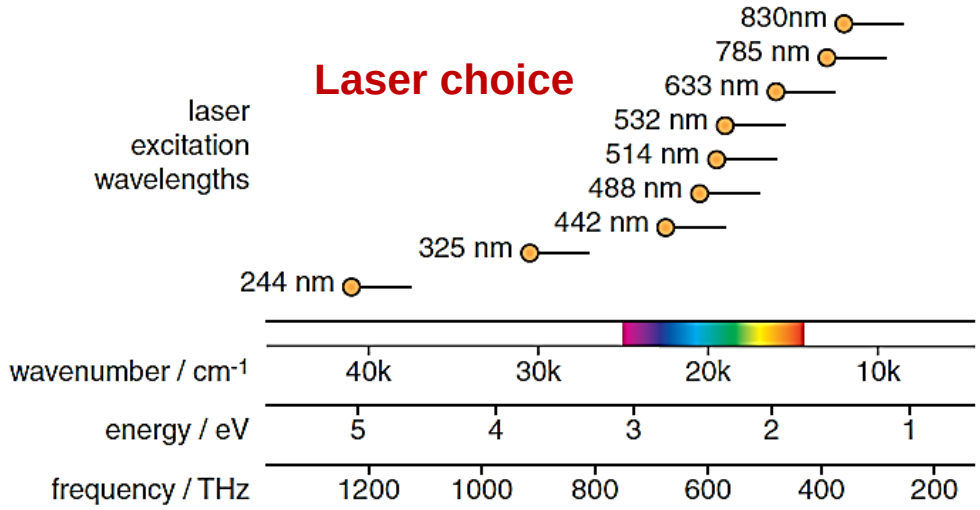

Higher energy ⇒ Higher Raman intensity: $I_{Raman} \sim (\omega_{scattered})^4$ ⇒… Fluorescence!!!

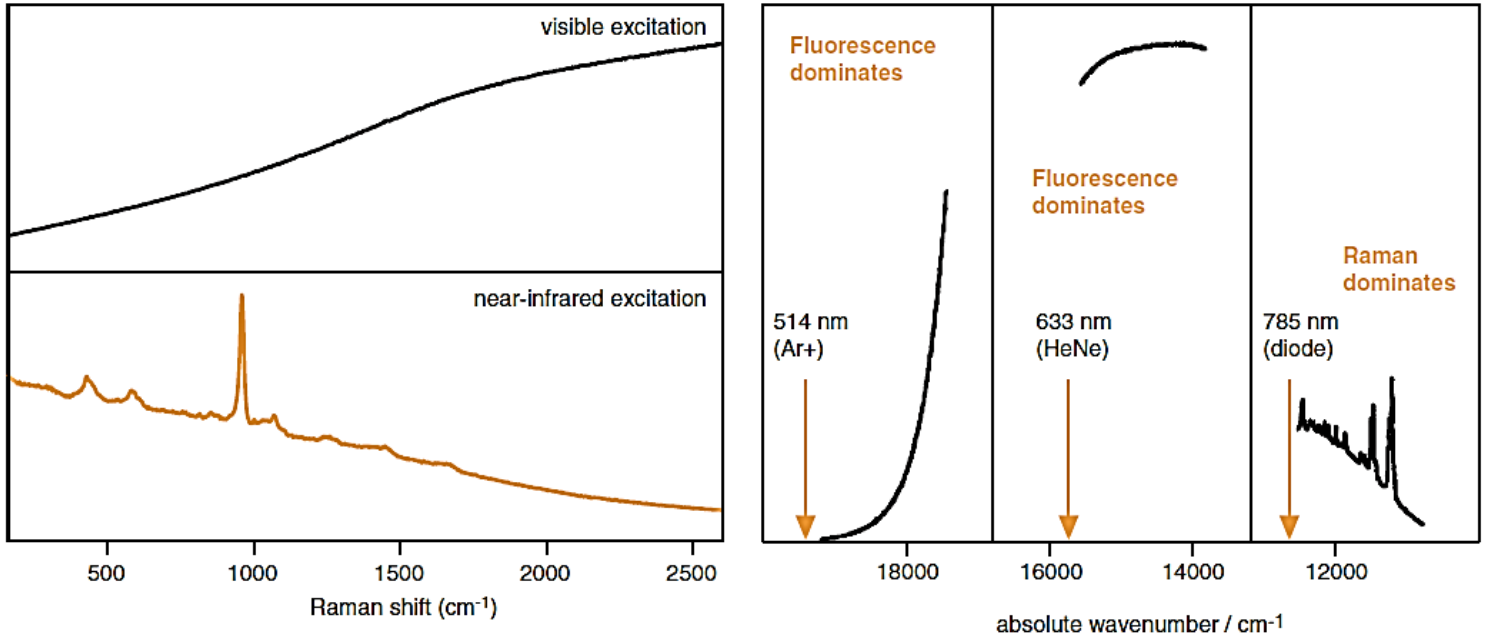

ΠΕΙΡΑΜΑΤΙΚΕΣ ΤΕΧΝΙΚΕΣ

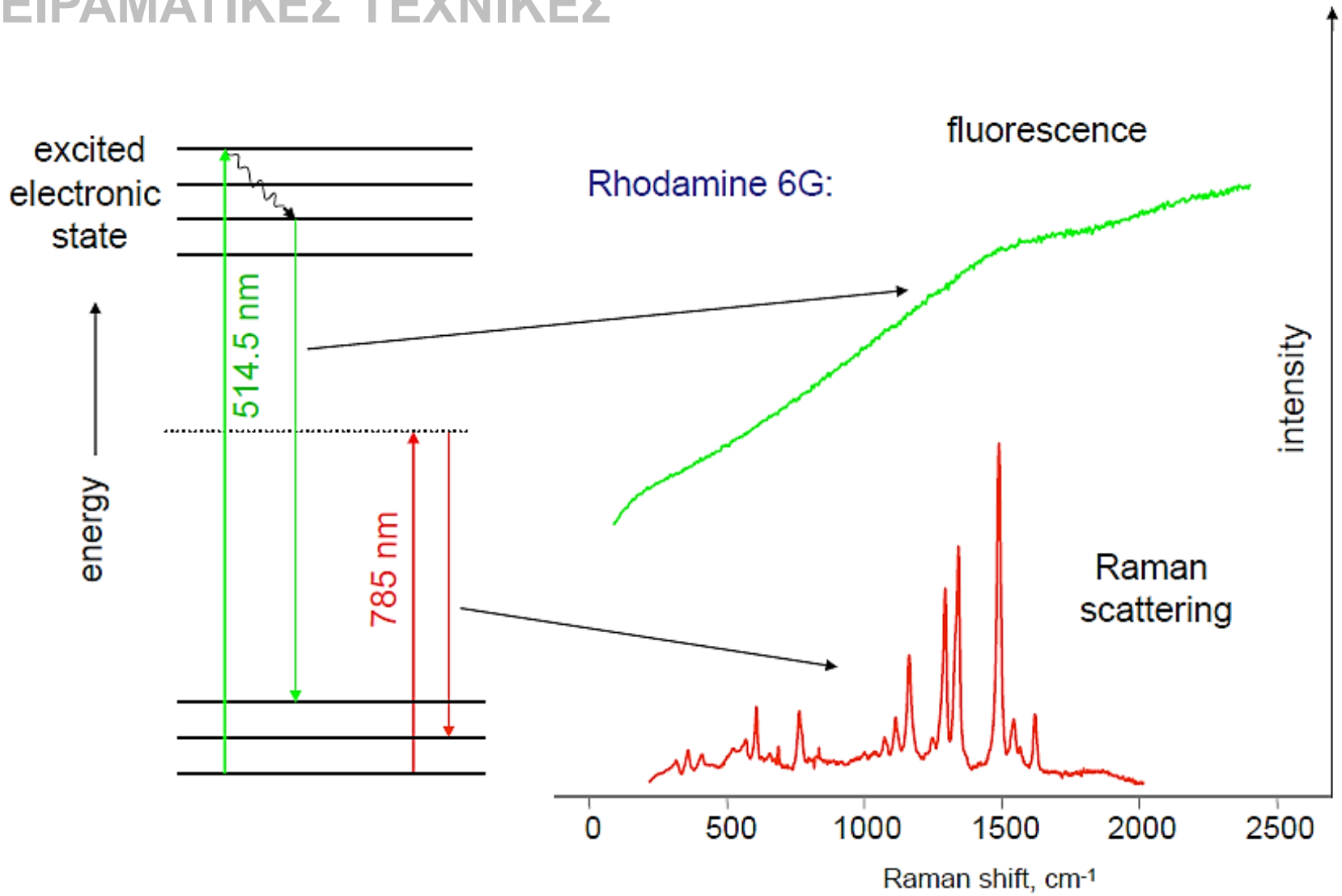

Williamson, Bowling, McCreery, ; *Applied Spectros.* **1989**, *43*, 372
Allred, McCreery, *Applied Spectroscopy* **1990**, *44*, 1229.

ΠΕΙΡΑΜΑΤΙΚΕΣ ΤΕΧΝΙΚΕΣ

- Laser
- **Rayleigh Rejection filter**
- Diffraction grating
- Detector (CCD)

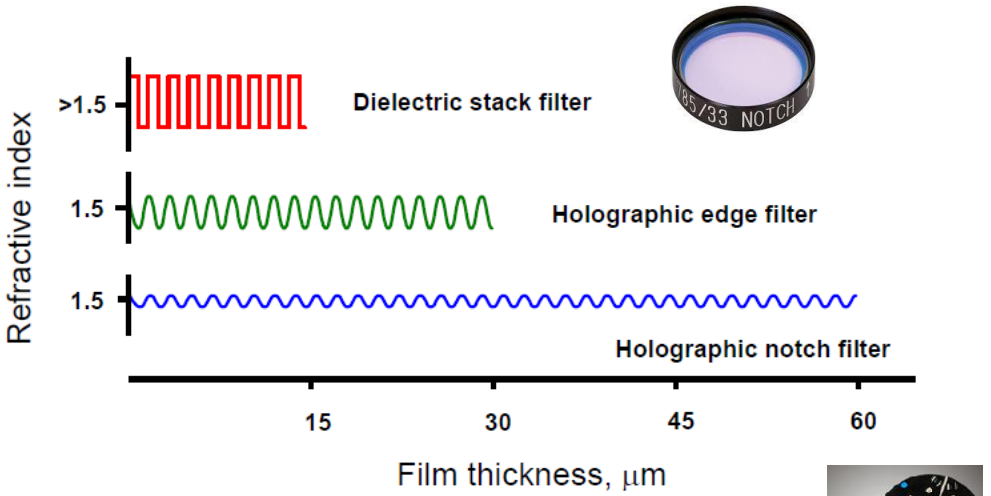

Stokes

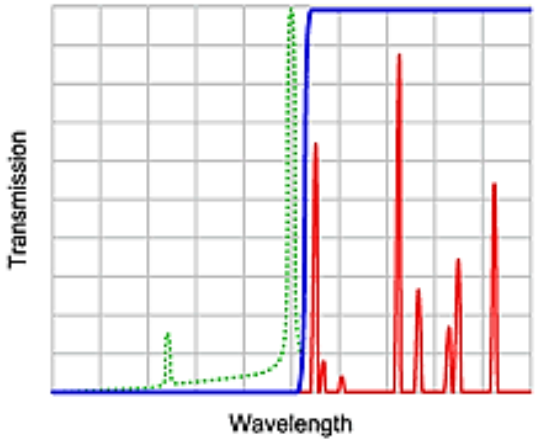

Edge

Stokes and Anti-Stokes

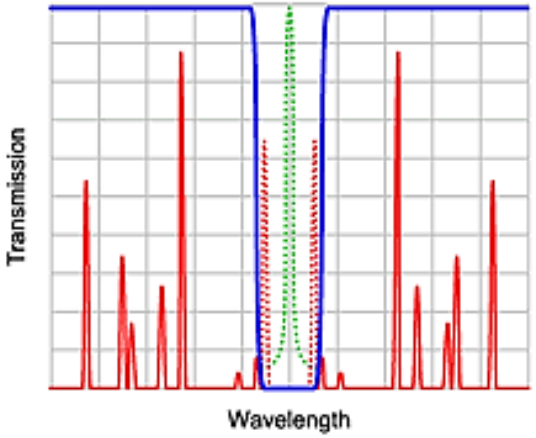

Notch

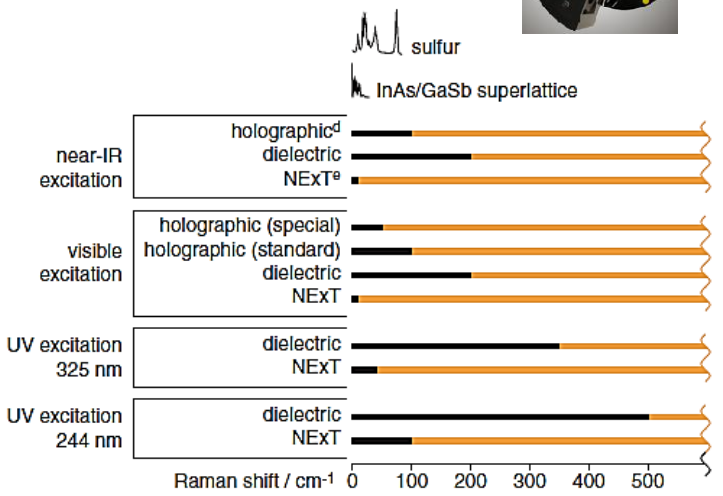

ΠΕΙΡΑΜΑΤΙΚΕΣ ΤΕΧΝΙΚΕΣ

- Laser
- Rayleigh Rejection filter
- Diffraction grating
- **Detector (CCD, PMT)**

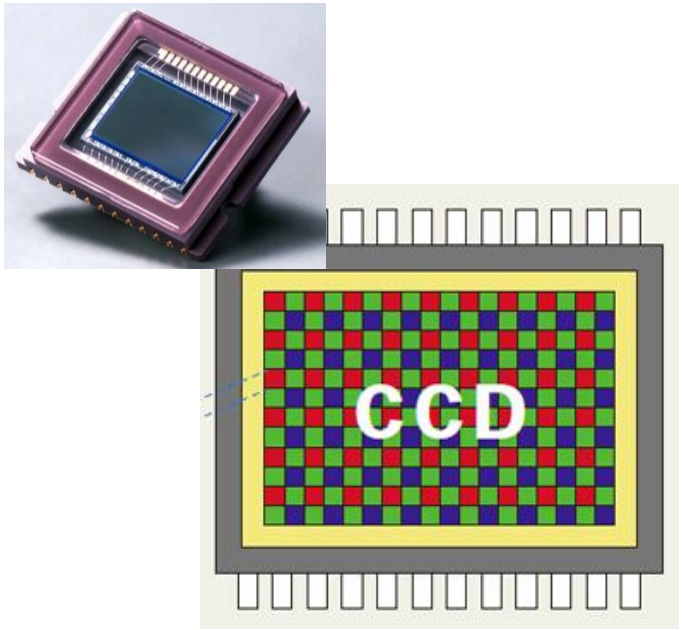

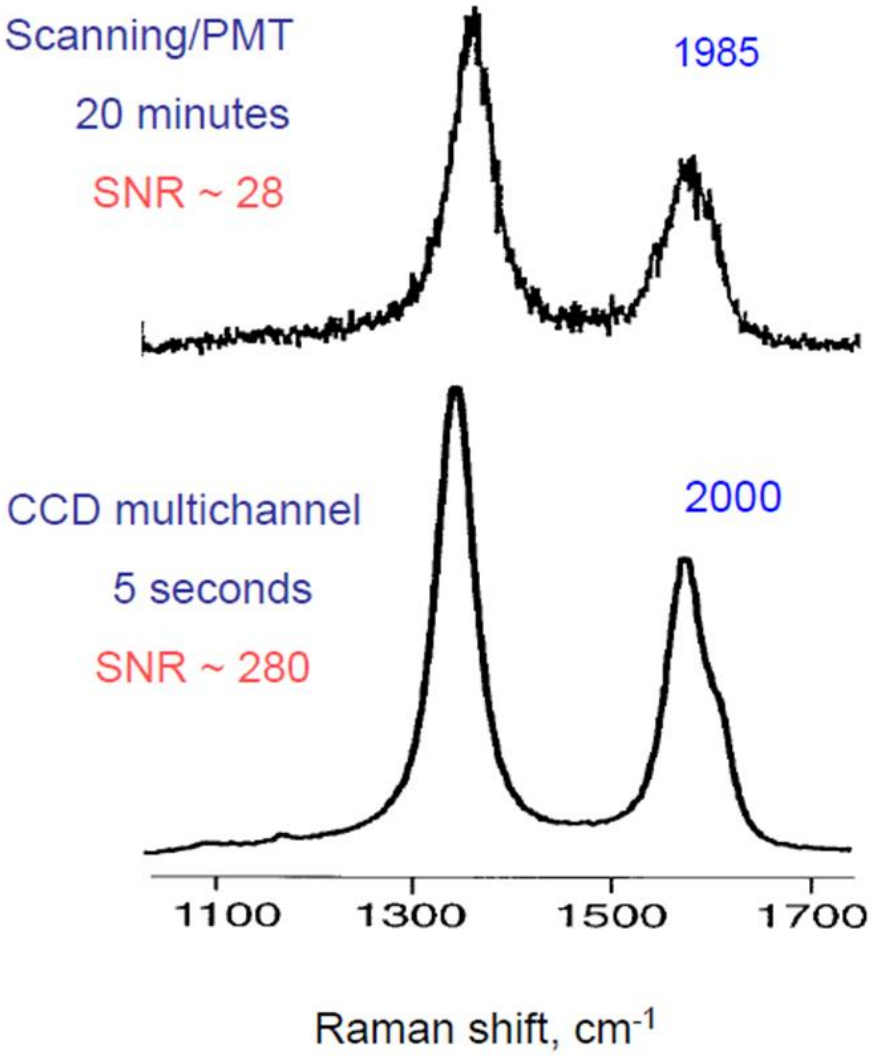

Fourier transform (FT) – infrared (IR) spectrometer

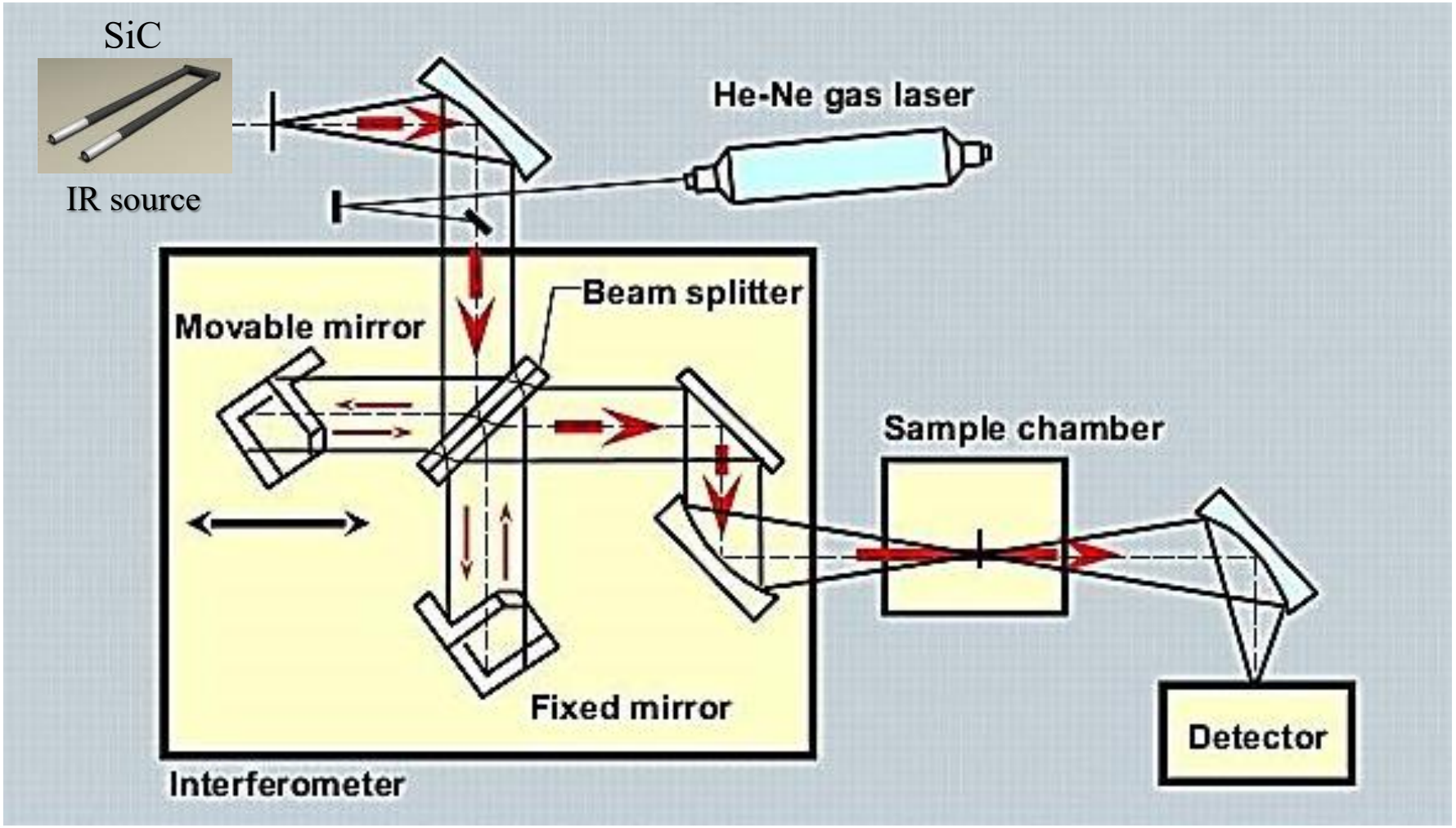

Michelson interferometer

$$I(x) = S(\bar{\nu})\cos(2\pi\bar{\nu}x)$$

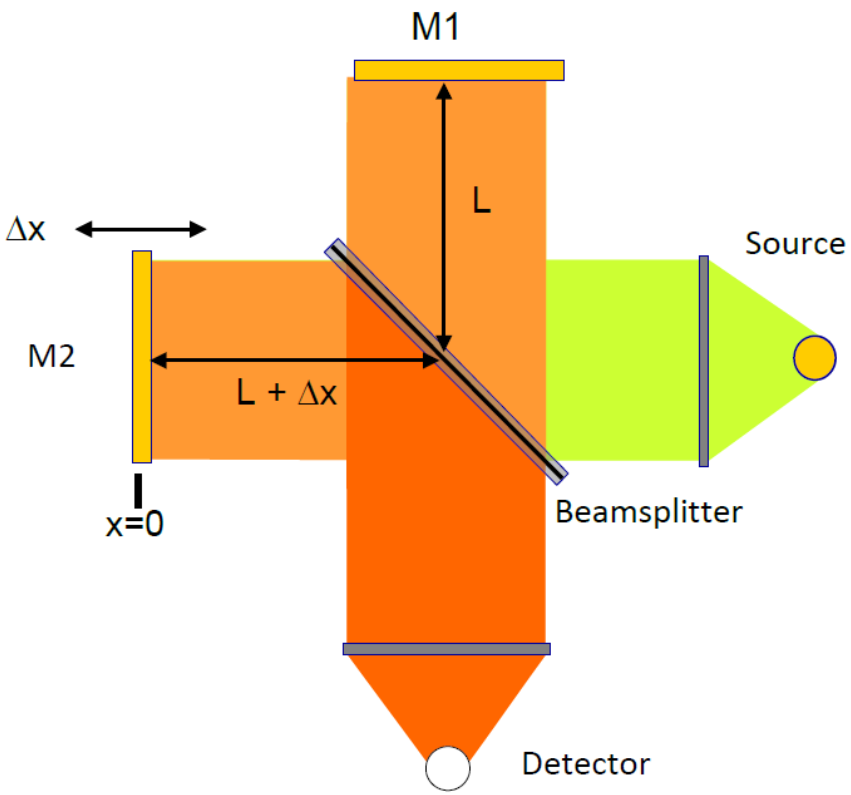

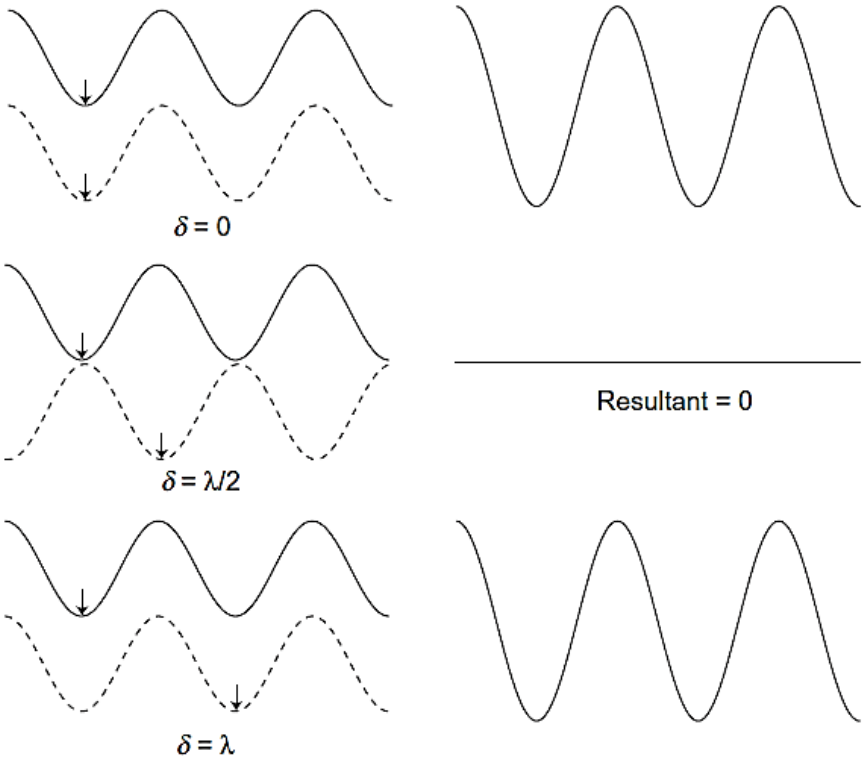

$$2\Delta x = n\lambda \quad (n = 0, 1, 2, 3, \ldots)$$

$$2\Delta x = n\frac{\lambda}{2}, \text{ για } \lambda = 0, 1, 2, 3, \ldots$$

Michelson interferometer

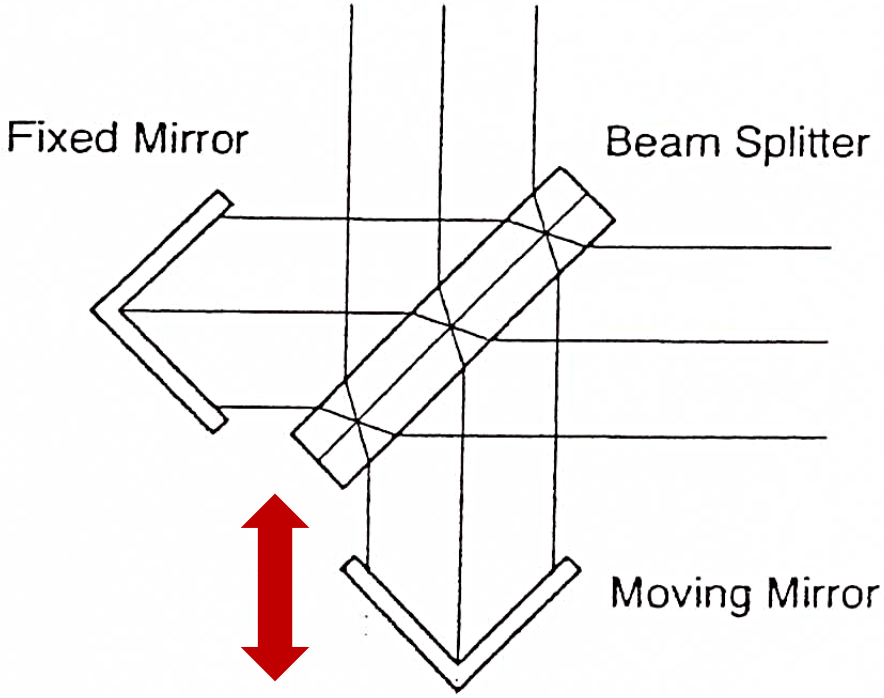

$$2\Delta x = n\lambda \quad (n = 0, 1, 2, 3, \ldots)$$

$$2\Delta x = n\frac{\lambda}{2}, \text{ για } \lambda = 0, 1, 2, 3, \ldots$$

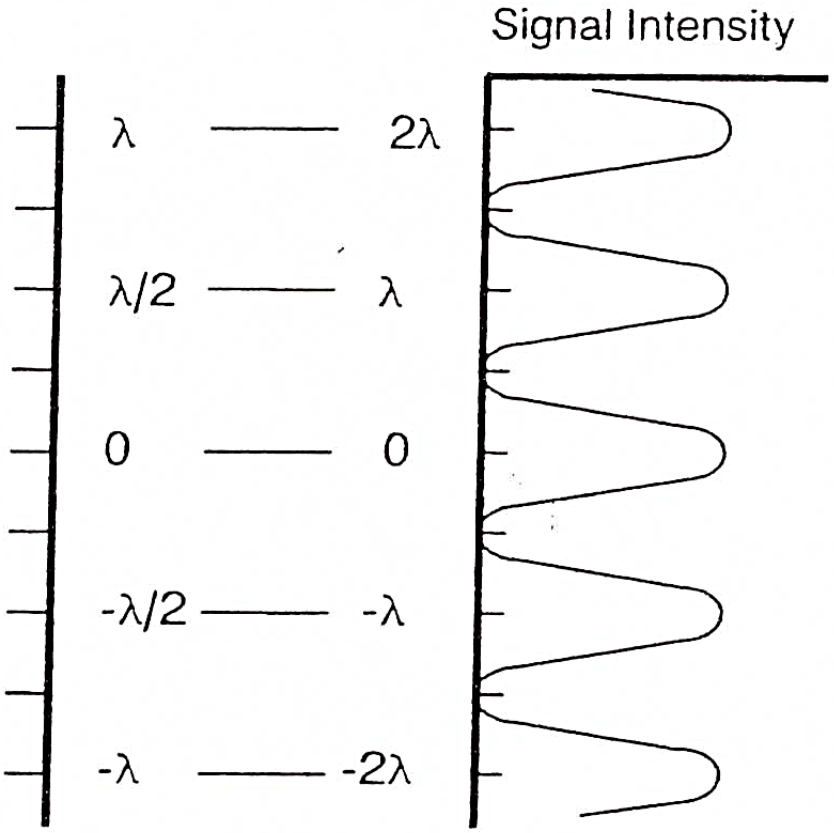

Michelson interferometer

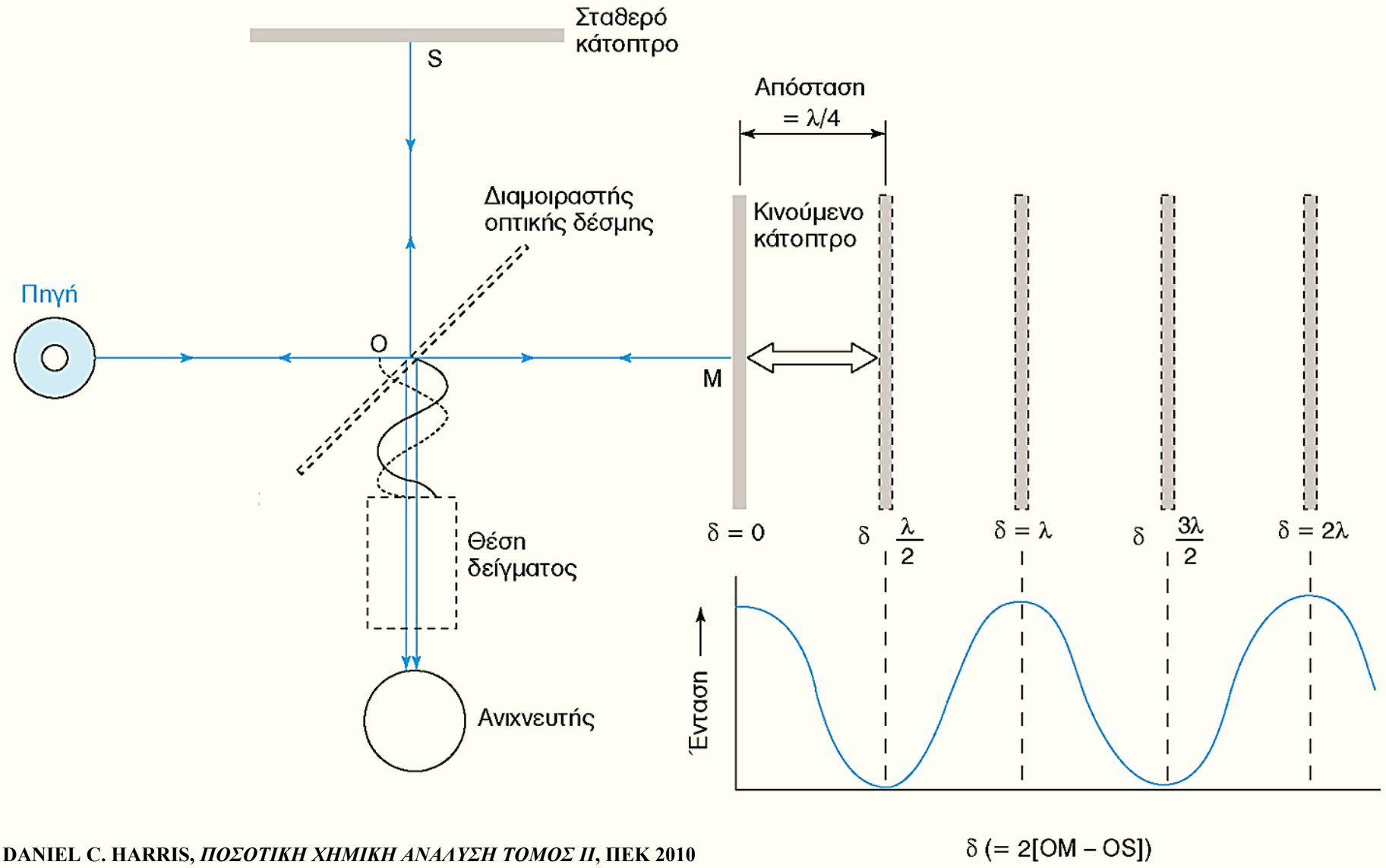

Interferograms

Monochromatic

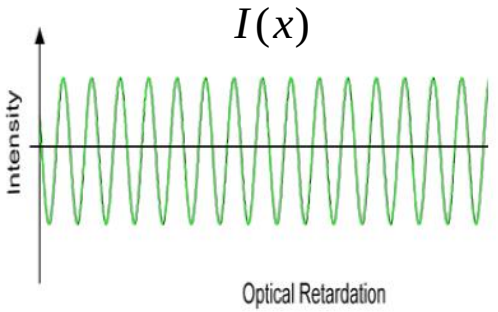

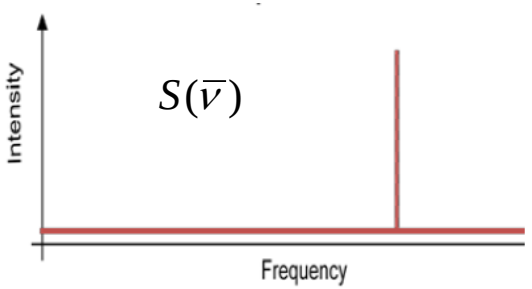

Dichromatic

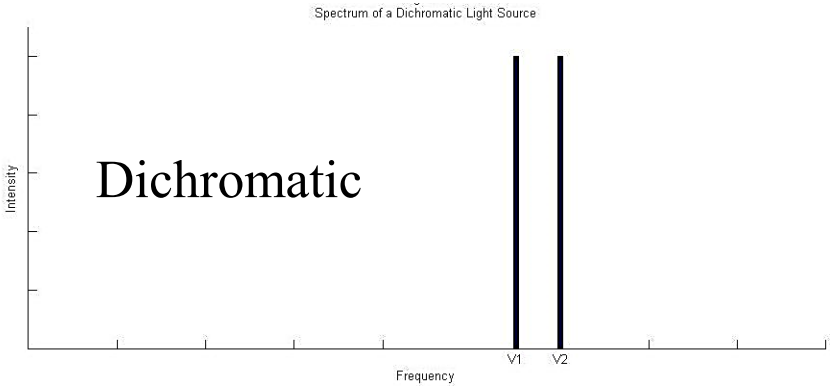

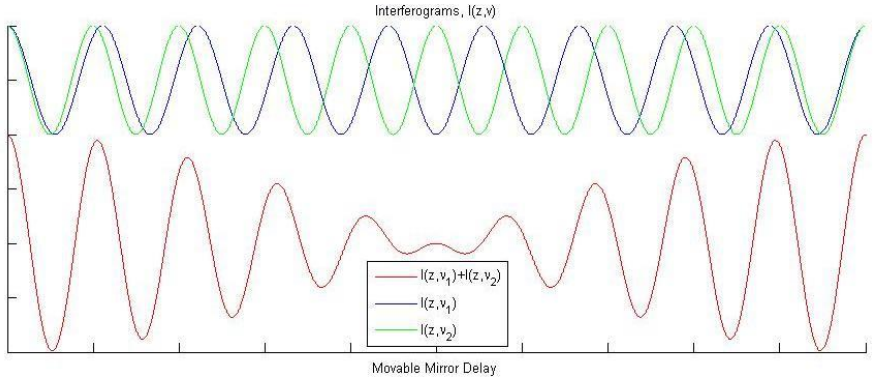

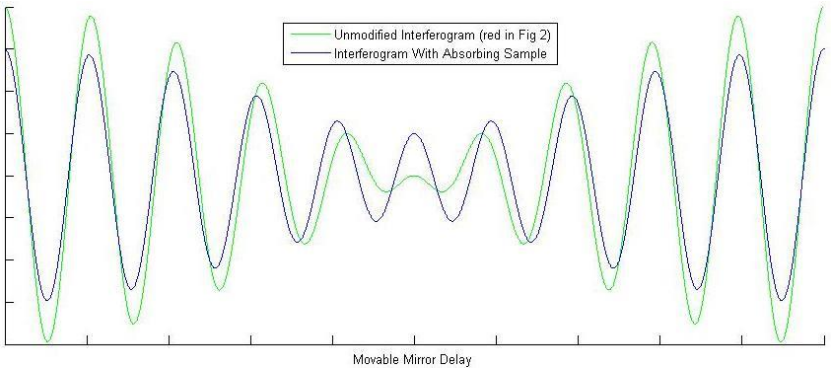

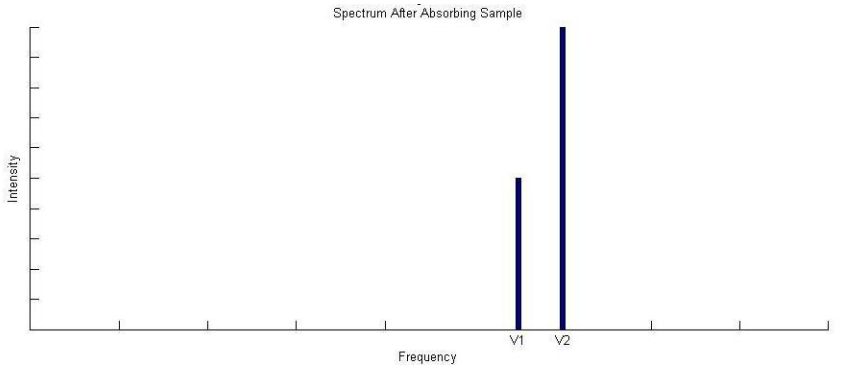

Interferograms

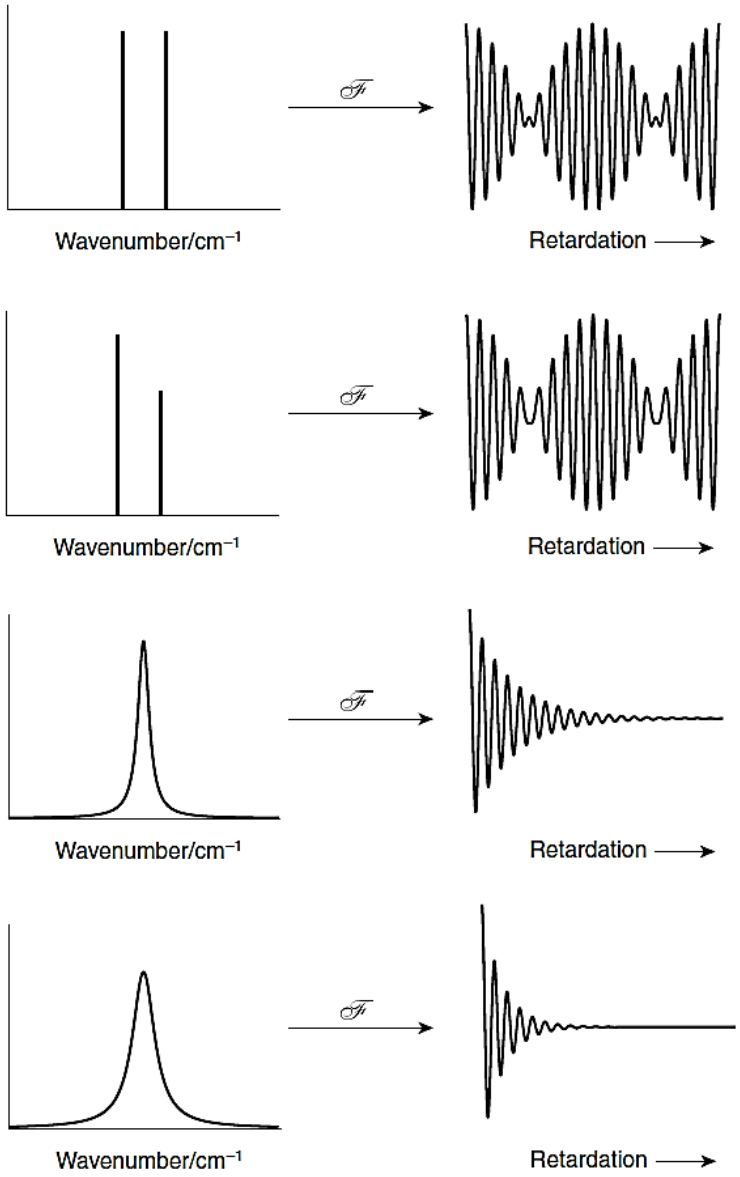

Apodization

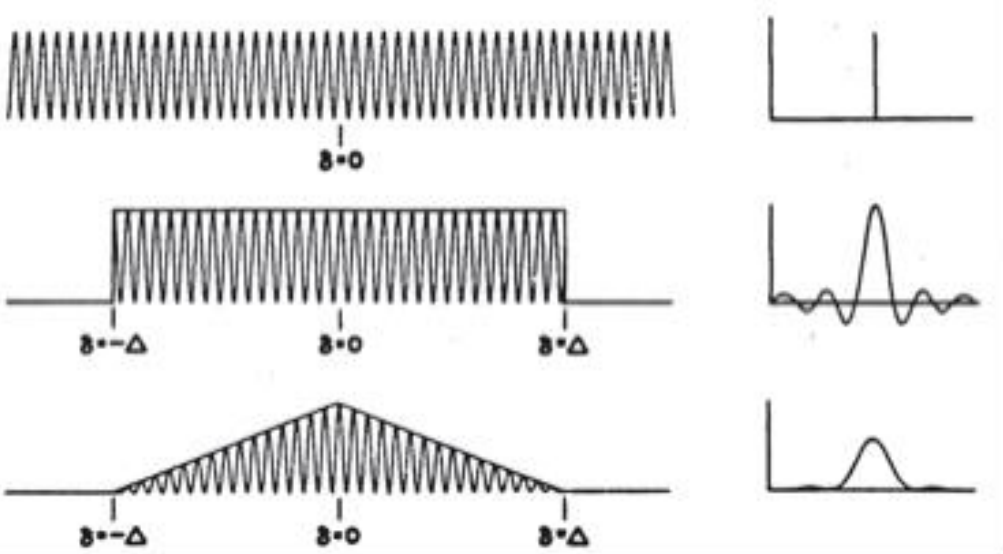

Spectral resolution

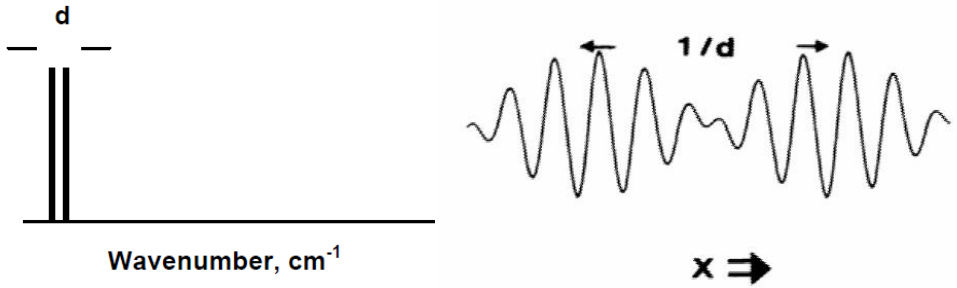

FT-IR spectrum

Υπόβαθρο (αέρας)

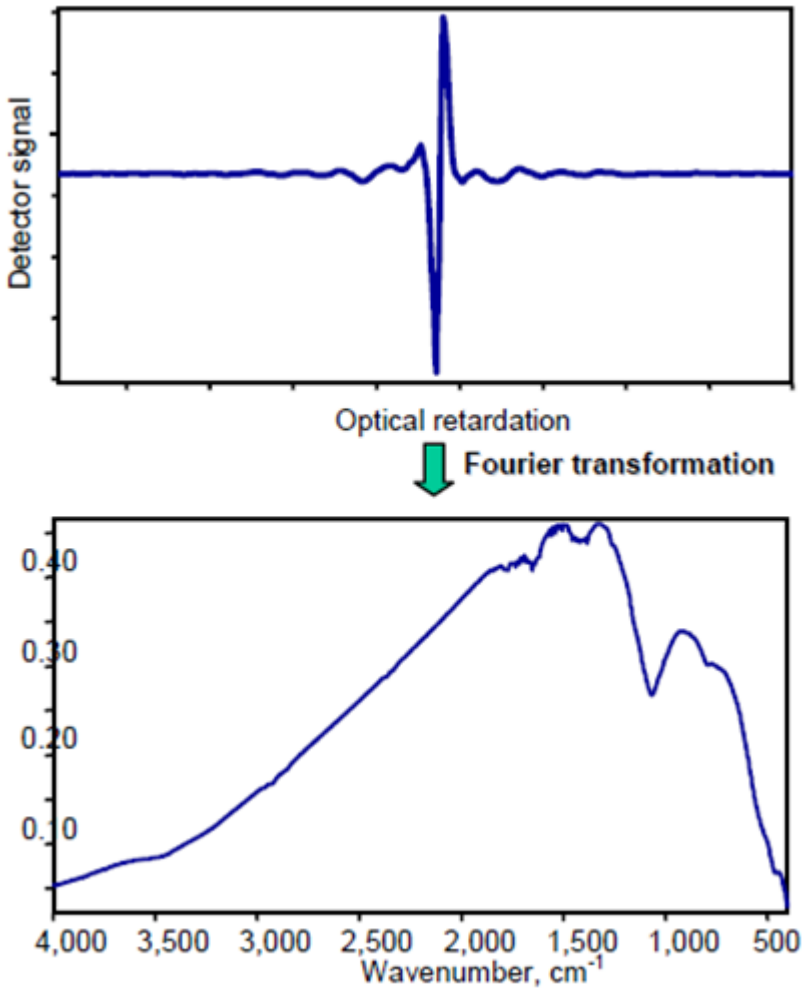

Φάσμα αναφοράς R(ν)

Δείγμα

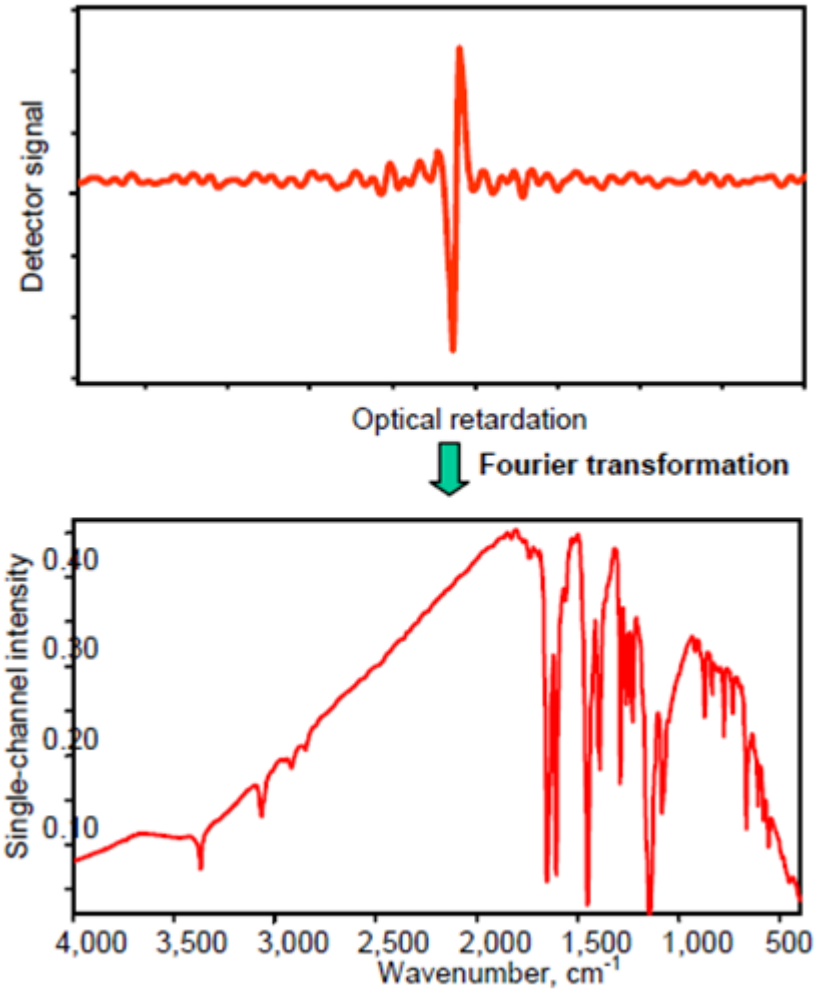

Φάσμα δείγματος S(ν)

FT-IR spectrum

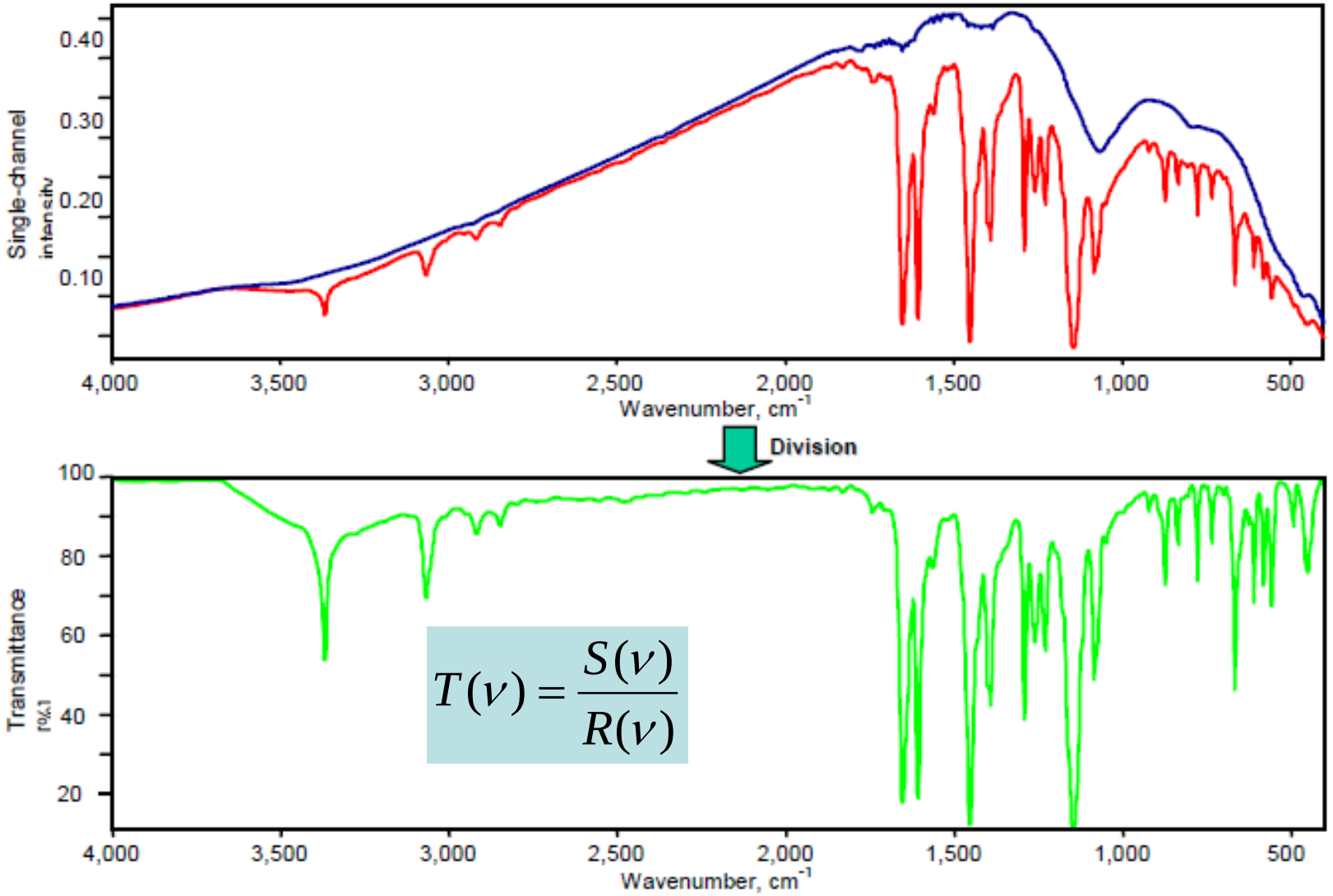

$$T(\nu) = \frac{S(\nu)}{R(\nu)}$$

FT-IR spectrometer

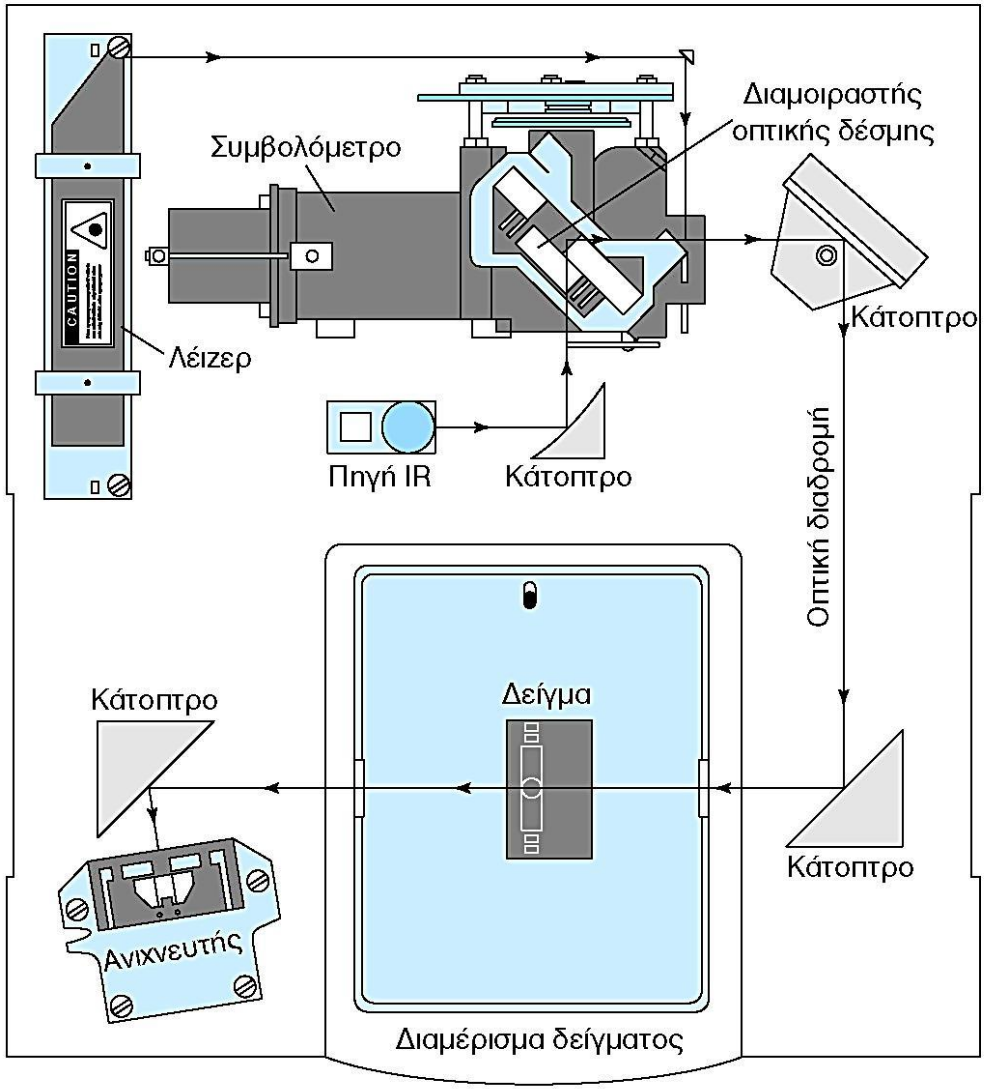

DANIEL C. HARRIS, *ΠΟΣΟΤΙΚΗ ΧΗΜΙΚΗ ΑΝΑΛΥΣΗ ΤΟΜΟΣ ΙΙ*, ΠΕΚ 2010

FT-IR spectrometer

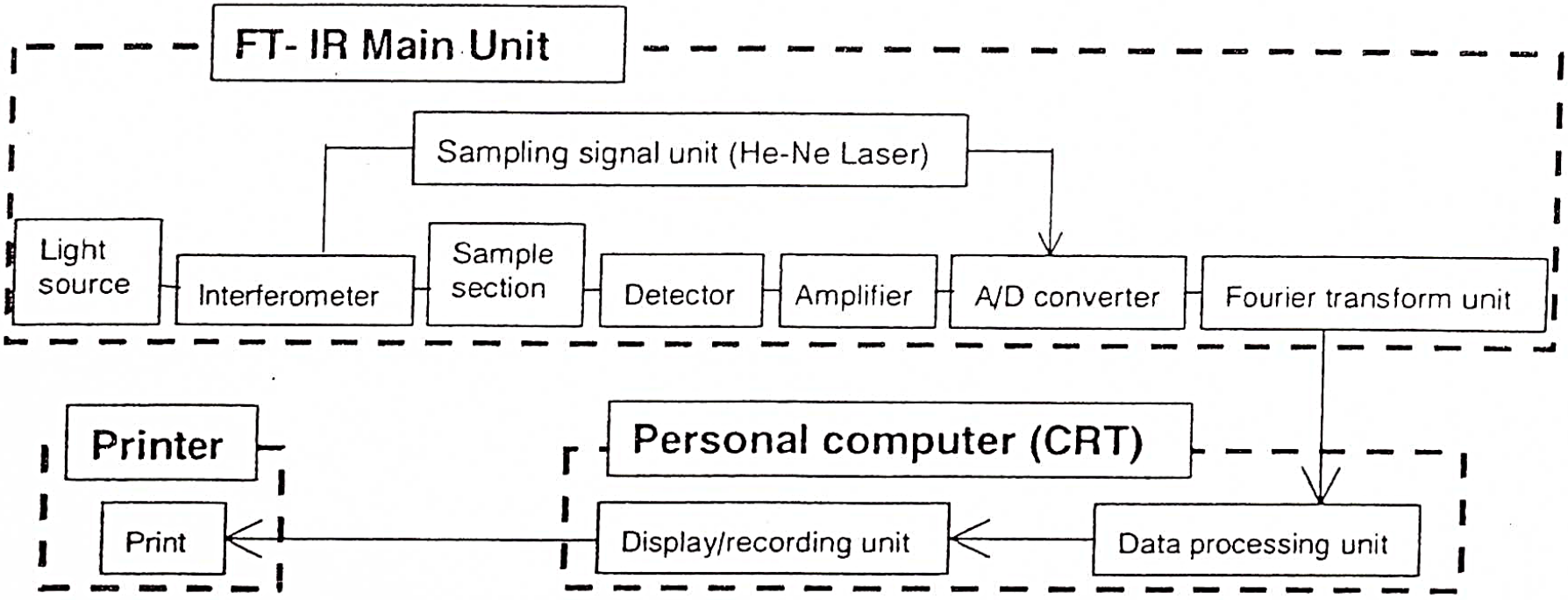

Near Infrared Table

BRUKER

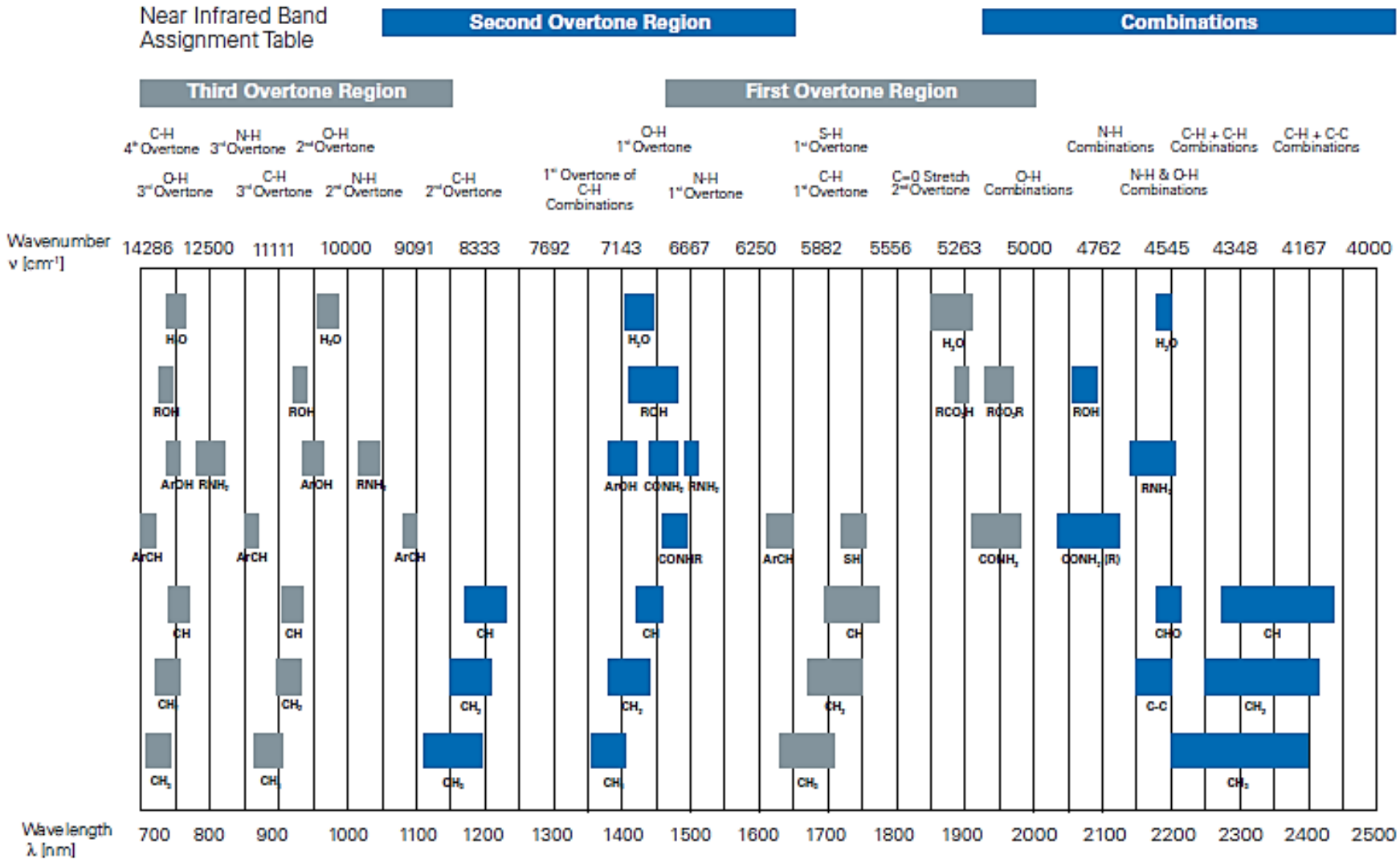

Sources

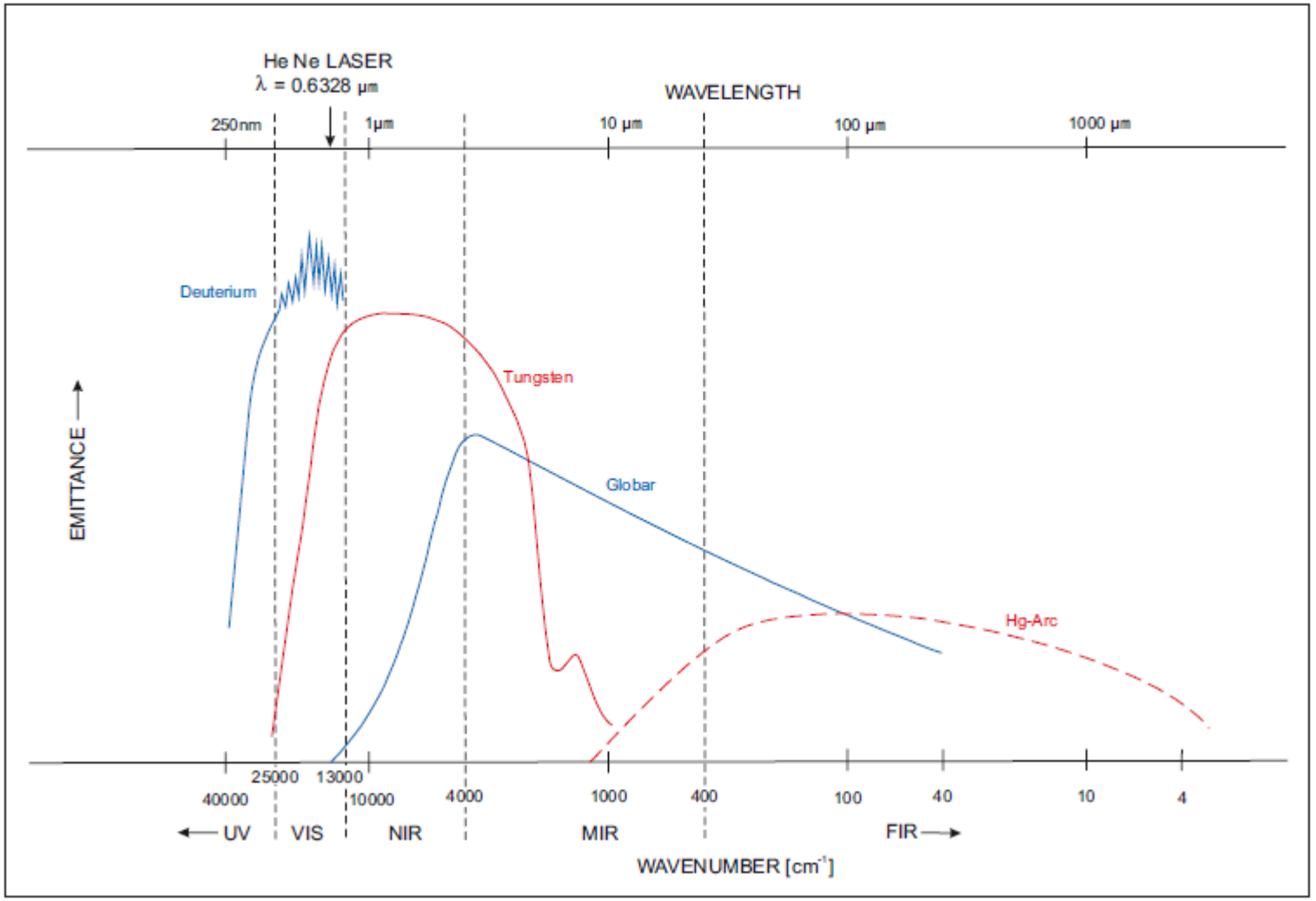
He Ne LASER
λ = 0.6328 μm
WAVELENGTH
250nm
1μm
10 μm
100 μm
1000 μm
Deuterium
Tungsten
Globar
Hg-Arc
EMITTANCE
25000
13000
40000
10000
4000
1000
400
100
40
10
4
UV
VIS
NIR
MIR
FIR
WAVENUMBER [cm-1]

Detectors

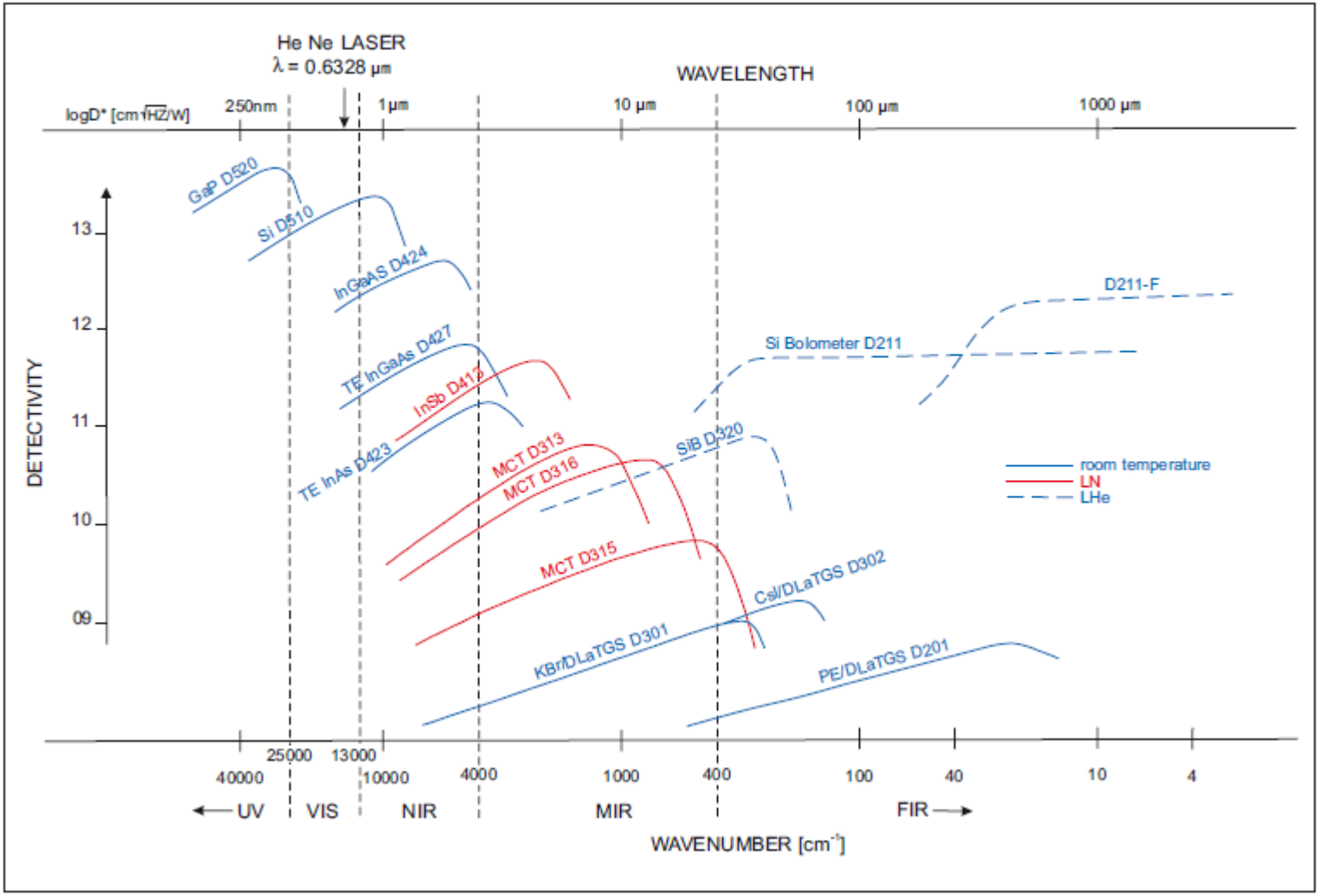
He Ne LASER
λ = 0.6328 µm
WAVELENGTH
logD* [cm√HZ/W]
250nm
1µm
10 µm
100 µm
1000 µm
GaP D520
Si D510
InGaAS D424
TE InGaAs D427
InSb D412
TE InAs D423
MCT D313
MCT D316
MCT D315
SiB D320
Si Bolometer D211
D211-F
room temperature
LN
LHe
CsI/DLaTGS D302
KBr/DLaTGS D301
PE/DLaTGS D201
DETECTIVITY
13
12
11
10
09
25000
13000
40000
10000
4000
1000
400
100
40
10
4
UV
VIS
NIR
MIR
FIR
WAVENUMBER [cm-1]

Beamsplitters

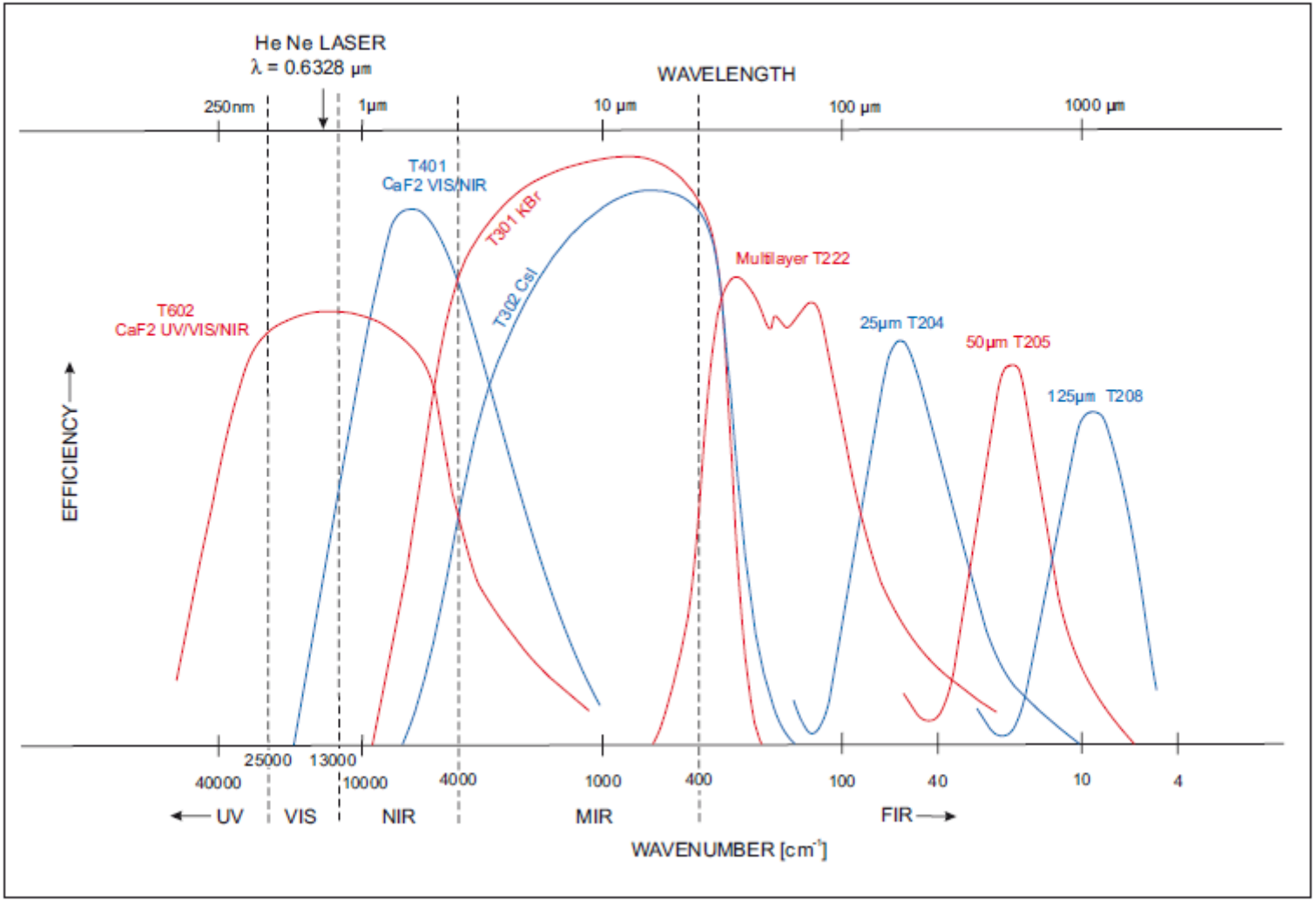

FT-IR reflection techniques

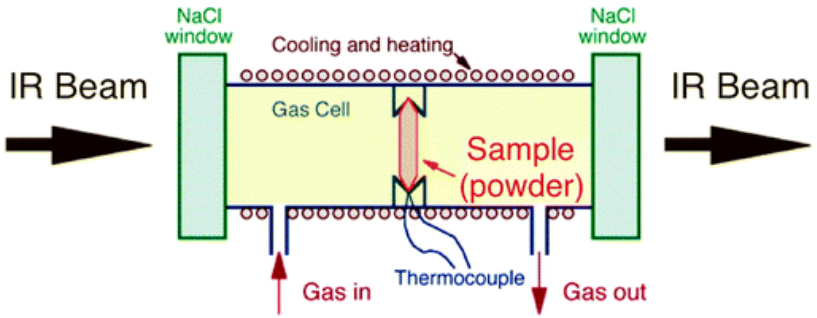

Transmission (TIR)

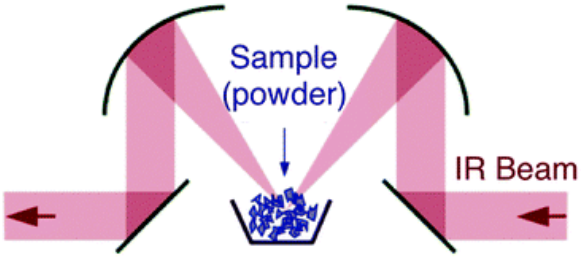

Diffuse-Reflectance (DRIFTS)

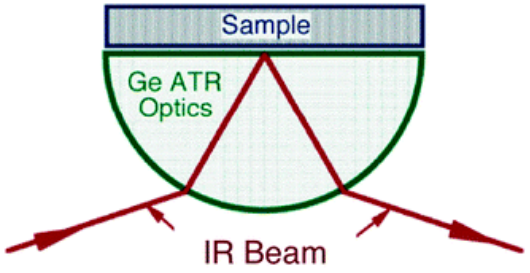

Attenuated Total Reflection (ATR)

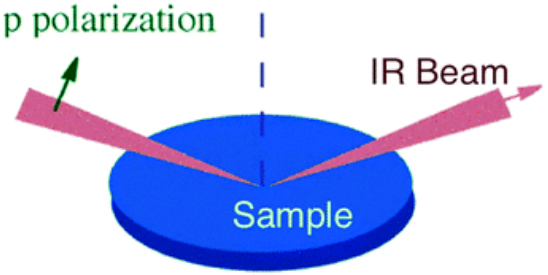

Reflection-Absorption (RAIRS)

Attenuated Total Reflection (ATR

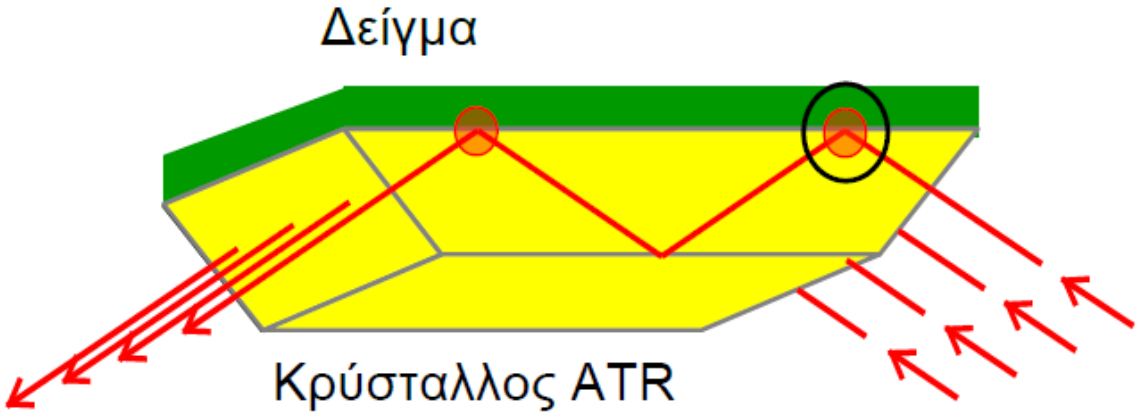

$$\theta_c = \sin^{-1}\left(\frac{n_2}{n_1}\right)$$

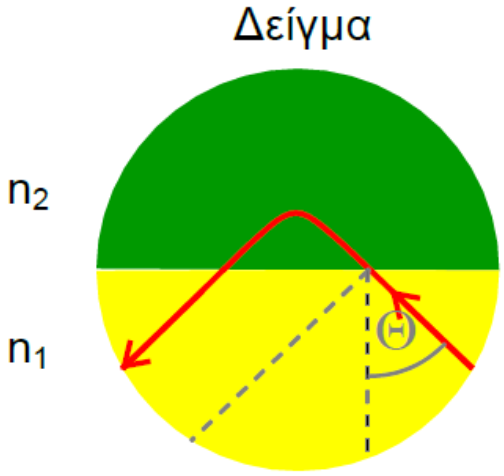

Δείκτης διάθλασης

$n_1 > n_2$

Attenuated Total Reflection (ATR

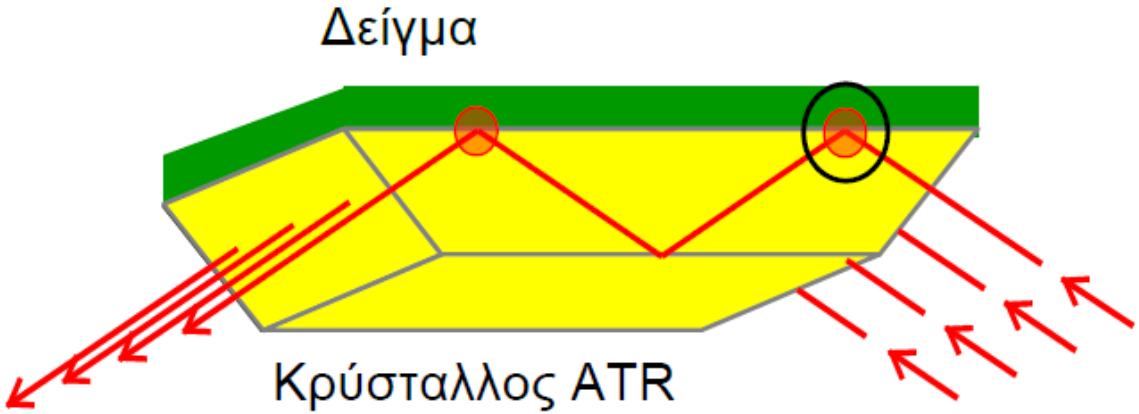

$$d_p = \frac{\lambda}{2\pi n_p (\sin^2\theta - n_{sp}^2)^{1/2}}$$

Material	Refr. Index	Depth of Penetration (μ)
ZnSe	2.4	1.66
AMTIR	2.5	1.46
Ge	4.0	0.65
Si	3.4	0.84
KRS-5	2.37	1.73

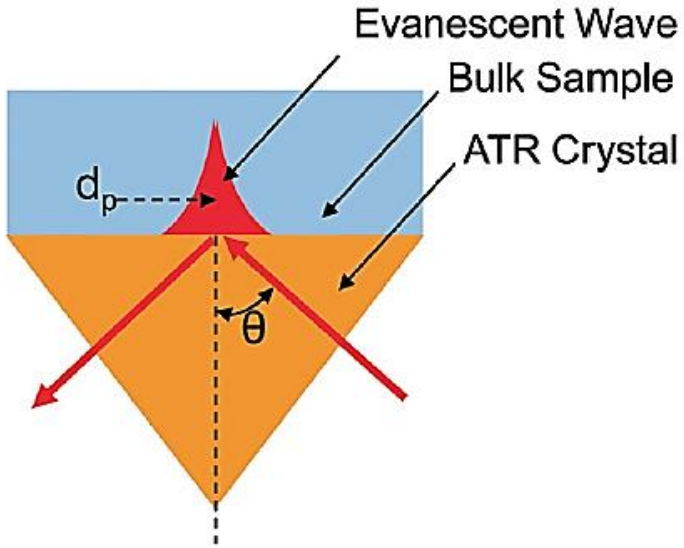

Attenuated Total Reflection (ATR

Material	Refractive Index at 1000 cm^{-1}	Spectral Range (cm^{-1})	Safe pH
Zinc Selenide	2.4	20000-630	5-9
AMTIR (As/Se/Ge)	2.5	11000-630	1-9
Germanium	4.0	5500-780	1-14
Silicon	3.4	8300-1500	1-12
KRS-5	2.37	17900-400	5-8

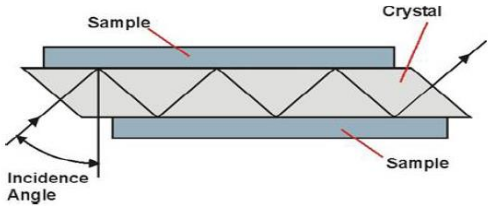

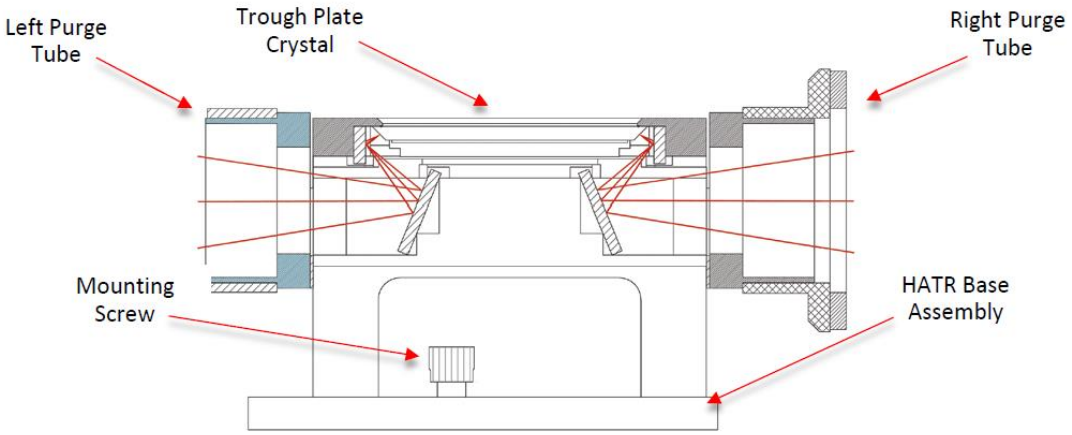

FT-Raman spectrometer

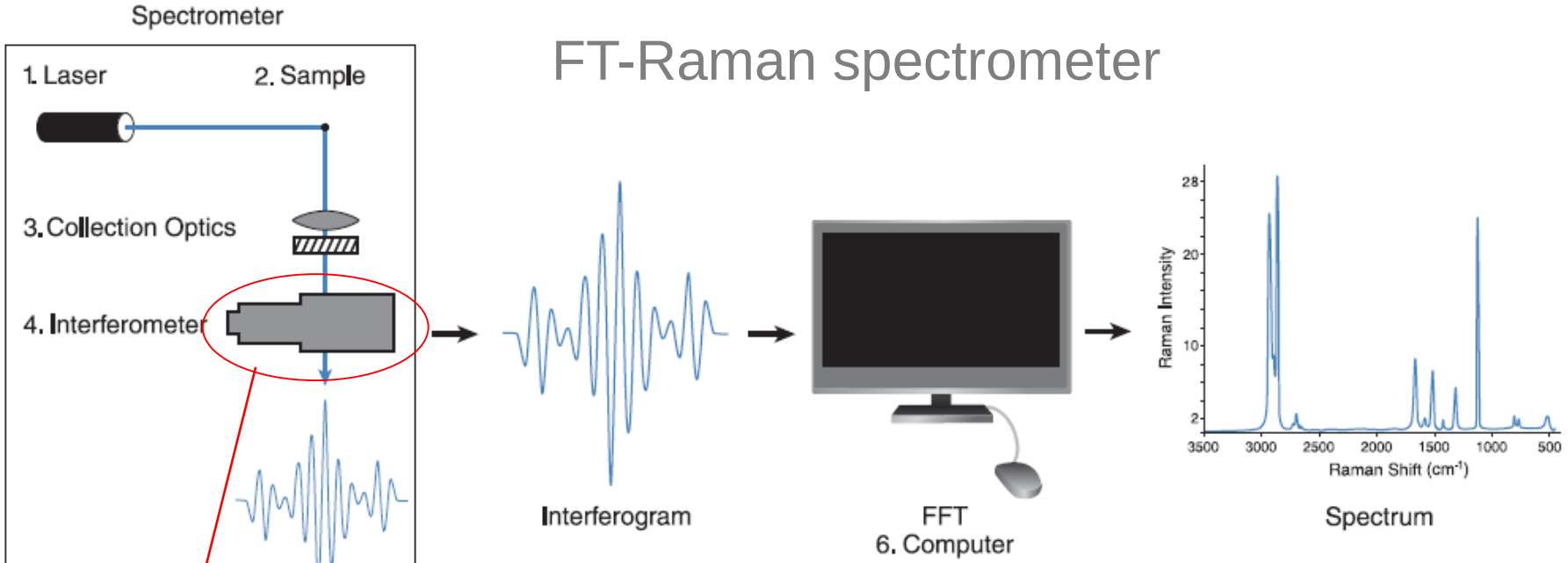

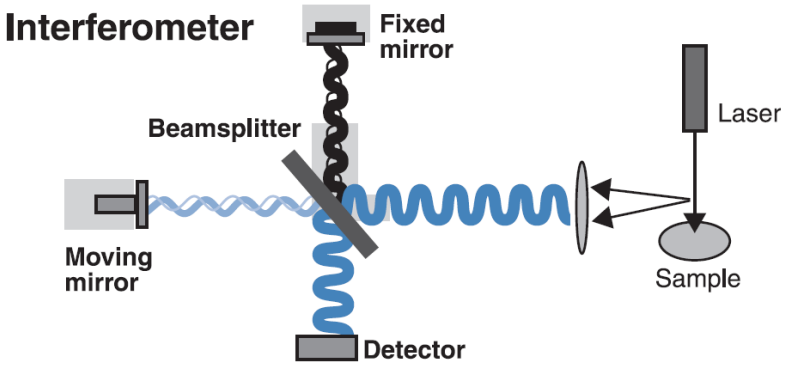

Feature	Dispersive	(FT-Raman)
Available Wavelength	<200nm to 850nm	1064nm
Fluorescence	More fluorescence (Except UV)	Better fluorescence avoidance
Detector	CCD	Ge or GaAs
Best Spectral Resolution	Typically 1-4 cm^{-1}	~0.5cm^{-1}

FT-Raman disadvantages

Three classes of compound prove intractable to FT-Raman analysis:

- **Aqueous phase samples.** These may strongly absorb both the exciting laser radiation and the Raman scattered light
- **Samples at elevated temperatures.** Above 250 °C intense black body emission can mask the Raman signal
- **Black samples.** These can strongly absorb, heat up, and produce intense background emission, or even degrade

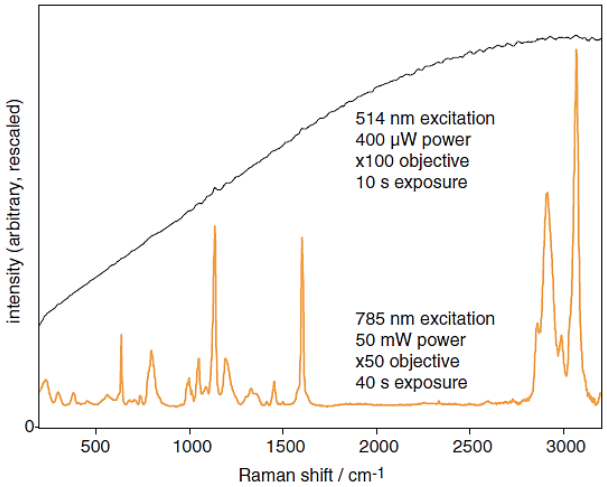

Raman spectra of
poly(sodium 4-styrenesulfonate)
(514 nm and 785 nm excitation, 50x objective)

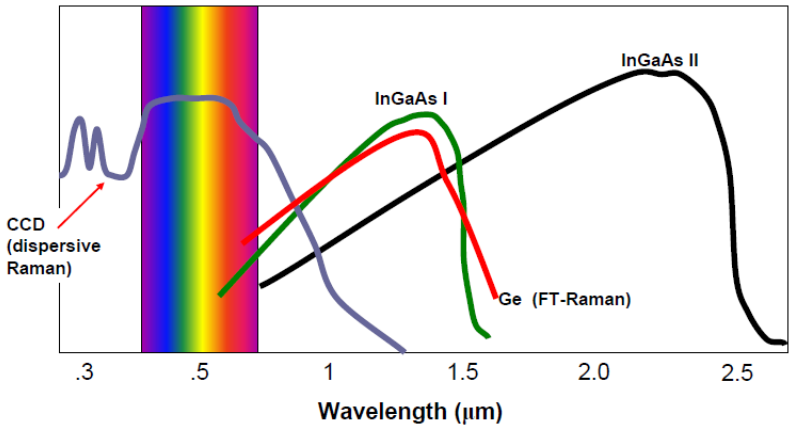

Silicon detectors (i.e. CCDs) are not sensitive to light beyond ~1100 nm,

Combine a 1064 nm laser
with a dispersive spectrograph
and specialized InGaAs array
detector (DeltaNu/Intevac)

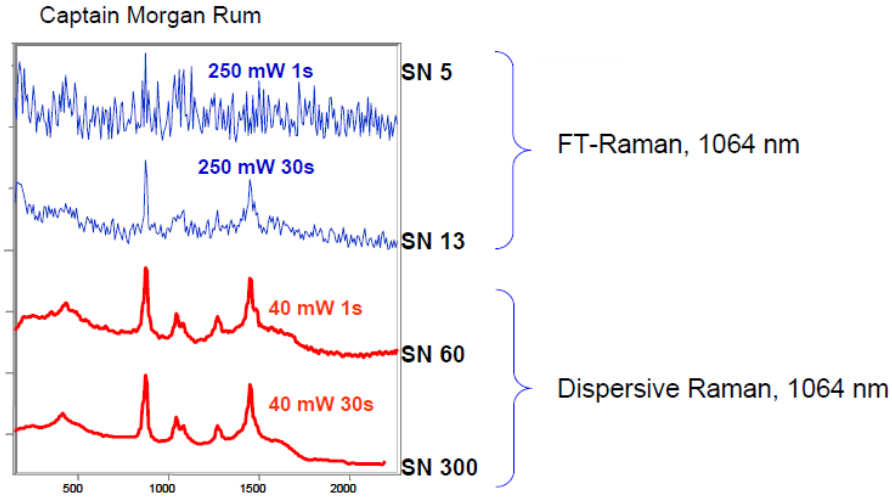

(slide from Keith Carron)

Most popular and efficient choice nowadays
Single grating
micro-Raman
spectrometer

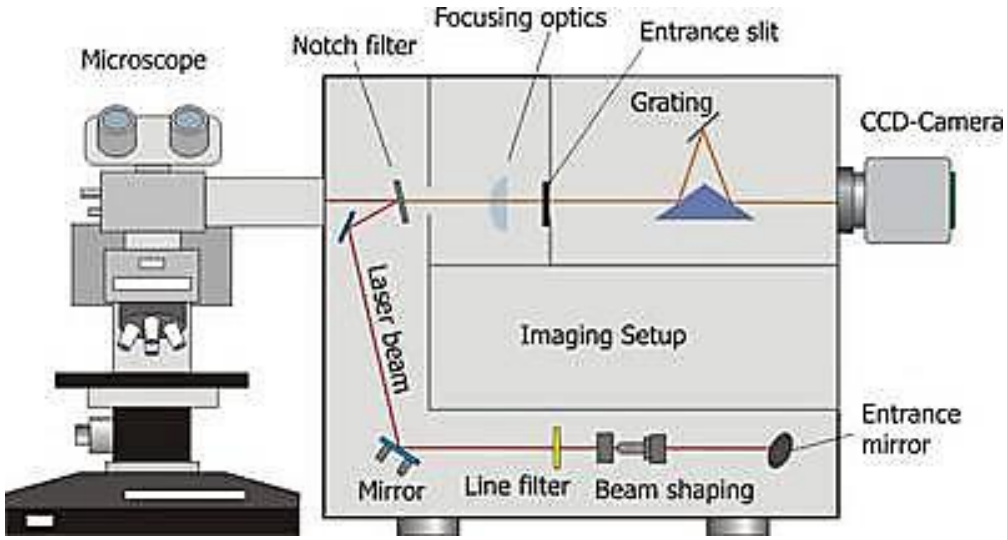

Raman imaging

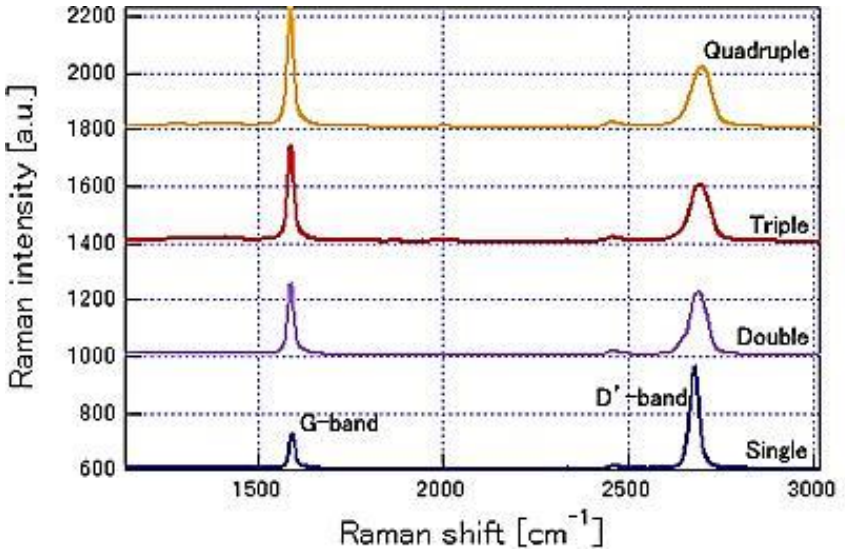

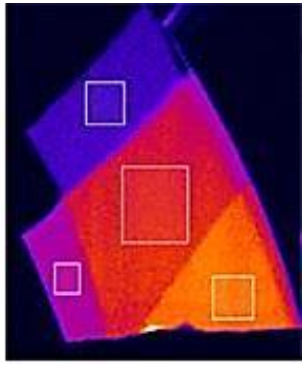

Graphene

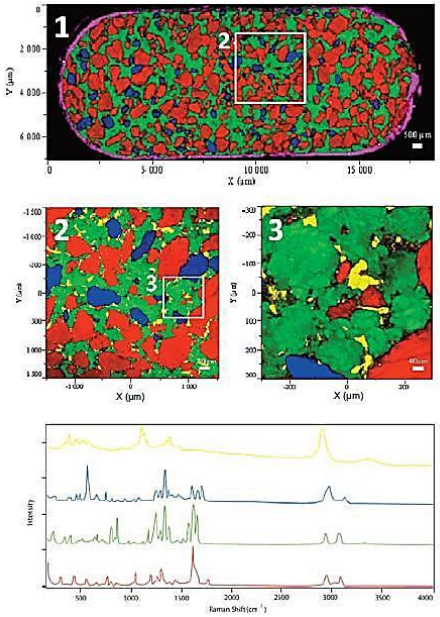

Aspirin, paracetamol, caffeine, cellulose

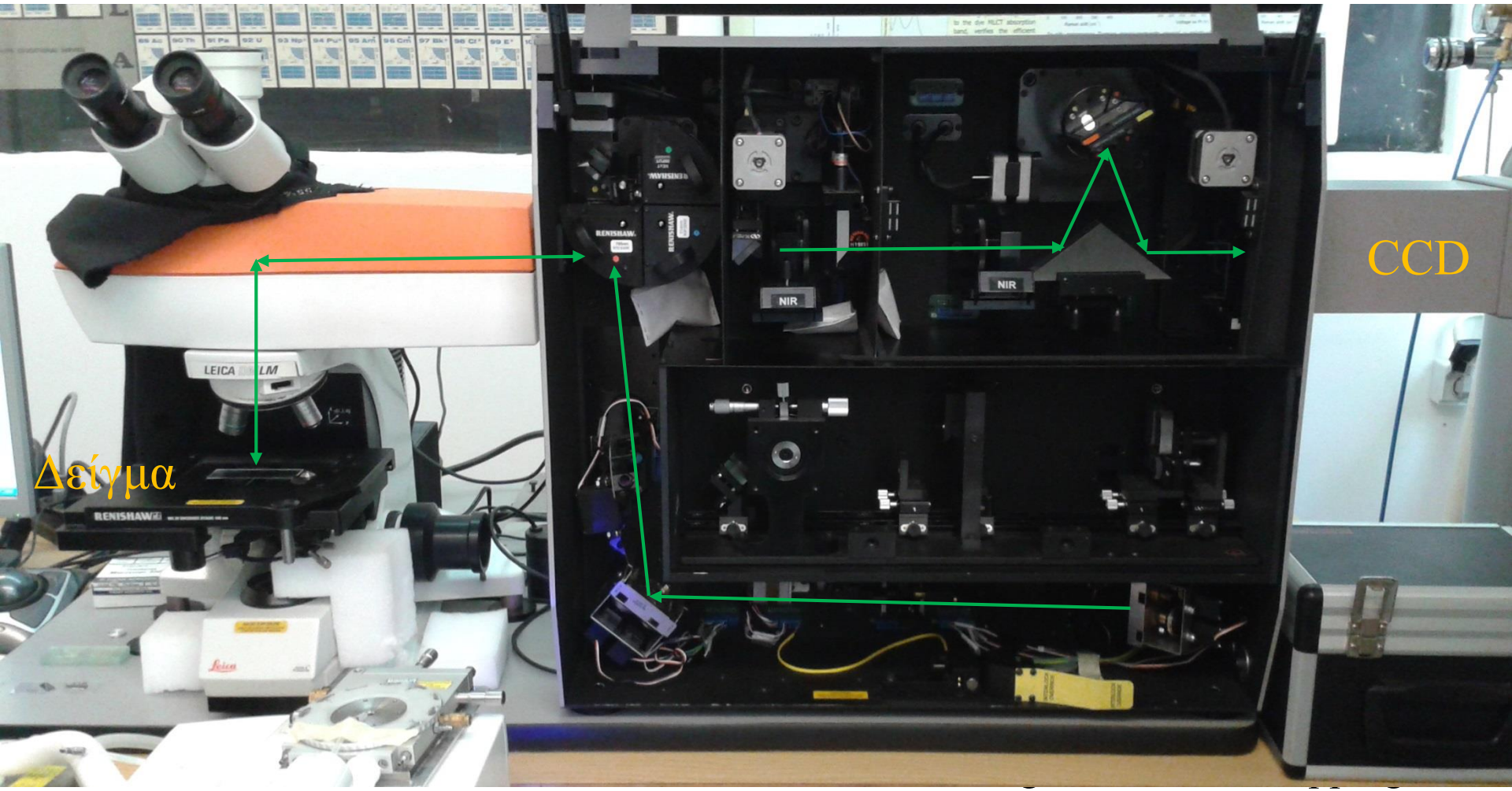
Δείγμα
CCD
NIR
NIR
RENISHAW
LEICA

Corrosion properties of $[C_nmim][C(CN)_3]$ by micro-Raman spectroscopy

Immersion of mild steel (MS) in $[C_2mim]$ $[C(CN)_3]$ at 80 °C for 1 and 10 days

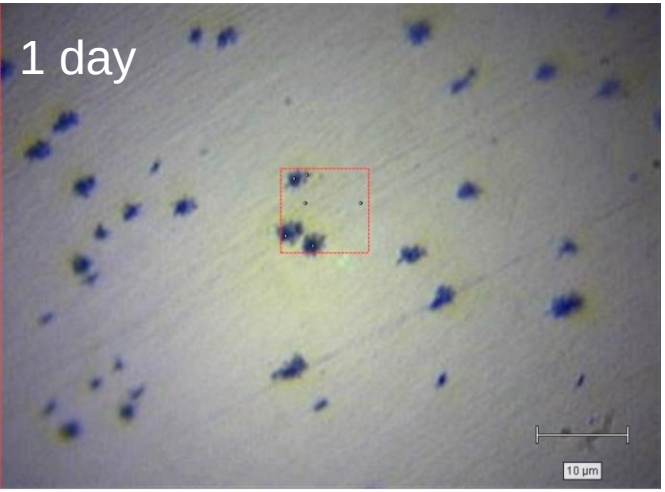

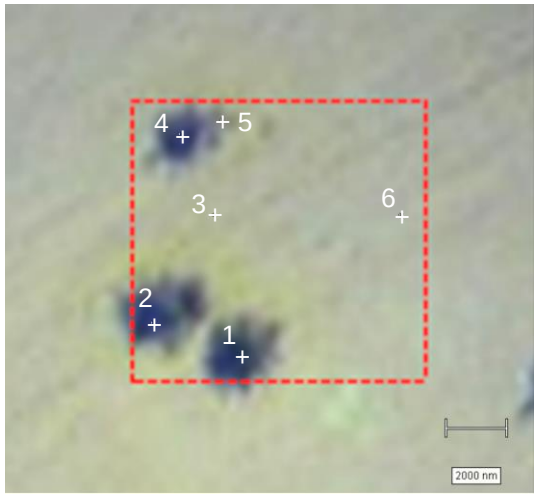

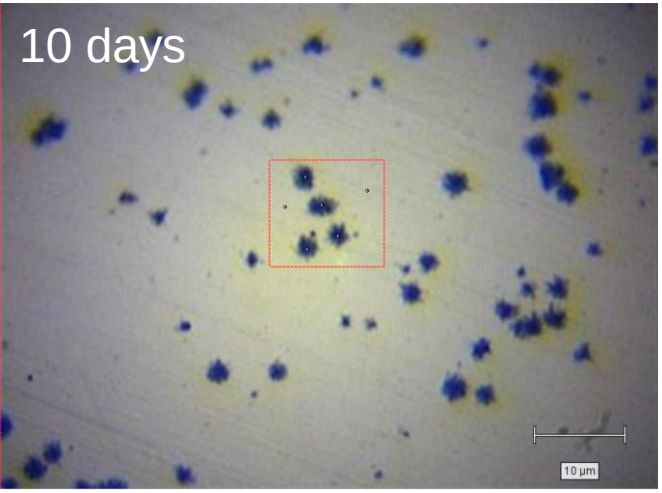

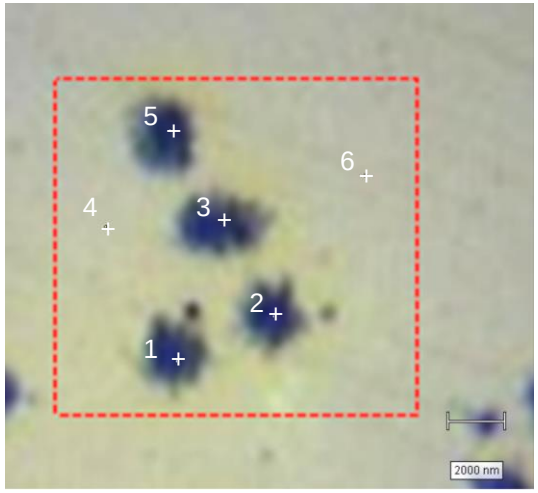

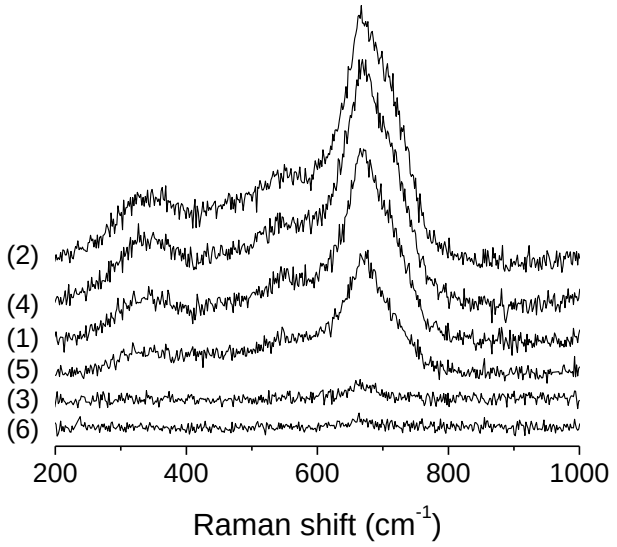

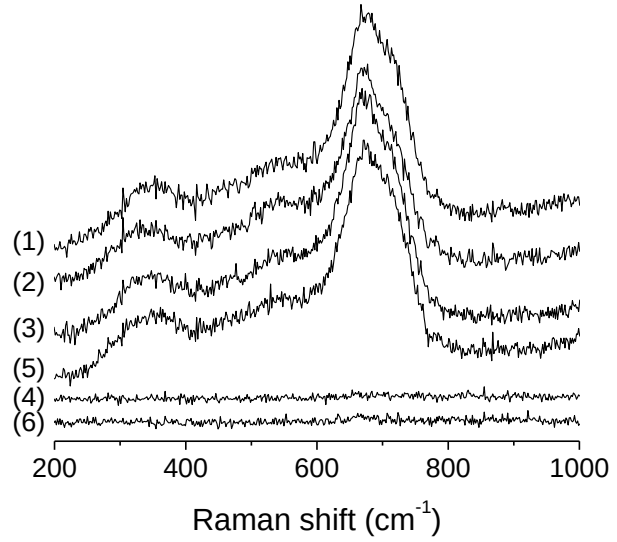

Immersion at 80 °C for 10 days

Mild steel in $[C_4mim]$ $[C(CN)_3]$

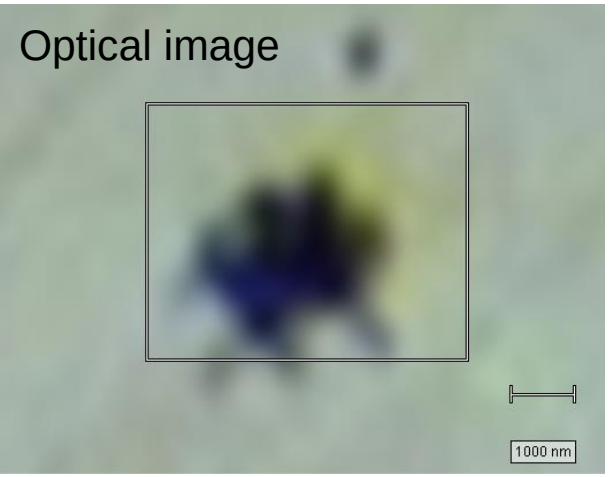

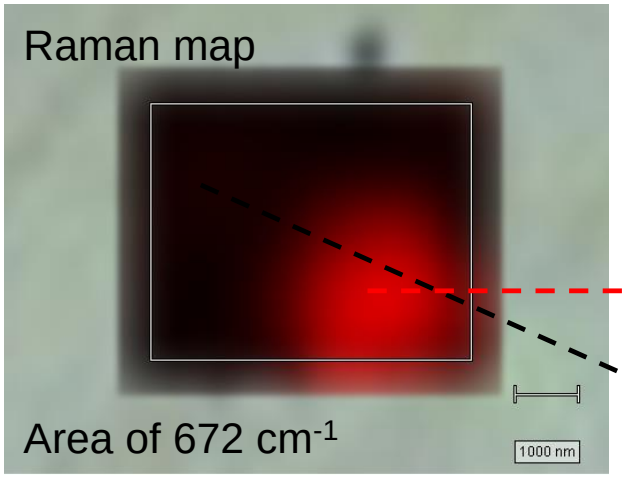

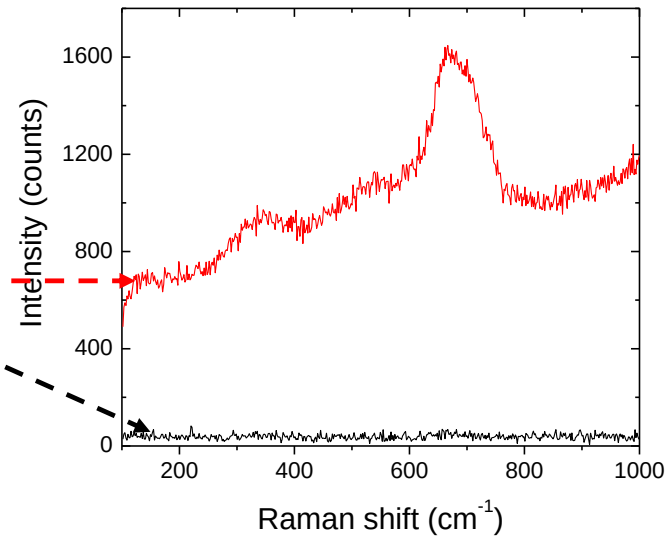

Mild steel in $[C_8mim]$ $[C(CN)_3]$

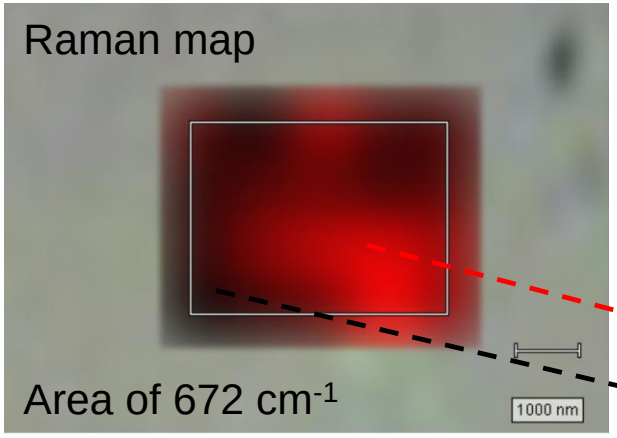

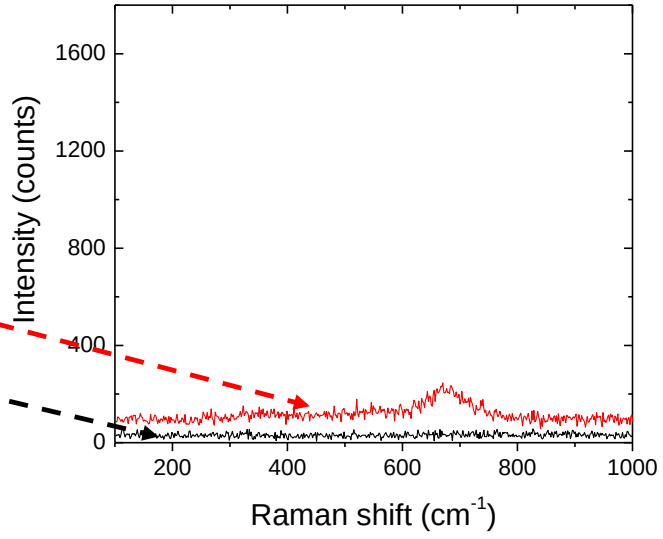

Demokritos
National Centre for Scientific Research
Institute of Physical Chemistry

Micro-Raman spectroscopy:
Phase Identification- crystallinity of nanomaterials

Amorphous titania
vs
Crystalline titania

Vibrations of ethylene glycol molecules and carbon

Ethylene glycol TiO_2 nanotubes

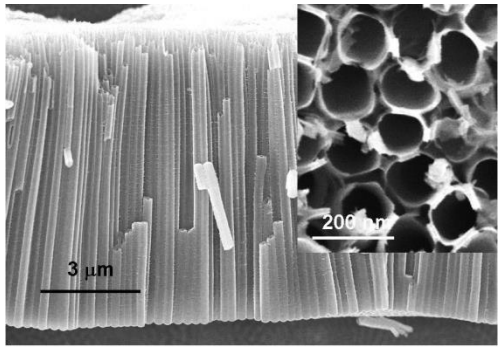

RBA TiO_2 nanotubes

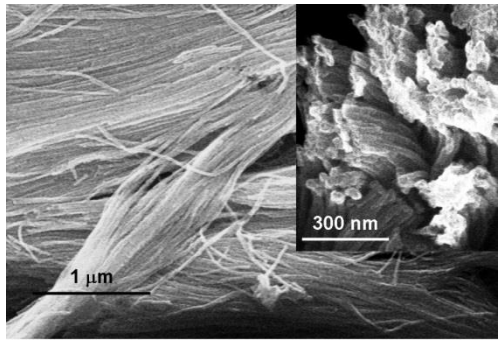

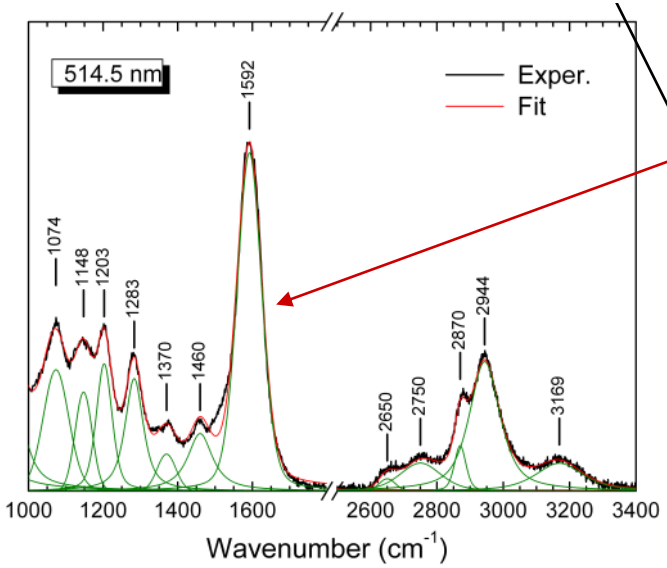

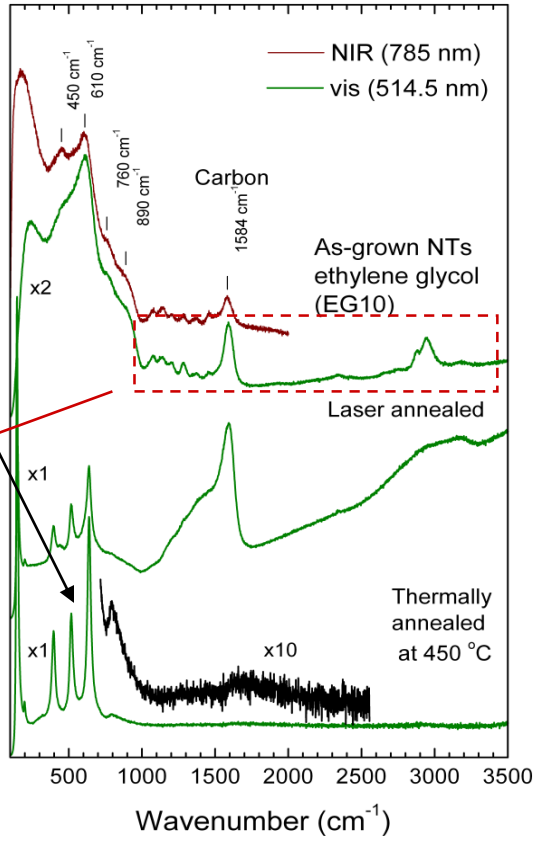

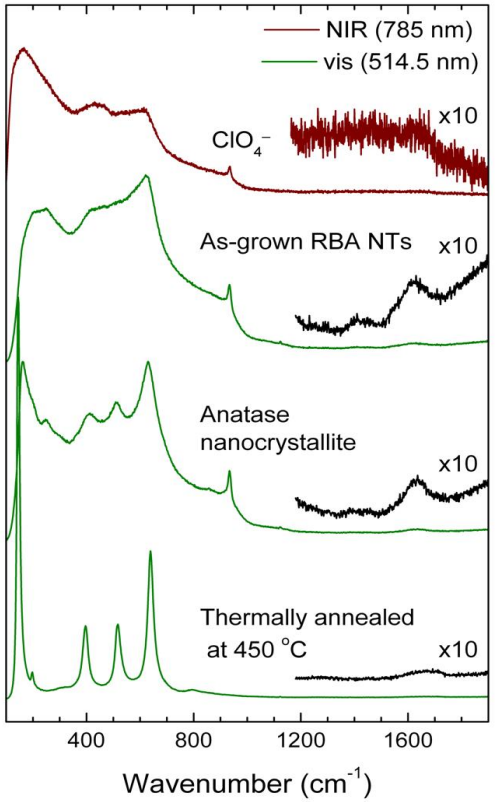

Micro-Raman on Hybrid Nanostructures

Micro-Raman at variable laser excitation wavelengths (Resonance Raman) can do it !!!

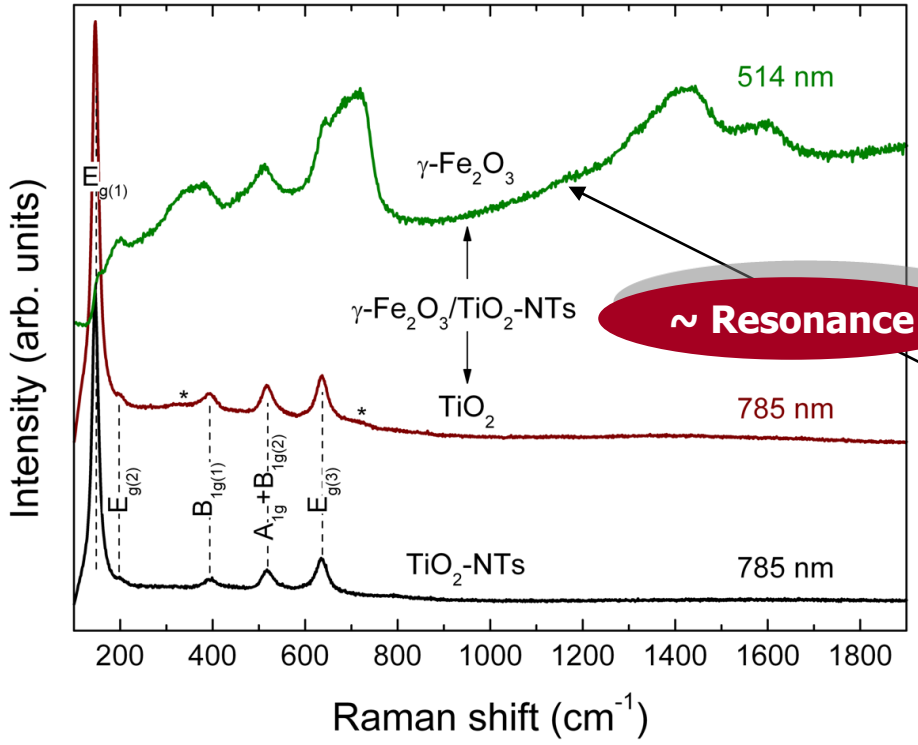

~ Resonance

Maghemite γ-Fe_2O_3

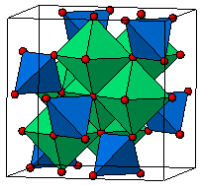

E_g ~ 2.2 eV
λ ~ 560 nm

Anatase TiO_2

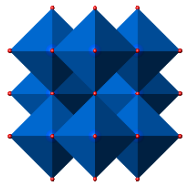

E_g ~ 3.2 eV
λ ~ 390 nm

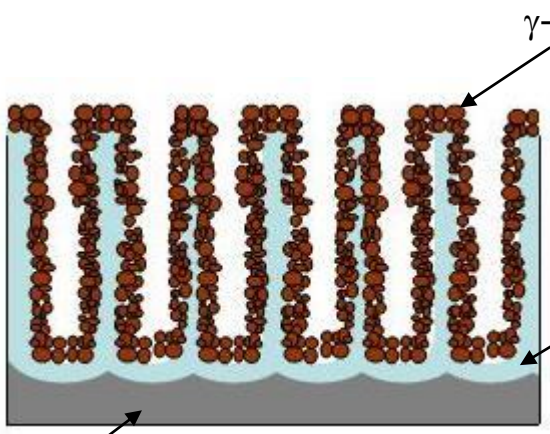

The individual oxides on the hybrid nanostructure are clearly discriminated though the resonance Raman as the excitation energy at 514 nm (2.4 eV) approaches the band-gap (~2.2 eV) of maghemite (γ-Fe_2O_3) (minor phase) causing the enhancement of its modes, which appear only as weak shoulders on the dominant anatase modes (major phase) at the off-resonance conditions of the NIR Raman spectra.

Micro-Raman on Hybrid Nanostructures

Phase transformation of the iron-oxide nanoparticles upon thermal treatment

In-situ local heating through the laser beam

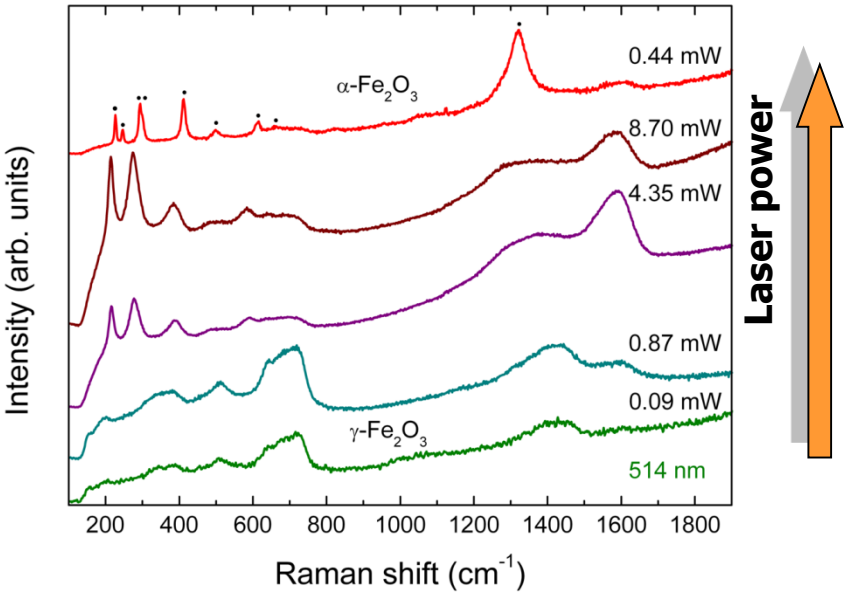

Ex-situ Raman measurements after thermal treatment at 500 °C

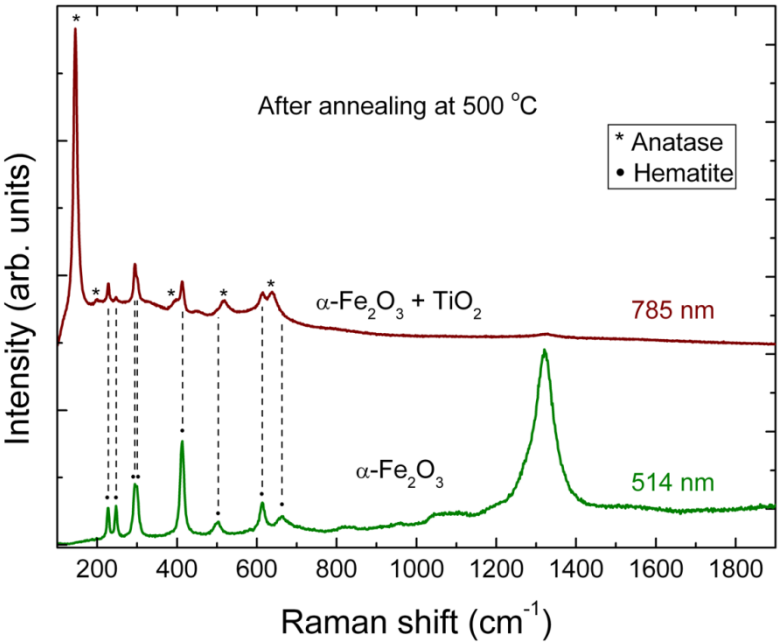

In-situ Raman monitoring of the phase transformation by increasing the laser power at 514 nm, where the γ-Fe_2O_3 NPs absorb strongly. Heating is performed through the focusing objective on the Raman microscope stage.
Local temperature: anti-Stokes

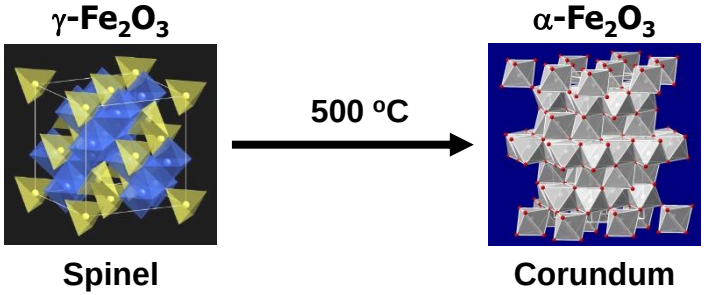

Demokritos
National Centre for Scientific Research
Institute of Physical Chemistry

Hybrid dye/semiconductor interfaces

Dye sensitization on TiO_2 nanotubes

Crystallization of TiO_2 nanotube substrate

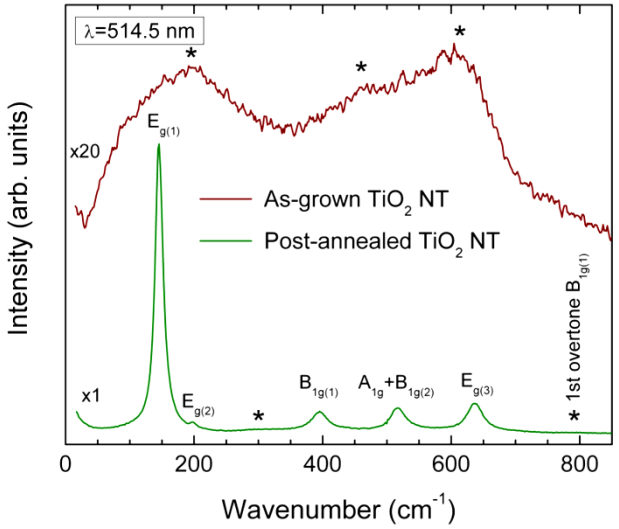

Frequency shifts and broadening of the bipyridine ring stretching (1470-1615 cm^{-1}) modes as well as the C-C inter-ring and C-O stretching modes (1250-1320 cm^{-1})

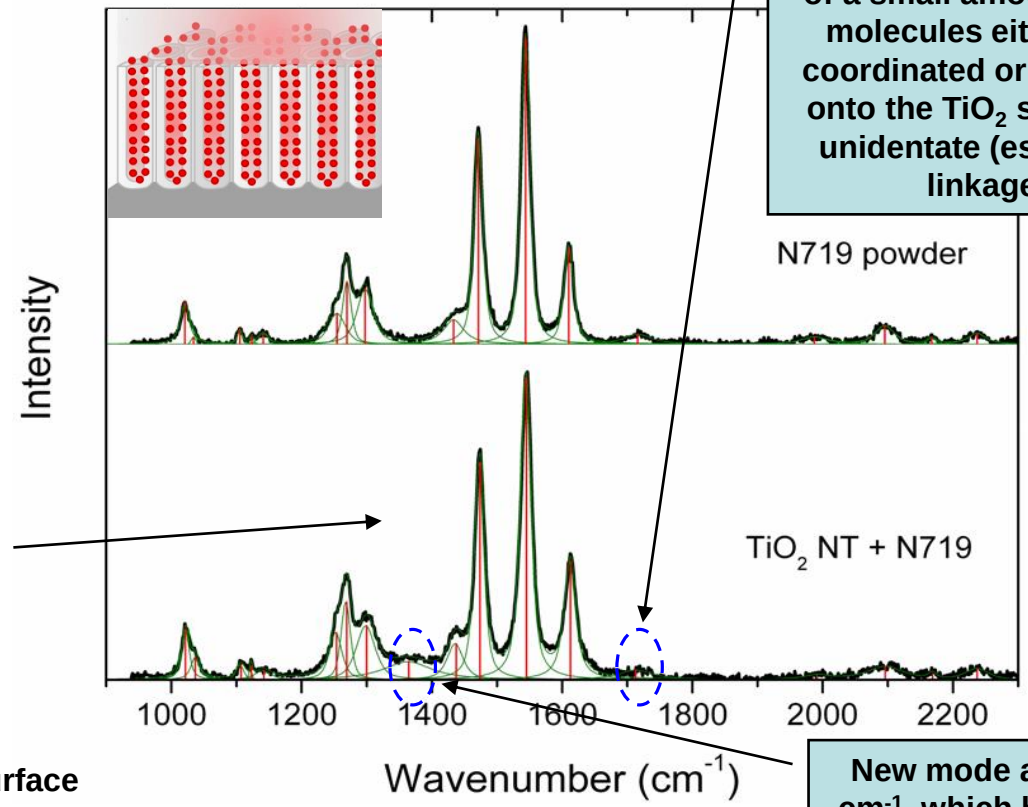

Weak C=O stretching mode at ~1720 cm-1, pointing to the presence of a small amount of dye molecules either non-coordinated or adsorbed onto the TiO_2 surface by unidentate (ester-type) linkages

New mode at ~1370 cm^{-1}, which has been assigned to the symmetric COO- stretching mode pointing to Bidentate or Bridging coordination

Dye coordination on the semiconductor surface

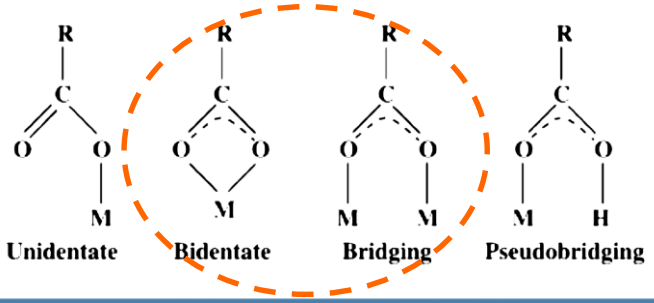

Analysis of the organic dye anchoring mode onto the semiconductor surface

Demokritos
National Centre for Scientific Research
Institute of Physical Chemistry

Hybrid amorphous carbon/polymer interfaces

Diamond-like carbon (DLC) on polyethylene terephthalate (PET) films

Deposited by plasma enhanced chemical vapour deposition PECVD at different bias voltages

Disordered/amorphous Carbon

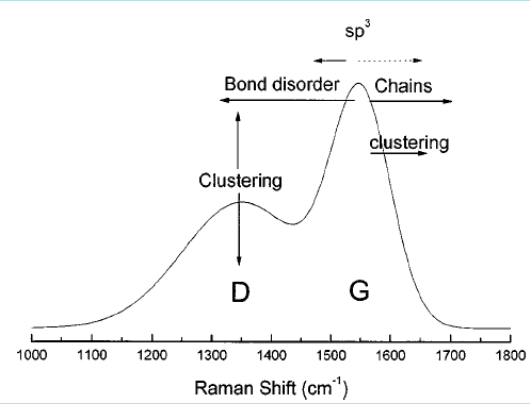

G mode: Bond stretching of sp^2 carbon atoms in both aromatic rings and chains

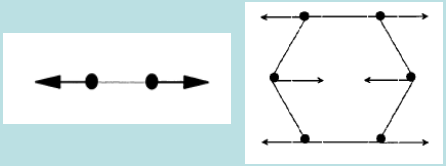

D-mode: Breathing of rings

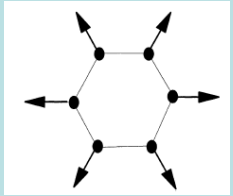

Use of different **objectives** and the **confocal** mode to resolve the very thin DLC layers deposited on PET under the lowest bias voltage

$$\Delta z \approx \frac{\lambda}{NA^2}$$

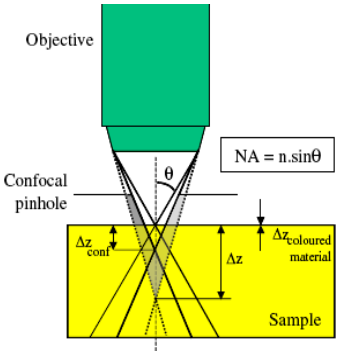

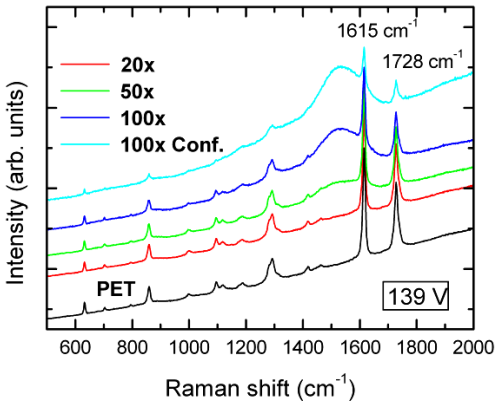

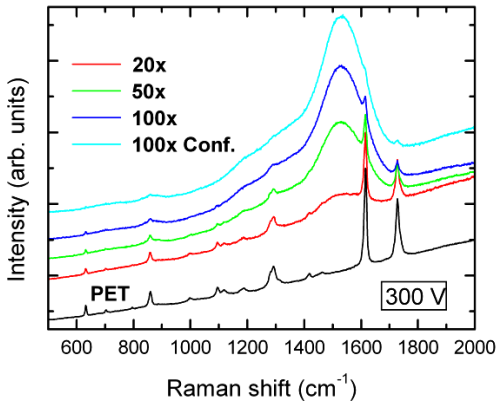

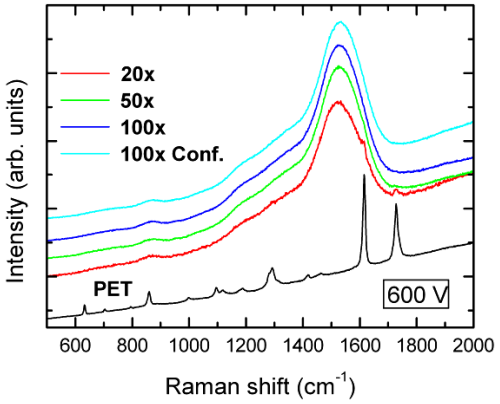

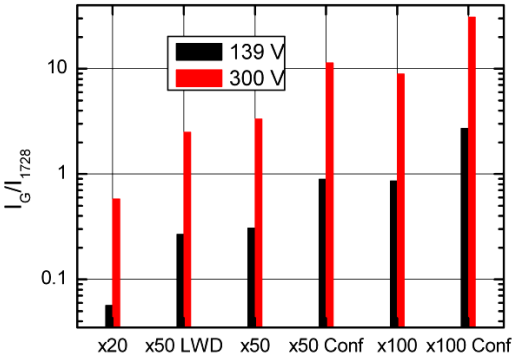

Collection optics

Optical parameters for the lateral spatial resolution

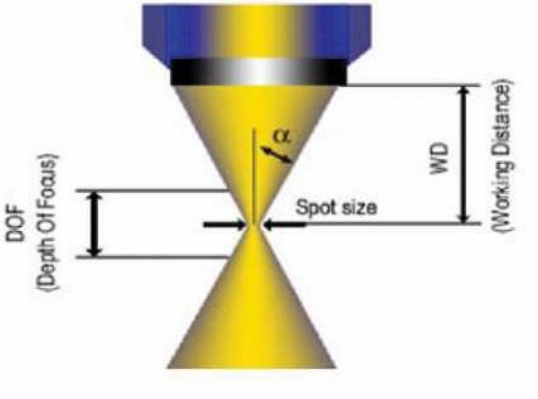

Laser spot size

$$d_w = \frac{1.22\,\lambda}{NA}$$

Diffraction limited resolution d given by the Rayleigh criterium

$$d = \frac{0.61\,\lambda}{n\,\sin\alpha} = \frac{0.61\,\lambda}{NA}$$

e. g. with 633nm HeNe laser and x100 objective with NA = 0,9

d = 430 nm

HORIBA Scientific

Collection optics

- Depending on the experiment **and the sample** different collecting optics are used
- Therefore micro Raman instruments are equipped with different objectives with different numerical aperture

Objective	N.A.	Working distance [mm]
x100	0.90	0.21
x50	0.75	0.38
x10	0.25	10.6
x100 LWD	0.80	3.4
x50 LWD	0.50	10.6

Dispersive micro-Raman spectrometer

Collection optics

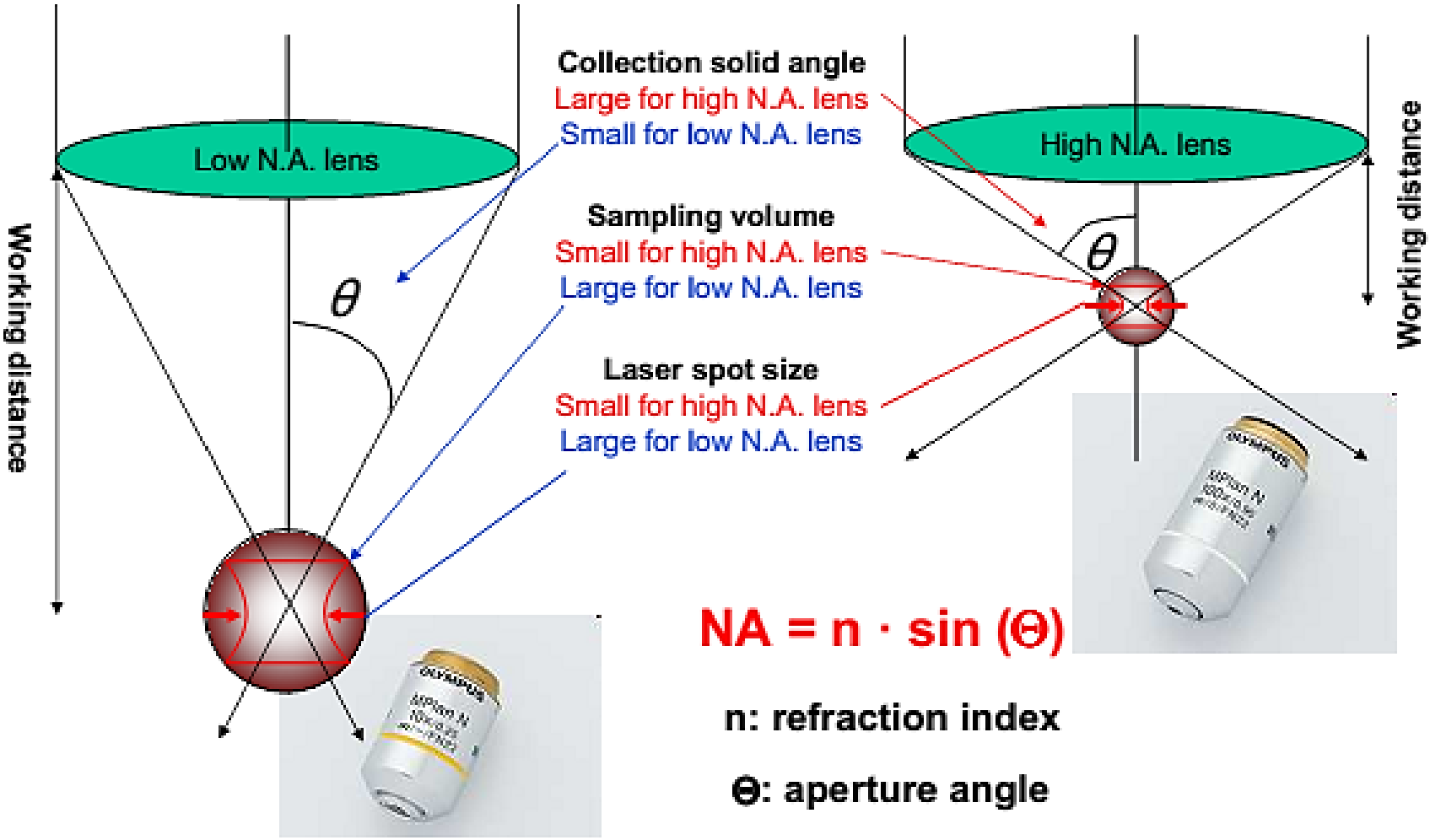

$$NA = n \cdot \sin(\Theta)$$

n: refraction index

Θ: aperture angle

Nanomaterials

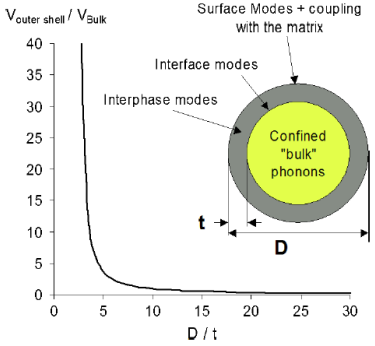

Surface/Interface Acoustic modes

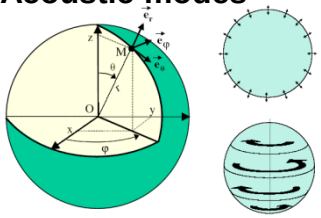

"Antenna effects"

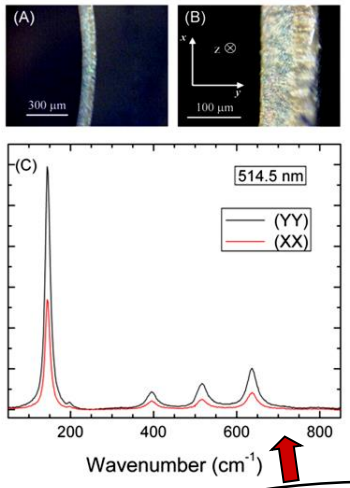

Mapping nanostructures

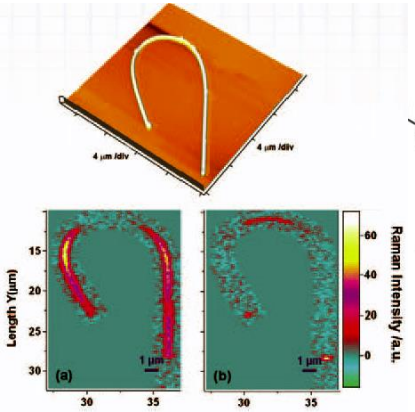

Device characterization Photoelectrochemical cells

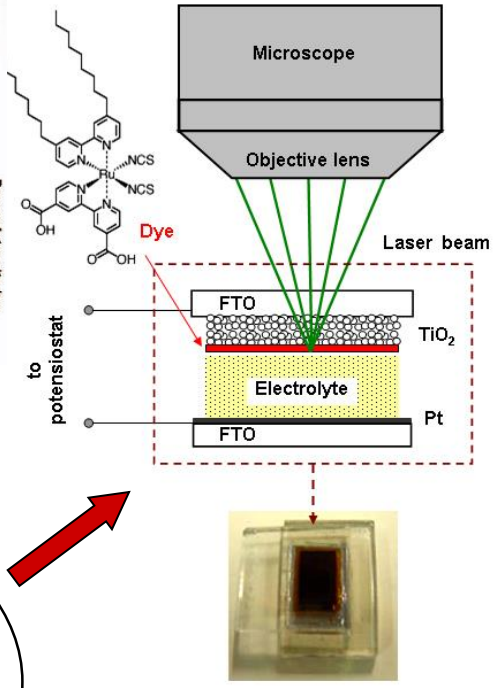

Micro-Raman

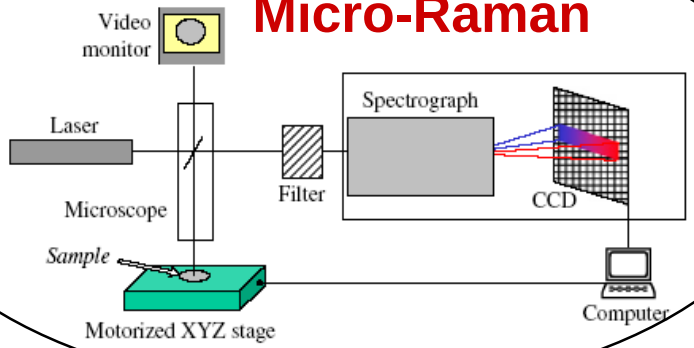

Confocal Raman

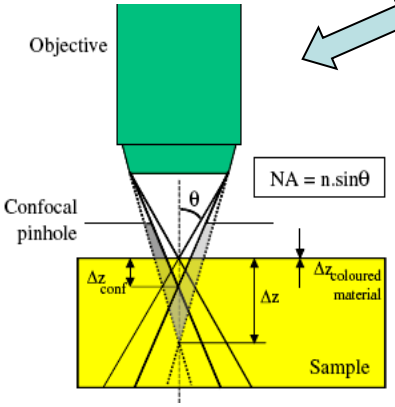

Fiber optical probes Portable Raman

Electrochemical cell

Variable temperatures

Mapping stage

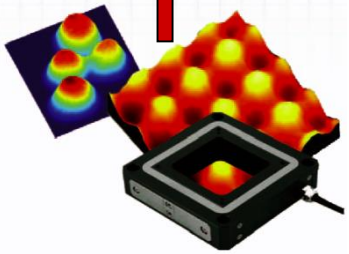

Environmental analysis & monitoring

Increasing lateral resolution…

OPTICAL MICROSCOPY

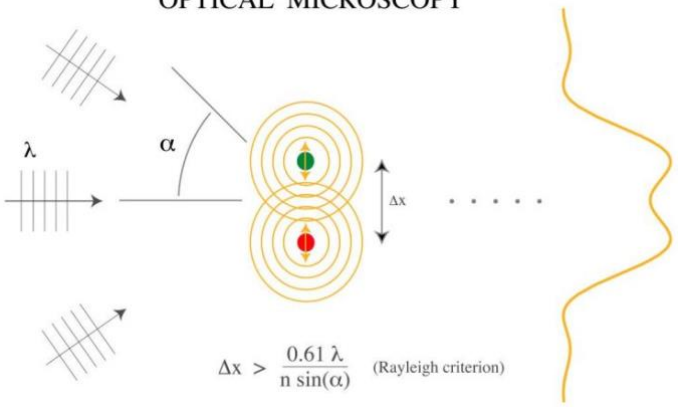

Rayleigh Criterion: Diffraction limit of the far field microscopy is of the order of the wavelength of the incident light. **Resolution> 500 nm**.

APERTURE NEAR-FIELD MICROSCOPY

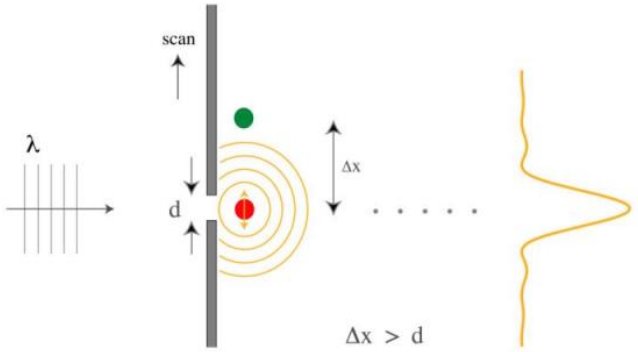

E.H. Synge, Phil.Mag. **6**, 356, 1928 , D.W. Pohl et al., Appl.Phys.Lett. **44**, 651, 1984

Aperture **scanning near field microscopy** is a technique that allows for arbitrarily small details to be resolved. Lateral resolution ~ aperture size.

FIELD ENHANCEMENT MICROSCOPY

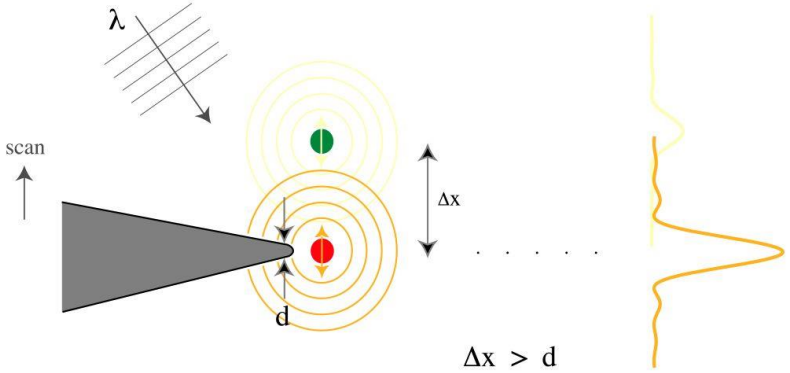

H. Furukawa and S. Kawata, Opt. Commun.**148**, 221, 1998
L. Novotny et al., Ultramicroscopy **71**, 21, 1998

Instead of using a small aperture, a metal tip is used to provide a local electric field enhancement (**TERS**). Lateral resolution is the size of the tip.

Near-field scanning optical microscopy (NSOM/SNOM)

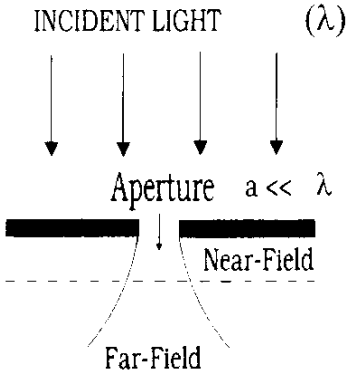

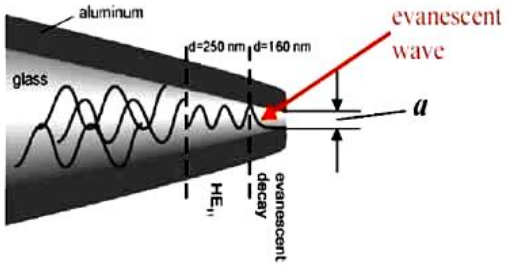

Aperture SNOM
Modes of operation

Transmission – Reflection – Collection

Tip-Enhanced Raman Scattering (TERS)

Apertureless SNOM

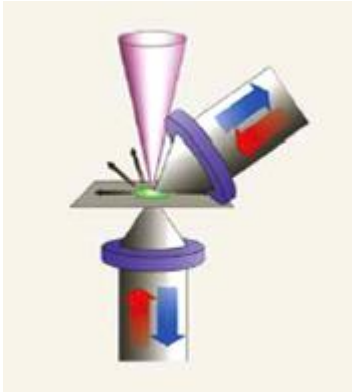

\+

Surface Enhanced Raman Scattering (SERS)

Tip-Enhanced Raman Scattering

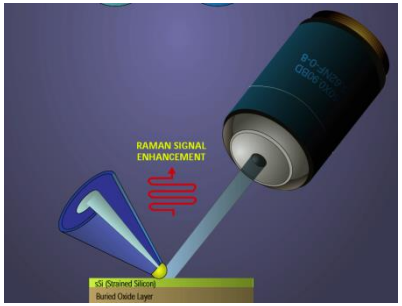

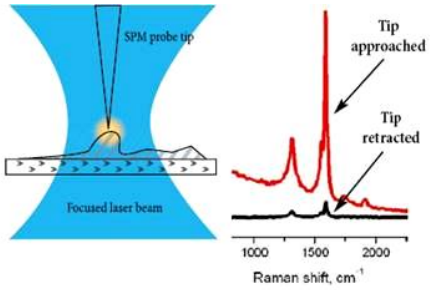
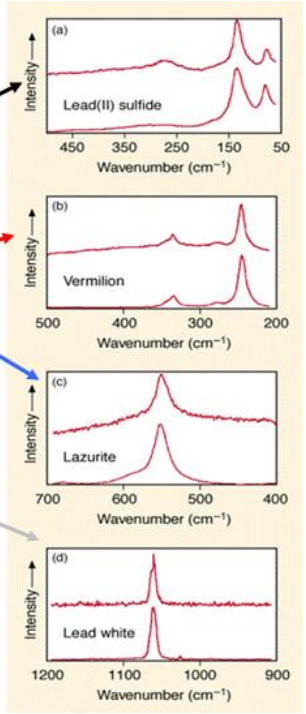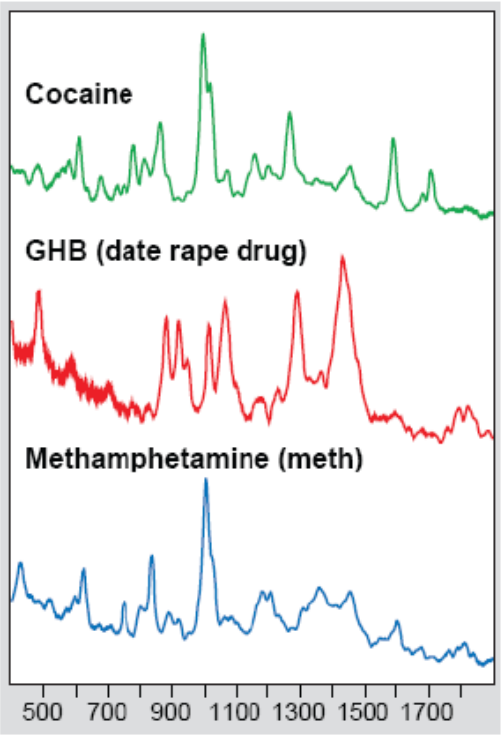
Portable Raman